Large cluster dynamical mean field calculations and the momentum-selective Mott transition

Emanuel Gull

Columbia University
IN THE CITY OF NEW YORK

April 22, 2011

Funding: NSF-DMR-1006282

A.J. Millis
A. Georges, M. Ferrero, N. Lin, O. Parcollet, P. Werner
S. Fuchs, P. Staar, P. Nukala, M. Summers, T. Pruschke, T. Schulthess, T. Maier
L. Pollet, E. Kozik, E. Burovski, M. Troyer

Phys. Rev. B 80, 045120 (2009)
Phys. Rev. B 80, 245102 (2009)
Phys. Rev. B 82, 045104 (2010)
Phys. Rev. B 82, 155101 (2010)
Phys. Rev. Lett. 106, 030401 (2011)
Phys. Rev. B 83, 075122 (2011)

Overview

- Introduction: the pseudogap in High Tc

- Methods and tools I: Cluster DMFT

- Methods and tools II: Impurity solvers

- Controlling DCA: Benchmarking the 3D Hubbard model

- Results for the 2D Hubbard model: Momentum selectivity, pseudogaps, Optical conductivities, Raman, ...

Experiments: Pseudogap

in high-Tc materials: Electronic spectral function is suppressed along the BZ face, but not along zone diagonal.

Key physics dependence on momentum around Fermi surface, Difference of spectral function around Fermi surface.

Doping dependence of region with quasiparticles

ARPES: Shen *et al.*, Science 307, 901 (2005)

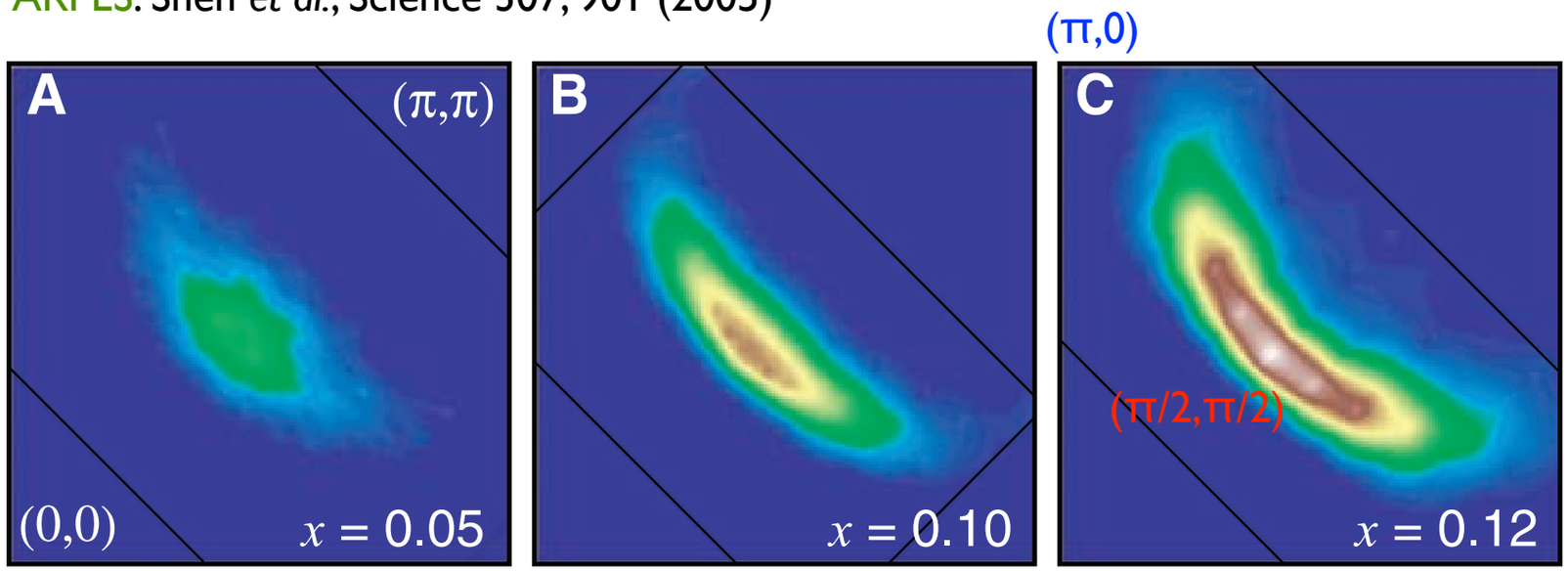

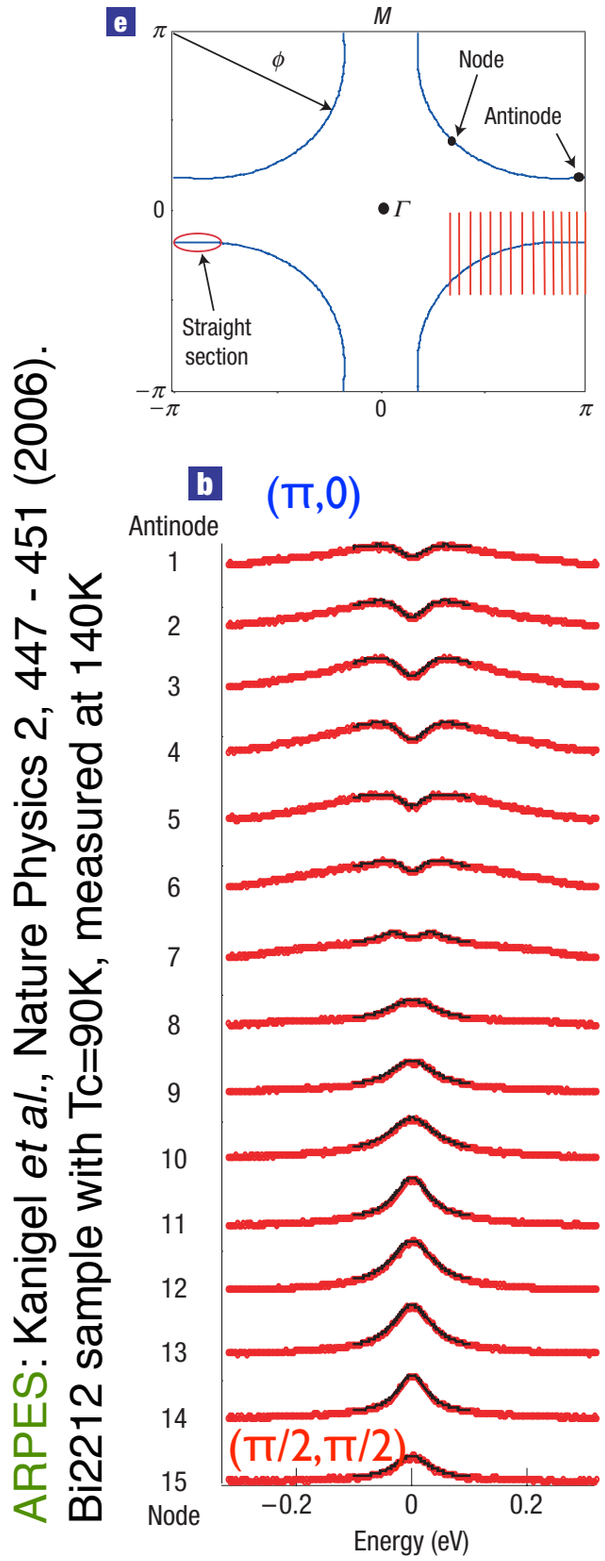

ARPES: Kanigel *et al.*, Nature Physics 2, 447 - 451 (2006). Bi2212 sample with Tc=90K, measured at 140K

Experiments: Pseudogap

Damascelli *et al.*, Rev. Mod. Phys 75, 2 (2003)

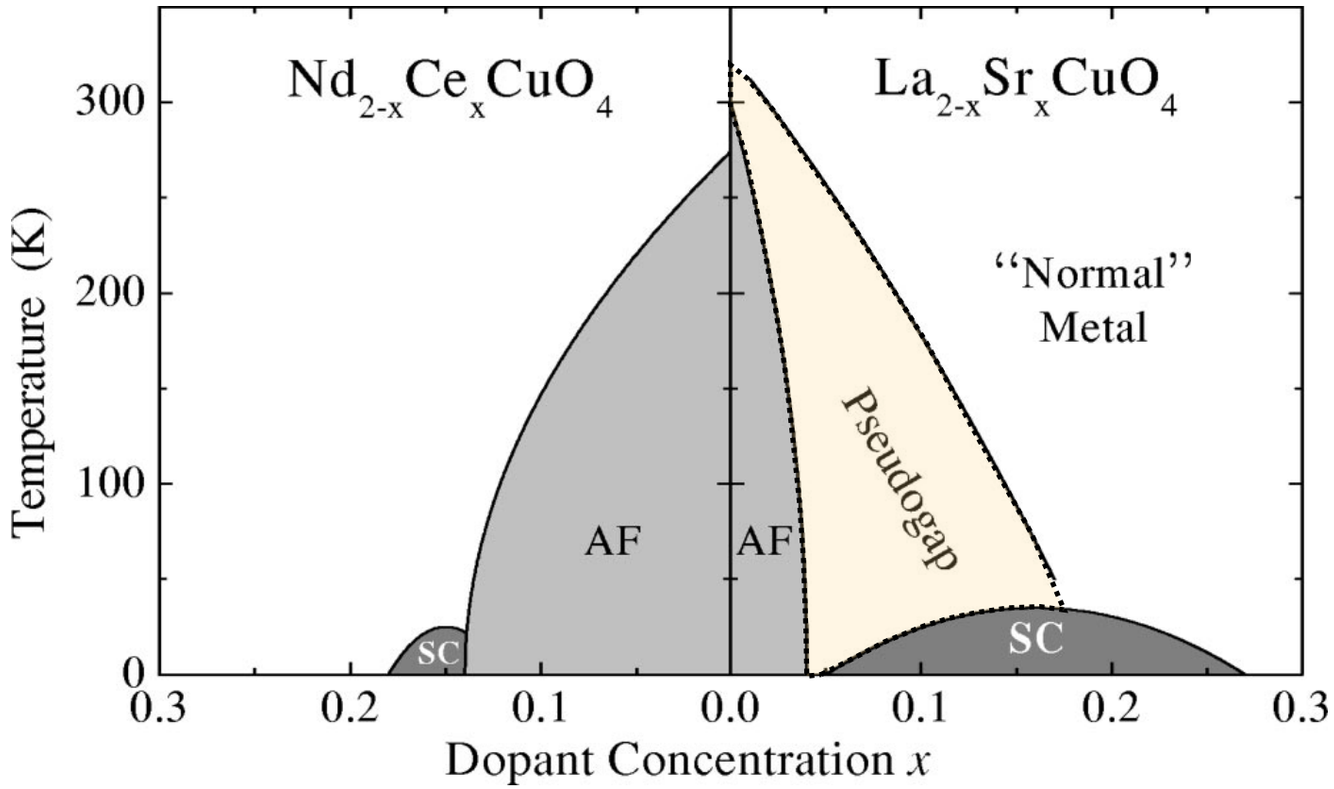

FIG. 1. Phase diagram of n- and p-type superconductors, showing superconductivity (SC), antiferromagnetic (AF), pseudogap, and normal-metal regions.

Hüfner *et al.*, Rep. Prog. Phys. 71, 062501(2008)

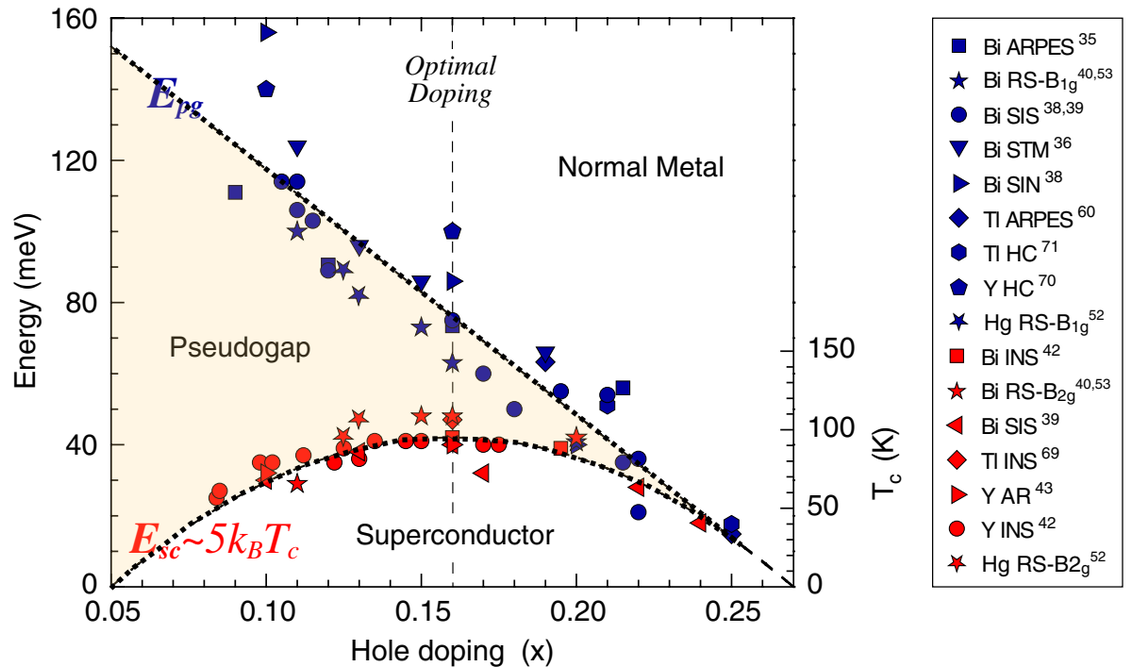

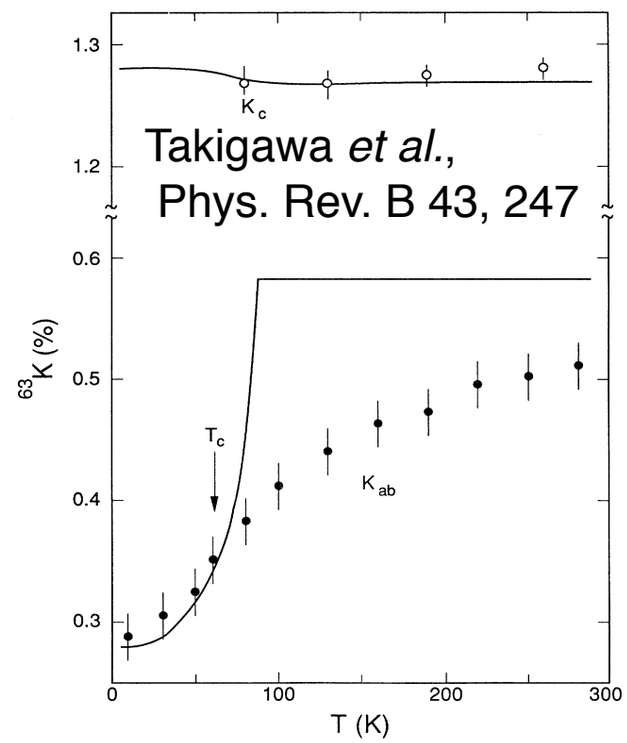

FIG. 3. Temperature dependence of the Cu(2) Knight shift (^{63}K) for $H \| \mathbf{c}$ (K_c) and $\mathbf{H} \perp \mathbf{c}$ (K_{ab}) together with the results in the $y \simeq 0$ material reported by Barrett *et al.* (Ref. 25) (solid line). The arrow indicates the value of T_c at 10 Oe.

Pseudogap* appears only on the hole doped side.

Dopings smaller than optimal doping.

Temperatures up to ~ 300K.

Signatures also in NMR, Tunneling, c-axis conductivities, Raman…

*...of this type...

Experiments: Overdoped Ti2201 / ADMR

French, Analytis, Carrington, Balicas, Hussey:
NJP 11, 05595 (2009)

Angle dependent magneto-resistance:

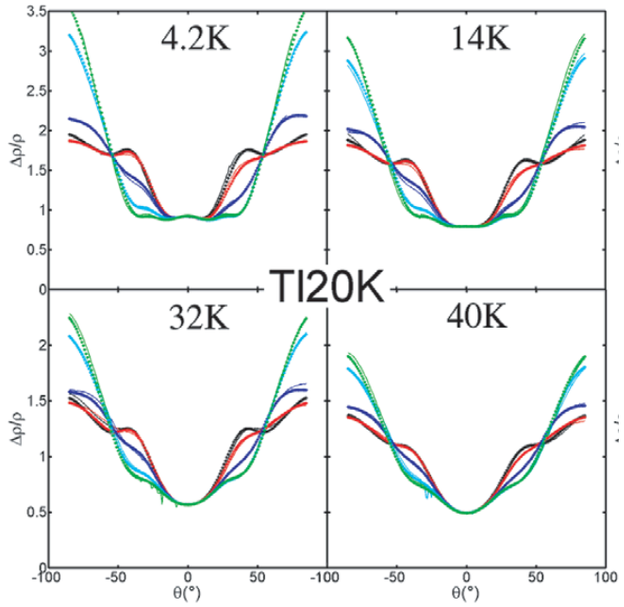

Data analysis:

$$\rho(T) = A + BT + CT^2$$

Angle dependent analysis:

$$\gamma_{\rm iso} \sim A + CT^2$$

$$\gamma_{\rm aniso} \sim BT(+CT^2)$$

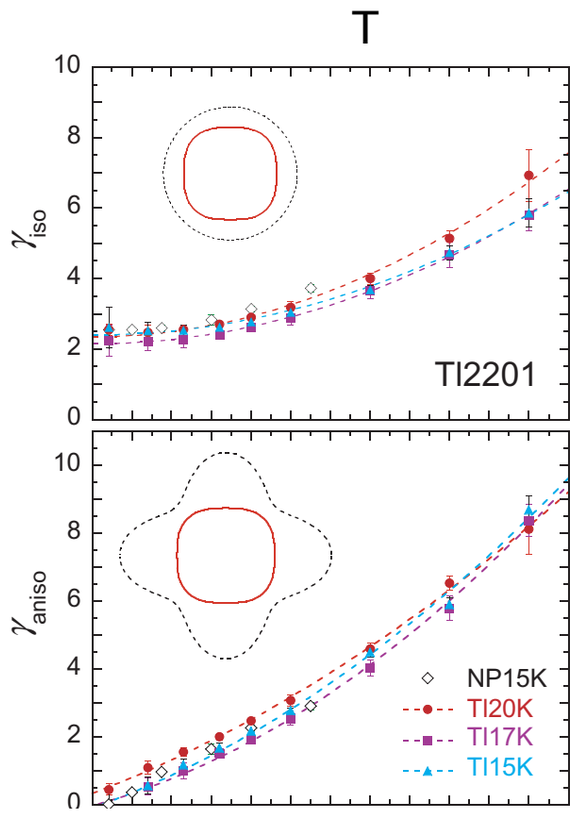

Figure 3. Temperature dependence of the isotropic (top panel) and anisotropic (middle panel) scattering rates determined from the ADMR measurements shown in figure 1. NP15K refers to the sample whose ADMR were measured at a single azimuthal angle [11]. The dashed lines in the top and middle panels are fits to $A + CT^2$ and $A + BT + CT^2$, respectively. The insets in each panel depict the Fermi surface (as red solid lines) and the corresponding scattering rates (as black dashed lines. Bottom panel: components of $\gamma_{\rm aniso}(T)$ (black long-dashed lines and green short-dashed lines) and $\gamma_{\rm iso}(T)$ (orange dots) for Tl15sK.

Anisotropic component of scattering rate: maximal near antinodal point, minimal near nodal point.

Momentum space differentiation!

Questions to theory

‘Explain’ momentum
space differentiation

‘Explain’ pseudogap

‘Explain’ experimental probes:
ARPES, ADMR, optical
conductivities, Raman, NMR,…

……we will try to give an answer in this talk……

Theory

$$H = -\sum_{\langle ij\rangle,\sigma} t_{ij}(c^{\dagger}_{i\sigma}c_{j\sigma} + c^{\dagger}_{j\sigma}c_{i\sigma}) + U\sum_{i} n_{i\uparrow}n_{i\downarrow}.$$

Hubbard model, with **t'**-anisotropy, treated in a **cluster DMFT** approximation.

No long range order (AFM, stripes, …), no multi-orbital physics

Open theoretical question (addressed in this talk): **how much of the physics already contained in this model?**

Simulations of **phase diagrams**

Large enough systems to show which features are **robust**

Variation of cluster size, cluster geometry, etc to **control approximation**

Computation of experimental probes

Phys. Rev. Lett. 106, 030401 (2011)

Cluster DMFT

Approximation to self energy:

$$\Sigma(k,\omega) = \sum_n \Sigma_n(\omega)\phi_n(k) \approx \sum_n^{N_c} \Sigma_n(\omega)\phi_n(k)$$

← Systematic truncation with cluster sites N_c

DMFT for $N_c = 1$

Basis functions

Example: Tiling of the BZ:

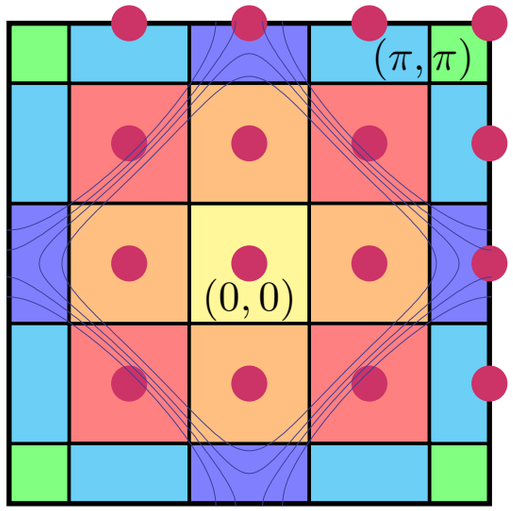

'Machinery' for obtaining approximated self energy: Cluster scheme. We use the DCA: ϕ constant on patches in the BZ

Cluster DMFT is a **controlled approximation**, exact for $N_c \to \infty$

Restriction to paramagnetic bath (no long-ranged AFM here)

$$\epsilon_p = -2t(\cos(p_x) + \cos(p_y)) - 4t' \cos(p_x)\cos(p_y)$$

DMFT: Metzner, Vollhardt, Phys. Rev. Lett. 62, 324 (1989),
Georges, Kotliar, Phys. Rev. B 45, 6479 (1992),
Jarrell, Phys. Rev. Lett. 69, 168 (1992),
Georges et al., Rev. Mod. Phys. 68, 13 (1996),

DCA: Hettler et al., Phys. Rev. B 58, R 7475 (1998),
Lichtenstein, Katsnelson, Phys. Rev. B 62, R9283 (2000)
CDMFT: Kotliar et al., Phys. Rev. Lett. 87, 186401 (2001)
T. Maier, et al., Rev. Mod. Phys. 77, 1027 (2005).

Cluster DMFT – impurity solvers

$$\Sigma(k,\omega) = \sum_n \Sigma_n(\omega)\phi_n(k) \approx \sum_n^{N_c} \Sigma_n(\omega)\phi_n(k)$$

Algorithm that produces $\Sigma_n(\omega)$: Mapping onto a quantum impurity problem & self-consistent hybridization with a "bath".

$$H_{\mathrm{QI}} = H_{\mathrm{loc}} + H_{\mathrm{hyb}} + H_{\mathrm{bath}}$$

$$H_{\mathrm{loc}} = \sum_i \epsilon_i (n_{i\uparrow} + n_{i\downarrow}) + U n_{i\uparrow} n_{i\downarrow}$$

$$H_{\mathrm{bath}} = \sum_{k\alpha} \epsilon_{k\alpha} c^\dagger_{k\alpha} c_{k\alpha}$$

$$H_{\mathrm{hyb}} = \sum_{k\alpha b} V_k^{\alpha b} c^\dagger_{k\alpha} d_b + H.c.$$

Computationally hard part: obtaining the impurity Green's function / self energy from this Hamiltonian:

• Solve large cluster impurity problems, at and away from half filling, for small and large interactions (density-density), at finite temperature.

• No further approximations (Δτ - errors, bath discretization, ...).

Review: E. Gull, A. J. Millis, A. I. Lichtenstein, A. N. Rubtsov, M. Troyer, P. Werner, arXiv:1012.4474 (Rev. Mod. Phys., in press)
E. Gull, P. Werner, O. Parcollet, M. Troyer, EPL 82,57003 (2008)

Cluster DMFT – impurity solvers

$$\Sigma(k,\omega) = \sum_n \Sigma_n(\omega)\phi_n(k) \approx \sum_n^{N_c} \Sigma_n(\omega)\phi_n(k)$$

Algorithm that produces $\sum_n(\omega)$: Mapping onto a quantum impurity problem & self-consistent hybridization with a "bath".

$$H_{\rm QI} = H_{\rm loc} + H_{\rm hyb} + H_{\rm bath}$$

$$H_{\rm loc} = \sum_i \epsilon_i (n_{i\uparrow} + n_{i\downarrow}) + U n_{i\uparrow} n_{i\downarrow}$$

$$H_{\rm bath} = \sum_{k\alpha} \epsilon_{k\alpha} c^\dagger_{k\alpha} c_{k\alpha}$$

$$H_{\rm hyb} = \sum_{k\alpha b} V_k^{\alpha b} c^\dagger_{k\alpha} d_b + H.c.$$

Only Candidates: Continuous-Time quantum Monte Carlo algorithms. We use: Continuous-Time Auxiliary Field (CT-AUX) algorithm.

Review: E. Gull, A. J. Millis, A. I. Lichtenstein, A. N. Rubtsov, M. Troyer, P. Werner, arXiv:1012.4474 (Rev. Mod. Phys., in press)
E. Gull, P. Werner, O. Parcollet, M. Troyer, EPL 82,57003 (2008)

Continuous-Time quantum Monte Carlo impurity solvers

Review: E. Gull, A. J. Millis, A. I. Lichtenstein, A. N. Rubtsov, M. Troyer, P. Werner, arXiv:1012.4474 (Rev. Mod. Phys., in press)

Diagrammatic expansion of the partition function of an impurity model in the interaction or the hybridization, sampling of the resulting series stochastically up to infinite order.

$$H_{\mathrm{QI}} = H_a + H_b$$

$$Z = \mathrm{Tr}\; T_\tau e^{-\beta H_a} \exp\left[-\int_0^\beta d\tau H_b(\tau)\right] = \sum_k (-1)^k \int_0^\beta d\tau_1 \ldots \int_{\tau_{k-1}}^\beta d\tau_k \mathrm{Tr}\left[e^{-\beta H_a} H_b(\tau_k) H_b(\tau_{k-1}) \ldots H_b(\tau_1)\right]$$

Hybridization Expansion

$H_a = H_{\mathrm{loc}};$

$H_{\mathrm{b}} = H_{\mathrm{hyb}} + H_{\mathrm{bath}}$

Exponential scaling in size of local Hilbert space

P. Werner, A. Comanac, L. de Medici, M. Troyer, and A. J. Millis, Phys. Rev. Lett. 97, 076405 (2006)

Continuous-Time Auxiliary Field

$H_a = H_{\mathrm{bath}} + H_{\mathrm{hyb}} + H^0_{\mathrm{loc}};$

$H_{\mathrm{b}} = H^I_{\mathrm{loc}}$

Efficiency dependent on type of interaction in H^I_{loc}

E. Gull, P. Werner, O. Parcollet, M. Troyer, EPL 82,57003 (2008)

E. Gull, P. Werner, O. Parcollet, M. Troyer, EPL 82,57003 (2008)

Continuous-Time Auxiliary Field impurity solver

Auxiliary field decoupling of interaction term s=±1

$$1 - \frac{\beta U}{K}\left(n_{i\uparrow}n_{i\downarrow} - \frac{n_{i\uparrow}+n_{i\downarrow}}{2}\right) = \frac{1}{2}\sum_{s=\pm 1}\exp\left(\gamma s(n_{i\uparrow}-n_{i\downarrow})\right),$$

$$\cosh(\gamma) = 1 + \frac{U\beta}{2K}.$$

s = 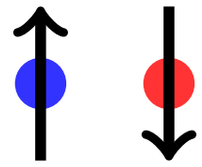

$$Z = \sum_{k=0}^{\infty}\sum_{s_1,\cdots s_k=\pm 1}\int_0^\beta d\tau_1 \cdots \int_{\tau_{k-1}}^\beta d\tau_k \left(\frac{K}{2\beta}\right)^k Z_k(\{s_k,\tau_k\}),$$

Partition function expansion

$$Z_k(\{s_i,\tau_i\}) \equiv \mathrm{Tr}\prod_{i=k}^{1}\exp(-\Delta\tau_i H_0)\exp(s_i\gamma(n_\uparrow - n_\downarrow)).$$

Compute trace of product of exponentials of one-body operators as determinant of matrix.

Stochastic sampling of diagrams of the partition function:

No truncation of expansion!

E. Gull, P. Werner, O. Parcollet, M. Troyer, EPL 82,57003 (2008)

Continuous-Time Auxiliary Field impurity solver

Auxiliary field decoupling of interaction term s=±1

$$1 - \frac{\beta U}{K}\left(n_{i\uparrow}n_{i\downarrow} - \frac{n_{i\uparrow}+n_{i\downarrow}}{2}\right) = \frac{1}{2}\sum_{s=\pm 1}\exp\left(\gamma s(n_{i\uparrow}-n_{i\downarrow})\right),$$

$$\cosh(\gamma) = 1 + \frac{U\beta}{2K}.$$

s =

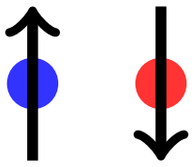

$$Z = \sum_{k=0}^{\infty}\sum_{s_1,\cdots s_k=\pm 1}\int_0^\beta d\tau_1 \cdots \int_{\tau_{k-1}}^\beta d\tau_k \left(\frac{K}{2\beta}\right)^k Z_k(\{s_k,\tau_k\}),$$

Partition function expansion

$$Z_k(\{s_i,\tau_i\}) \equiv \mathrm{Tr}\prod_{i=k}^{1}\exp(-\Delta\tau_i H_0)\exp(s_i\gamma(n_\uparrow - n_\downarrow)).$$

Compute trace of product of exponentials of one-body operators as determinant of matrix.

Stochastic sampling of diagrams of the partition function:

No truncation of expansion!

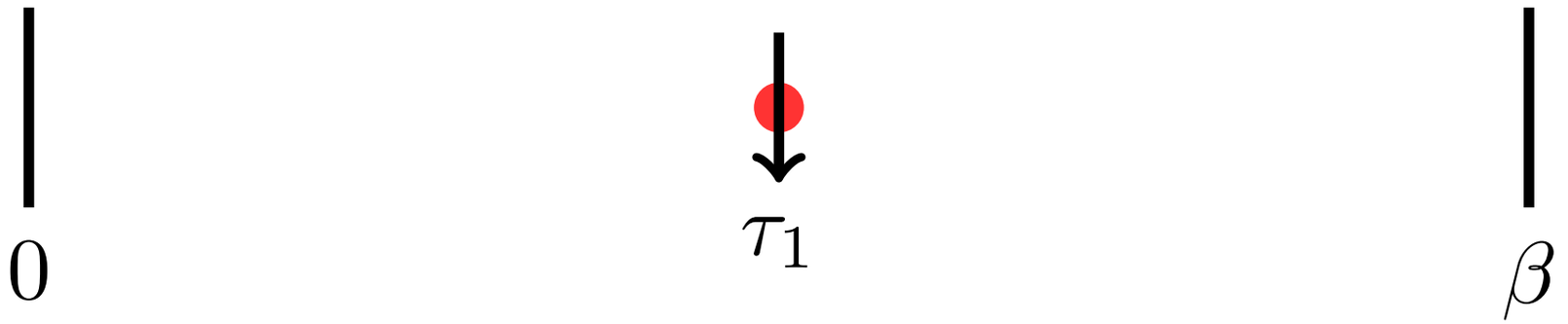

E. Gull, P. Werner, O. Parcollet, M. Troyer, EPL 82,57003 (2008)

Continuous-Time Auxiliary Field impurity solver

Auxiliary field decoupling of interaction term s=±1

$$1 - \frac{\beta U}{K}\left(n_{i\uparrow}n_{i\downarrow} - \frac{n_{i\uparrow}+n_{i\downarrow}}{2}\right) = \frac{1}{2}\sum_{s=\pm 1}\exp\left(\gamma s(n_{i\uparrow}-n_{i\downarrow})\right),$$

$$\cosh(\gamma) = 1 + \frac{U\beta}{2K}.$$

s =

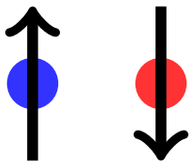

$$Z = \sum_{k=0}^{\infty}\sum_{s_1,\cdots s_k=\pm 1}\int_0^\beta d\tau_1 \cdots \int_{\tau_{k-1}}^\beta d\tau_k \left(\frac{K}{2\beta}\right)^k Z_k(\{s_k,\tau_k\}),$$

Partition function expansion

$$Z_k(\{s_i,\tau_i\}) \equiv \mathrm{Tr}\prod_{i=k}^{1}\exp(-\Delta\tau_i H_0)\exp(s_i\gamma(n_\uparrow - n_\downarrow)).$$

Compute trace of product of exponentials of one-body operators as determinant of matrix.

Stochastic sampling of diagrams of the partition function:

No truncation of expansion!

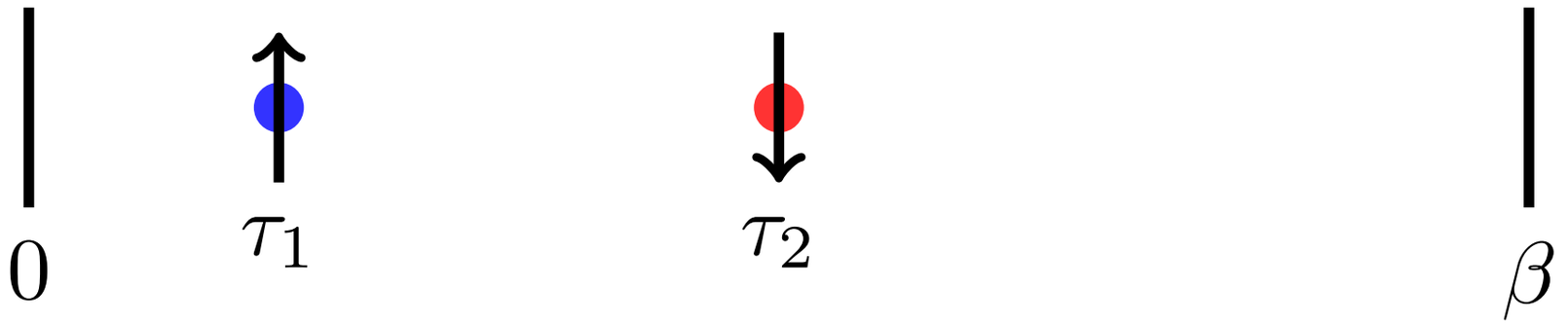

E. Gull, P. Werner, O. Parcollet, M. Troyer, EPL 82,57003 (2008)

Continuous-Time Auxiliary Field impurity solver

Auxiliary field decoupling of interaction term s=±1

$$1 - \frac{\beta U}{K}\left(n_{i\uparrow}n_{i\downarrow} - \frac{n_{i\uparrow}+n_{i\downarrow}}{2}\right) = \frac{1}{2}\sum_{s=\pm 1}\exp\left(\gamma s(n_{i\uparrow}-n_{i\downarrow})\right),$$

$$\cosh(\gamma) = 1 + \frac{U\beta}{2K}.$$

s =

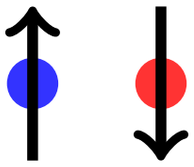

$$Z = \sum_{k=0}^{\infty}\sum_{s_1,\cdots s_k=\pm 1}\int_0^\beta d\tau_1 \cdots \int_{\tau_{k-1}}^\beta d\tau_k \left(\frac{K}{2\beta}\right)^k Z_k(\{s_k,\tau_k\}),$$

Partition function expansion

$$Z_k(\{s_i,\tau_i\}) \equiv \mathrm{Tr}\prod_{i=k}^{1}\exp(-\Delta\tau_i H_0)\exp(s_i\gamma(n_\uparrow - n_\downarrow)).$$

Compute trace of product of exponentials of one-body operators as determinant of matrix.

Stochastic sampling of diagrams of the partition function:

No truncation of expansion!

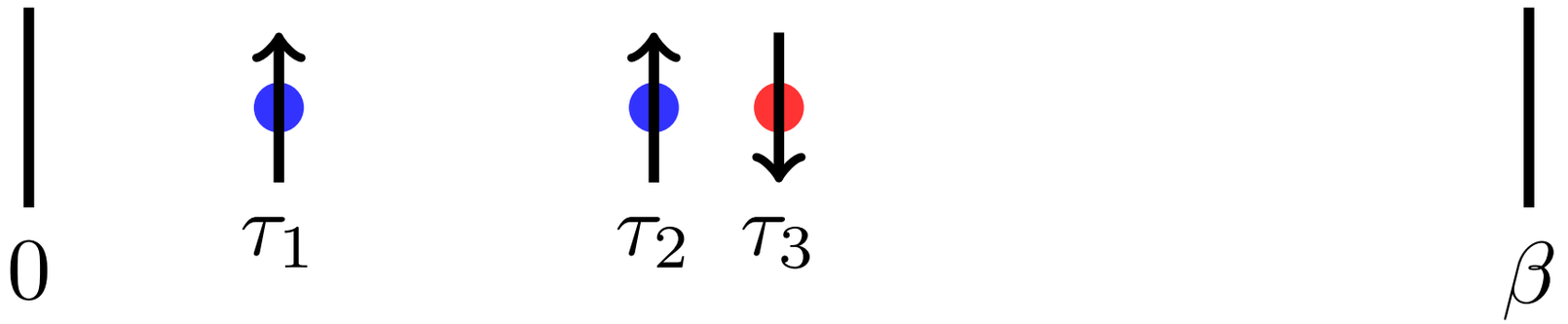

E. Gull, P. Werner, O. Parcollet, M. Troyer, EPL 82,57003 (2008)

Continuous-Time Auxiliary Field impurity solver

Auxiliary field decoupling of interaction term s=±1

$$1 - \frac{\beta U}{K}\left(n_{i\uparrow}n_{i\downarrow} - \frac{n_{i\uparrow}+n_{i\downarrow}}{2}\right) = \frac{1}{2}\sum_{s=\pm 1}\exp\left(\gamma s(n_{i\uparrow}-n_{i\downarrow})\right),$$

$$\cosh(\gamma) = 1 + \frac{U\beta}{2K}.$$

s =

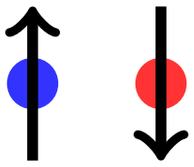

$$Z = \sum_{k=0}^{\infty}\sum_{s_1,\cdots s_k=\pm 1}\int_0^\beta d\tau_1 \cdots \int_{\tau_{k-1}}^\beta d\tau_k \left(\frac{K}{2\beta}\right)^k Z_k(\{s_k,\tau_k\}),$$

Partition function expansion

$$Z_k(\{s_i,\tau_i\}) \equiv \mathrm{Tr}\prod_{i=k}^{1}\exp(-\Delta\tau_i H_0)\exp(s_i\gamma(n_\uparrow - n_\downarrow)).$$

Compute trace of product of exponentials of one-body operators as determinant of matrix.

Stochastic sampling of diagrams of the partition function:

No truncation of expansion!

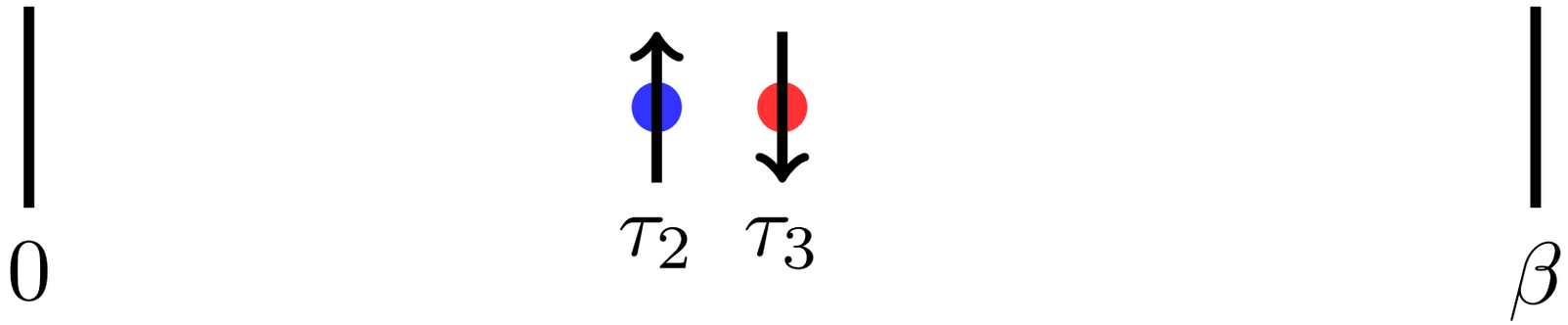

E. Gull, P. Werner, O. Parcollet, M. Troyer, EPL 82,57003 (2008)

Continuous-Time Auxiliary Field impurity solver

Auxiliary field decoupling of interaction term s=±1

$$1 - \frac{\beta U}{K}\left(n_{i\uparrow}n_{i\downarrow} - \frac{n_{i\uparrow}+n_{i\downarrow}}{2}\right) = \frac{1}{2}\sum_{s=\pm 1}\exp\left(\gamma s(n_{i\uparrow}-n_{i\downarrow})\right),$$

$$\cosh(\gamma) = 1 + \frac{U\beta}{2K}.$$

s =

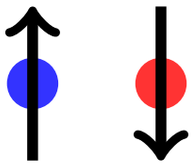

$$Z = \sum_{k=0}^{\infty}\sum_{s_1,\cdots s_k=\pm 1}\int_0^\beta d\tau_1 \cdots \int_{\tau_{k-1}}^\beta d\tau_k \left(\frac{K}{2\beta}\right)^k Z_k(\{s_k,\tau_k\}),$$

Partition function expansion

$$Z_k(\{s_i,\tau_i\}) \equiv \mathrm{Tr}\prod_{i=k}^{1}\exp(-\Delta\tau_i H_0)\exp(s_i\gamma(n_\uparrow - n_\downarrow)).$$

Compute trace of product of exponentials of one-body operators as determinant of matrix.

Stochastic sampling of diagrams of the partition function:

No truncation of expansion!

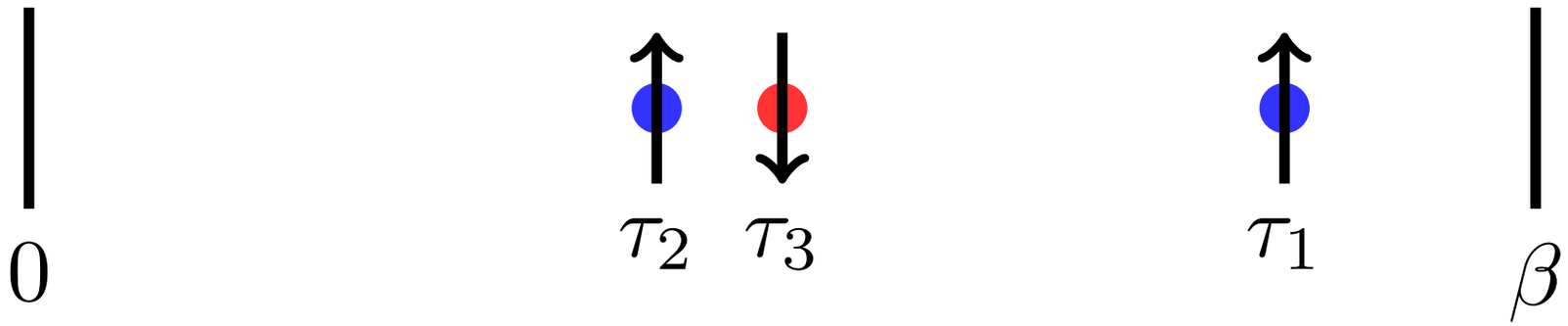

E. Gull, P. Werner, O. Parcollet, M. Troyer, EPL 82,57003 (2008)

Continuous-Time Auxiliary Field impurity solver

Auxiliary field decoupling of interaction term s=±1

$$1 - \frac{\beta U}{K}\left(n_{i\uparrow}n_{i\downarrow} - \frac{n_{i\uparrow}+n_{i\downarrow}}{2}\right) = \frac{1}{2}\sum_{s=\pm 1}\exp\left(\gamma s(n_{i\uparrow}-n_{i\downarrow})\right),$$

$$\cosh(\gamma) = 1 + \frac{U\beta}{2K}.$$

s =

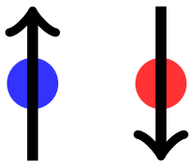

$$Z = \sum_{k=0}^{\infty}\sum_{s_1,\cdots s_k=\pm 1}\int_0^\beta d\tau_1 \cdots \int_{\tau_{k-1}}^\beta d\tau_k \left(\frac{K}{2\beta}\right)^k Z_k(\{s_k,\tau_k\}),$$

Partition function expansion

$$Z_k(\{s_i,\tau_i\}) \equiv \mathrm{Tr}\prod_{i=k}^{1}\exp(-\Delta\tau_i H_0)\exp(s_i\gamma(n_\uparrow - n_\downarrow)).$$

Compute trace of product of exponentials of one-body operators as determinant of matrix.

Stochastic sampling of diagrams of the partition function:

No truncation of expansion!

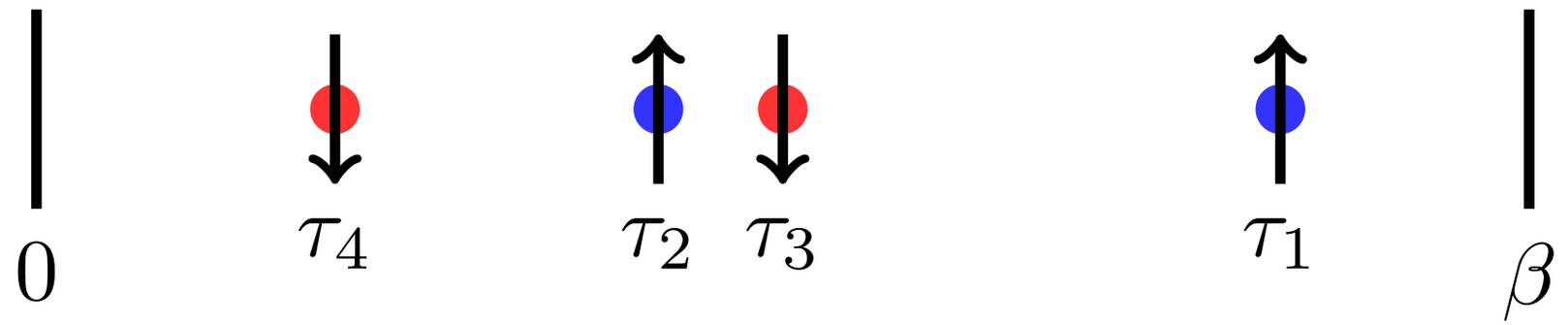

E. Gull, P. Werner, O. Parcollet, M. Troyer, EPL 82,57003 (2008)

Continuous-Time Auxiliary Field impurity solver

Auxiliary field decoupling of interaction term s=±1

$$1 - \frac{\beta U}{K}\left(n_{i\uparrow}n_{i\downarrow} - \frac{n_{i\uparrow}+n_{i\downarrow}}{2}\right) = \frac{1}{2}\sum_{s=\pm 1}\exp\left(\gamma s(n_{i\uparrow}-n_{i\downarrow})\right),$$

$$\cosh(\gamma) = 1 + \frac{U\beta}{2K}.$$

s =

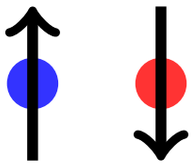

$$Z = \sum_{k=0}^{\infty}\sum_{s_1,\cdots s_k=\pm 1}\int_0^\beta d\tau_1 \cdots \int_{\tau_{k-1}}^\beta d\tau_k \left(\frac{K}{2\beta}\right)^k Z_k(\{s_k,\tau_k\}),$$

Partition function expansion

$$Z_k(\{s_i,\tau_i\}) \equiv \mathrm{Tr}\prod_{i=k}^{1}\exp(-\Delta\tau_i H_0)\exp(s_i\gamma(n_\uparrow - n_\downarrow)).$$

Compute trace of product of exponentials of one-body operators as determinant of matrix.

Stochastic sampling of diagrams of the partition function:

No truncation of expansion!

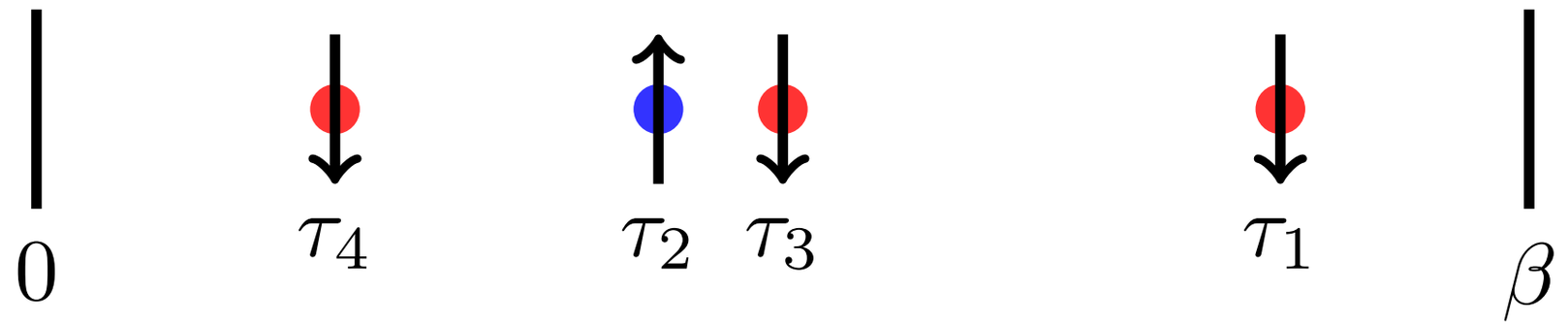

E. Gull, P. Werner, O. Parcollet, M. Troyer, EPL 82,57003 (2008)

Continuous-Time Auxiliary Field impurity solver

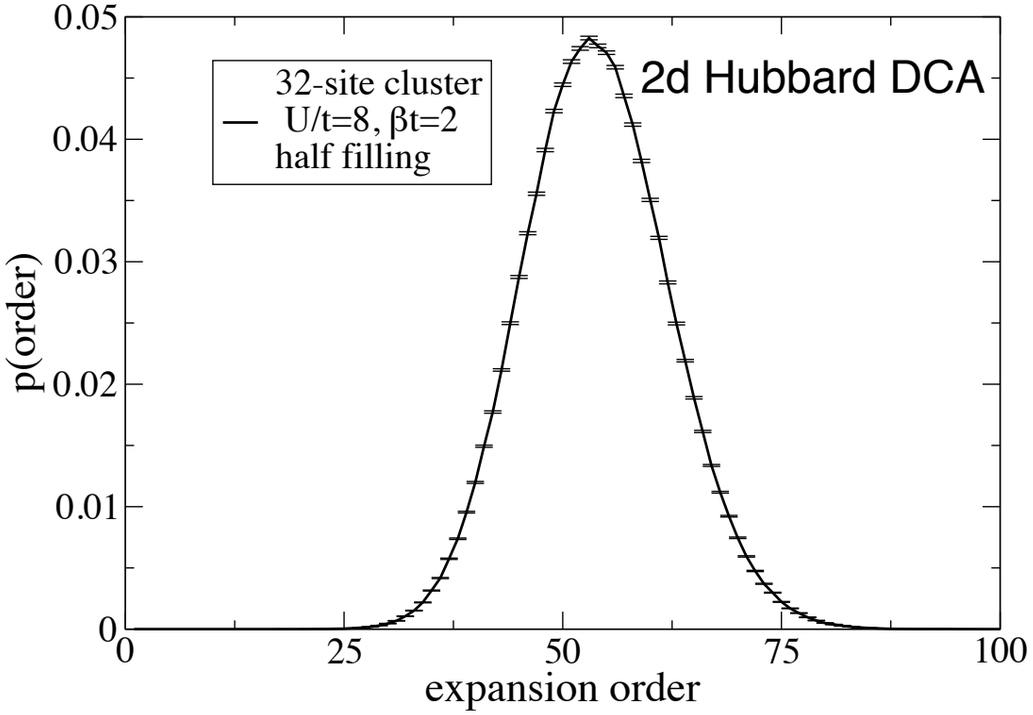

Expansion order

Average expansion order as a function of interaction

Average expansion order as a function of inverse temperature

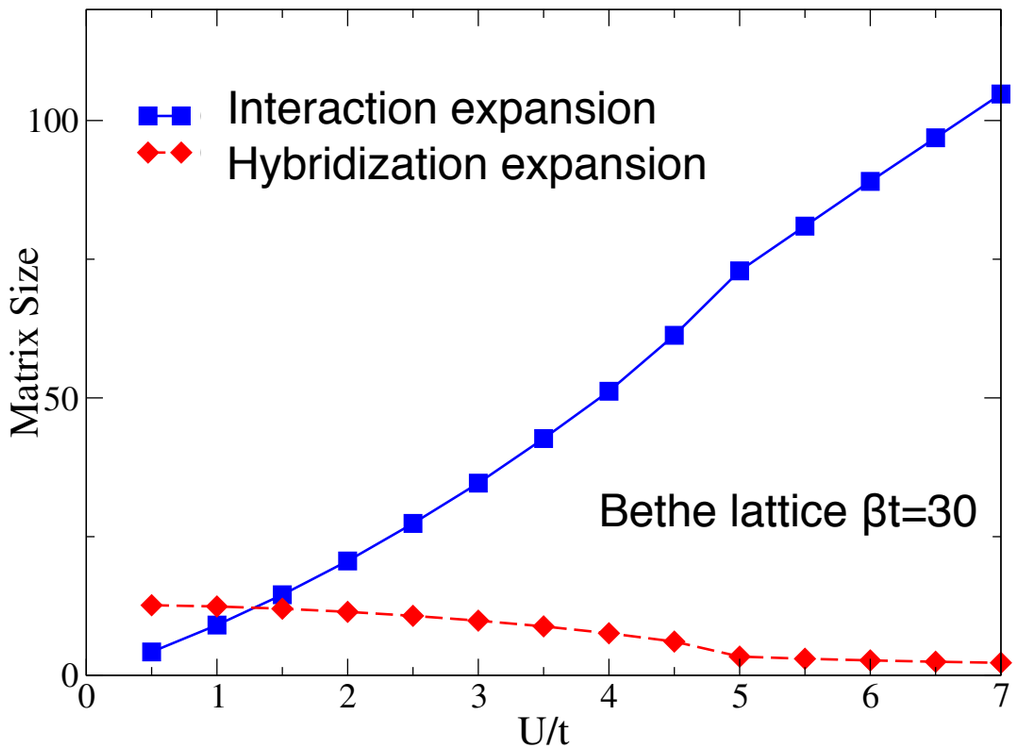

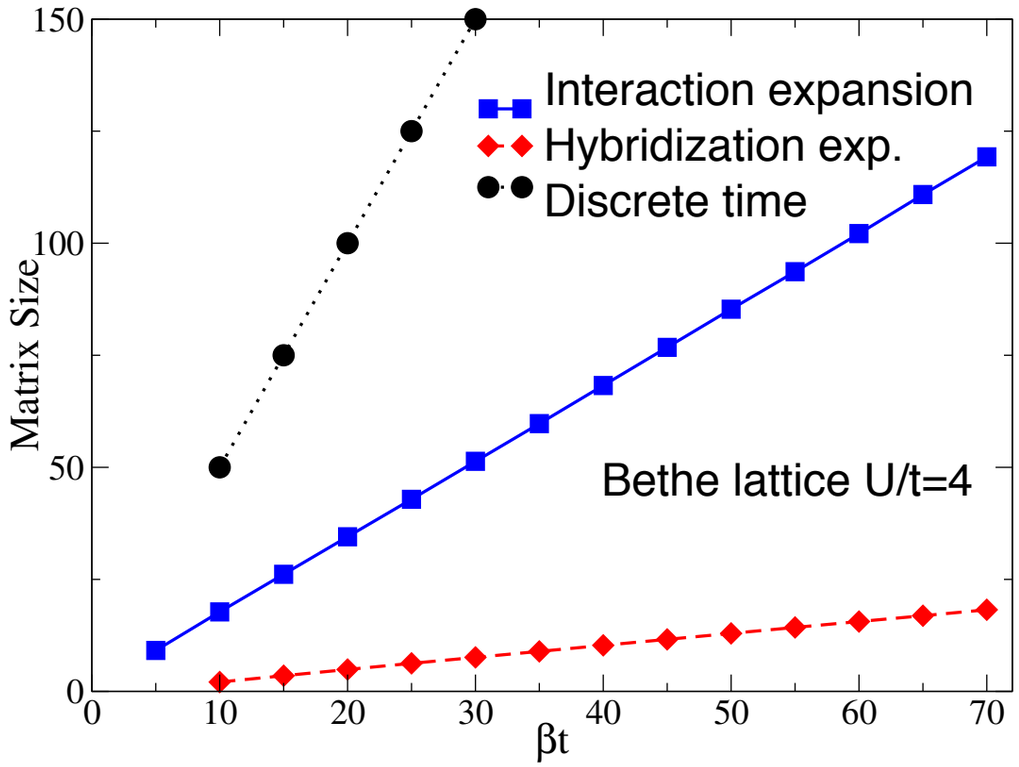

E. Gull, P. Staar, S. Fuchs, P. Nukala, M. Summers, T. Pruschke, T.C. Schulthess, T. Maier, Phys. Rev. B 83, 075122 (2011)

Sub-Matrix updates

Standard updates in auxiliary field impurity solvers: rank one operations (ger), $O(N^2)$ operations for $O(N^2)$ data: dominated by data access.

$$N'_{ij} \leftarrow N_{ij} + (G_{ip} - \delta_{ip})\lambda_p \times N_{pj}$$

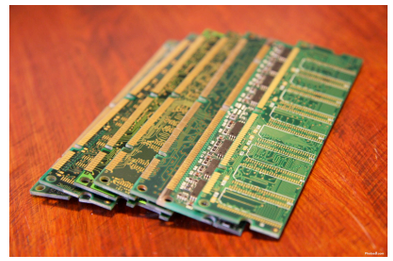

Sub-Matrix updates: based on matrix (gemm) operations: $O(N^3)$ operations on $O(N^2)$ data: runs at speed of (fast) CPU/Cache.

$$N_{ij}^{q+1} \leftarrow D_i^{-1} (N_{ij}^q - G_{ip_k}^q \times \Gamma_{p_k p_l}^{-1} \times N_{p_l j})$$

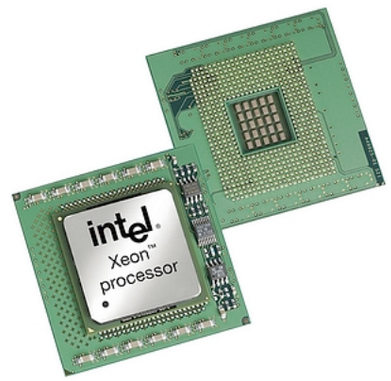

Linear algebra reformulated, overhead grows with size of Γ but operations 10x faster

E. Gull, P. Staar, S. Fuchs, P. Nukala, M. Summers, T. Pruschke, T.C. Schulthess, T. Maier, Phys. Rev. B 83, 075122 (2011)

Sub-Matrix updates

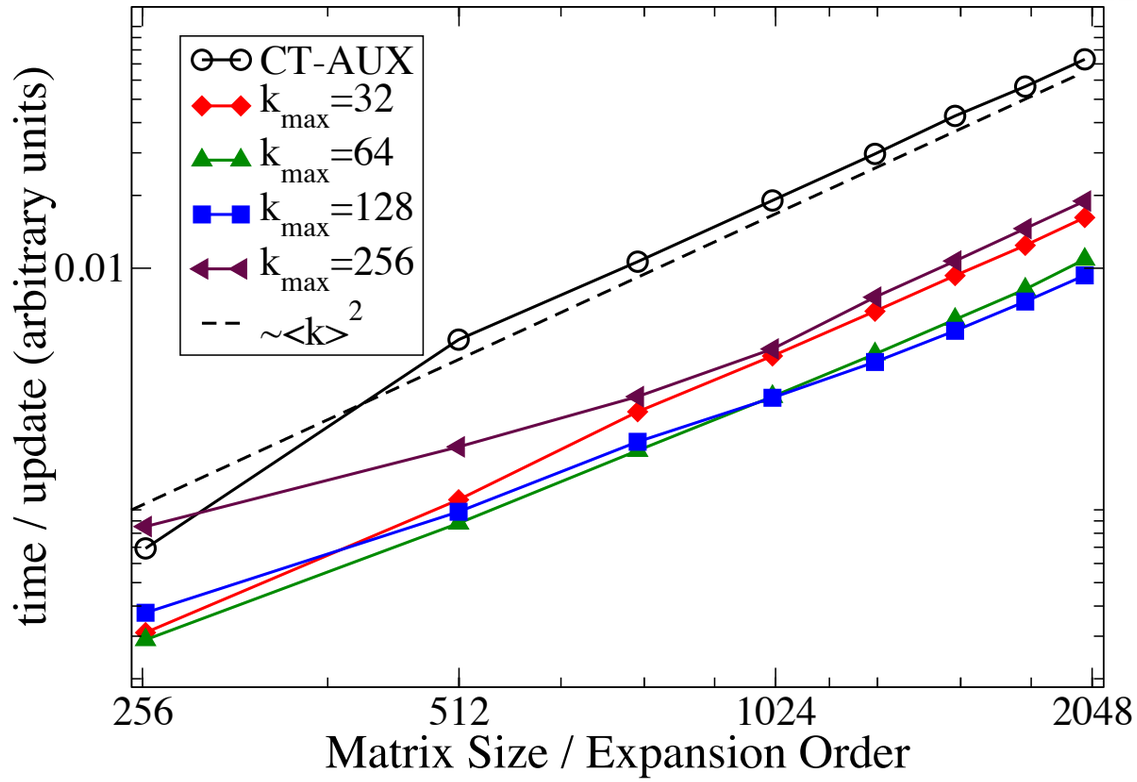

Scaling as a function of problem size

Scaling as a function of # of CPUs (single particle measurements)

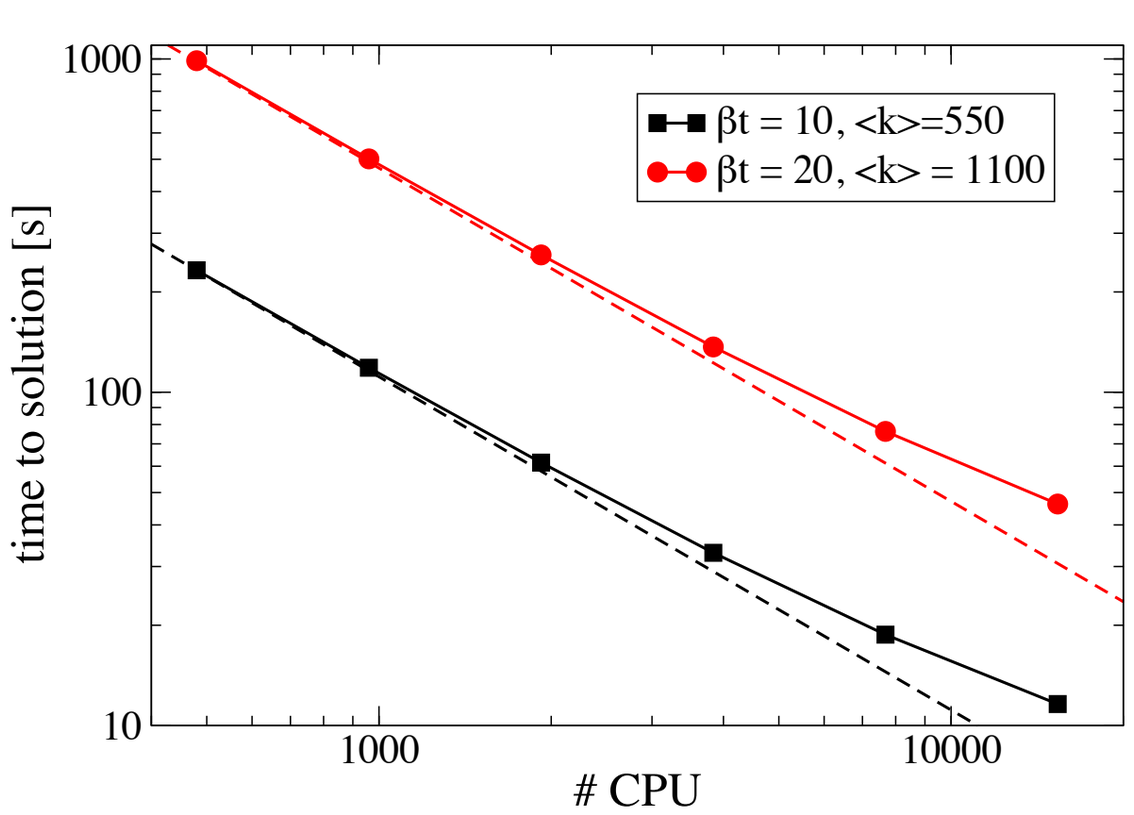

See also talk by Lode Pollet, L45.00011 (Tuesday)

Phys. Rev. Lett. 106, 030401 (2011)

Intermezzo: 3D Hubbard Model

‘Optical Lattice Emulator’: Goal is to experimentally simulate simple model Hamiltonians using cold atomic (fermionic) gases

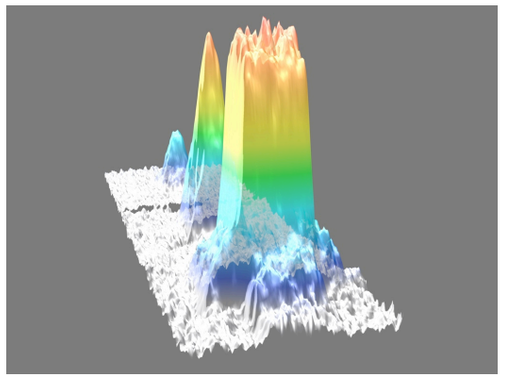

T. Esslinger, Annu. Rev. Condens. Matter Phys. 1, 129-152 (2010)

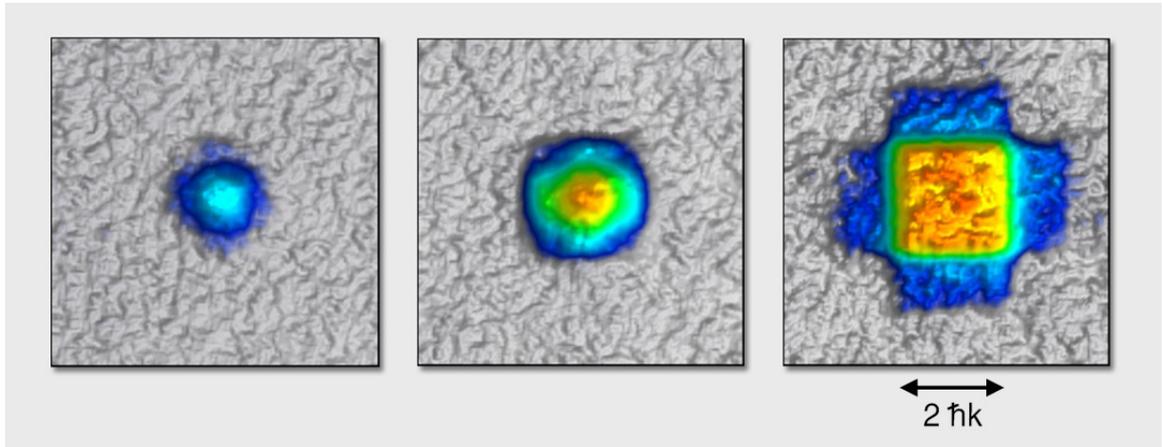

Test model: 3D Hubbard

$$H = -\sum_{\langle ij\rangle,\sigma} t_{ij}(c^{\dagger}_{i\sigma}c_{j\sigma} + c^{\dagger}_{j\sigma}c_{i\sigma}) + U\sum_{i} n_{i\uparrow}n_{i\downarrow}.$$

Temperatures in experiment are high (for now).

Phys. Rev. Lett. 106, 030401 (2011)

Questions to theory

When will we reach T_N?

What is the equation of state of this model? (for all fillings, as a function of U/t and T/t?)

Exact answer needed.

Phys. Rev. Lett. 106, 030401 (2011)

Controlling DCA

Solve quantum impurity model self-consistently for a range of cluster sizes:

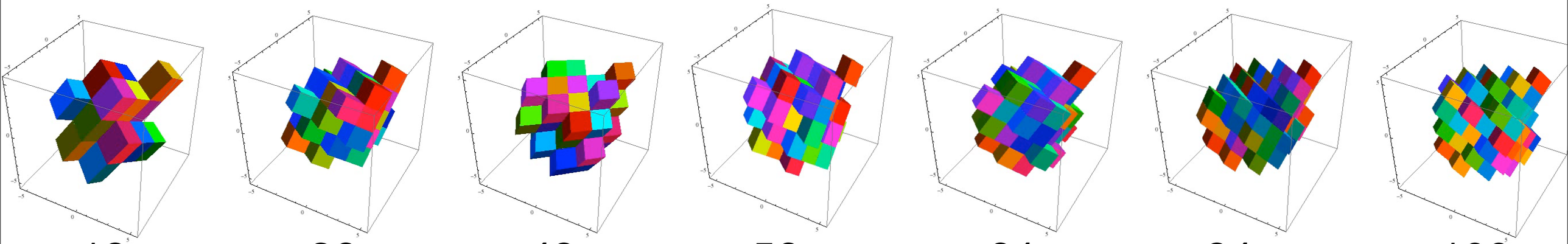

18 36 48 56 64 84 100

Compute thermodynamics: energy, density, entropy, free energy, double occupancy, spin correlation functions, …: Observable estimates and errors for a finite size system.

Extrapolate observable estimate to the infinite system size limit using known finite size scaling

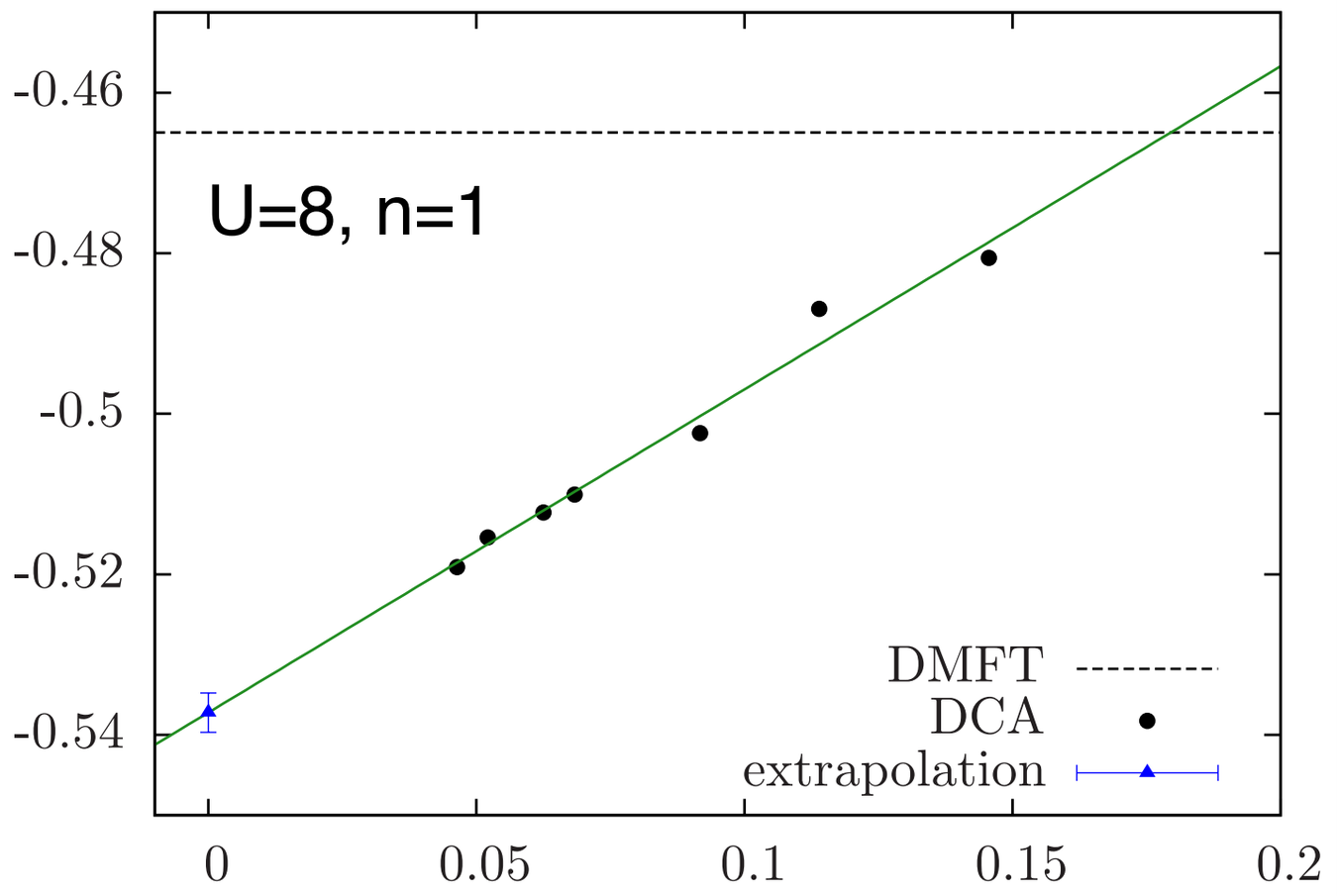

Fine size scaling behavior: Maier, Jarrell, Phys. Rev. B 65, 041104(R) (2002)

Phys. Rev. Lett. 106, 030401 (2011)

Controlling DCA

Validation against lattice QMC (1/2 filling) and HTSE (high T)

Comparison HTSE / DCA?
(6^{th} , 8^{th} ,10^{th} order)

HTSE order by order convergence: at U=8 correct down to T ~ 1.6t (at half filling). Worse away from half filling.

Agreement of 10th order HTSE with DCA down to T~1.4t.

Agreement with lattice QMC within error bars with for all T

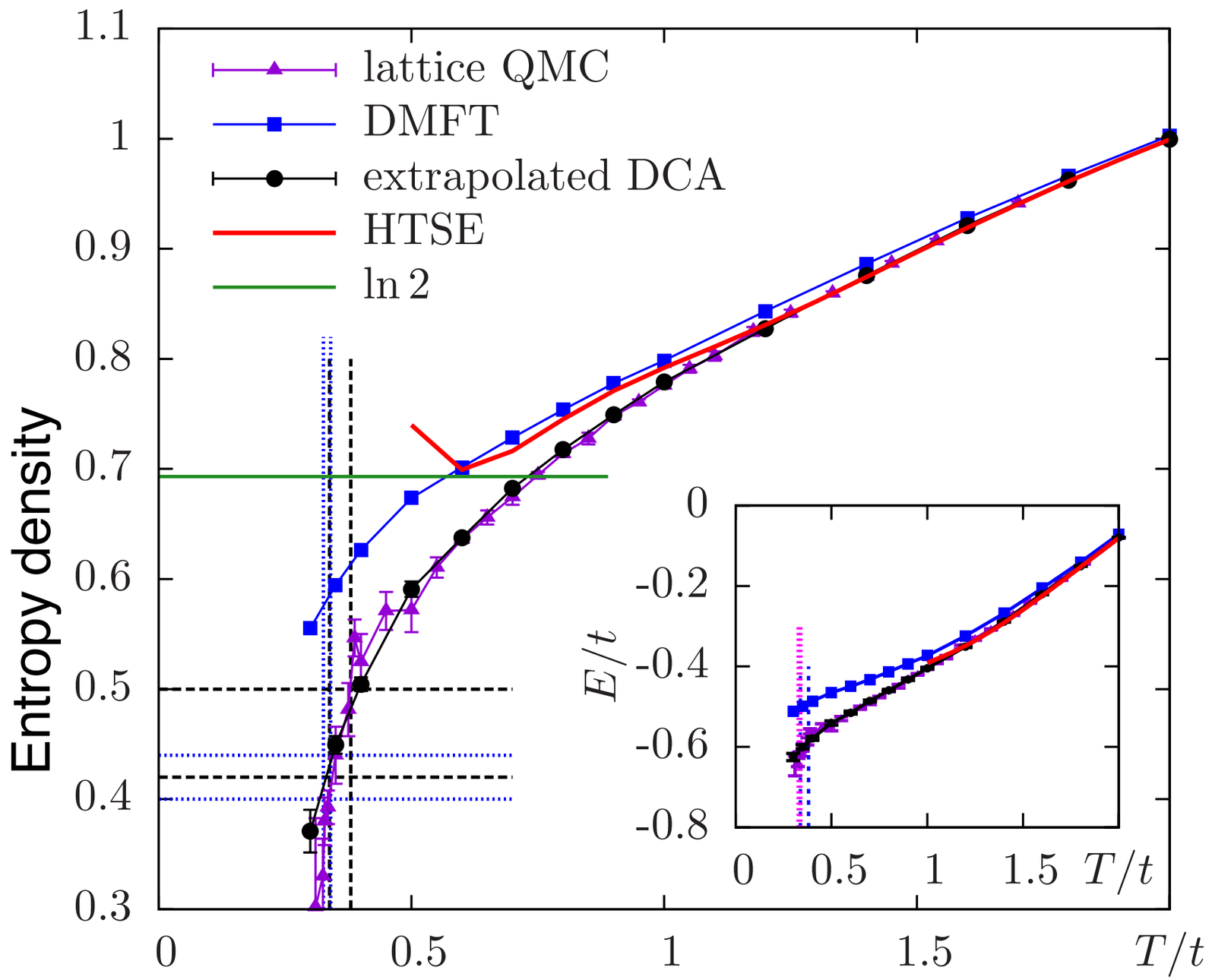

See also: in depth analysis of HTSE & DMFT by L. De Leo, J.S. Bernier, C. Kollath, A. Georges, V. W. Scarola, Phys. Rev. A 83, 023606 (2011)

Phys. Rev. Lett. 106, 030401 (2011)

Controlling DCA

How well does single site DMFT work?
(Single Site, PM self consistency)

First deviations at half filling are visible at
T ~ 1.6t [AFM T_N at ~0.5t]

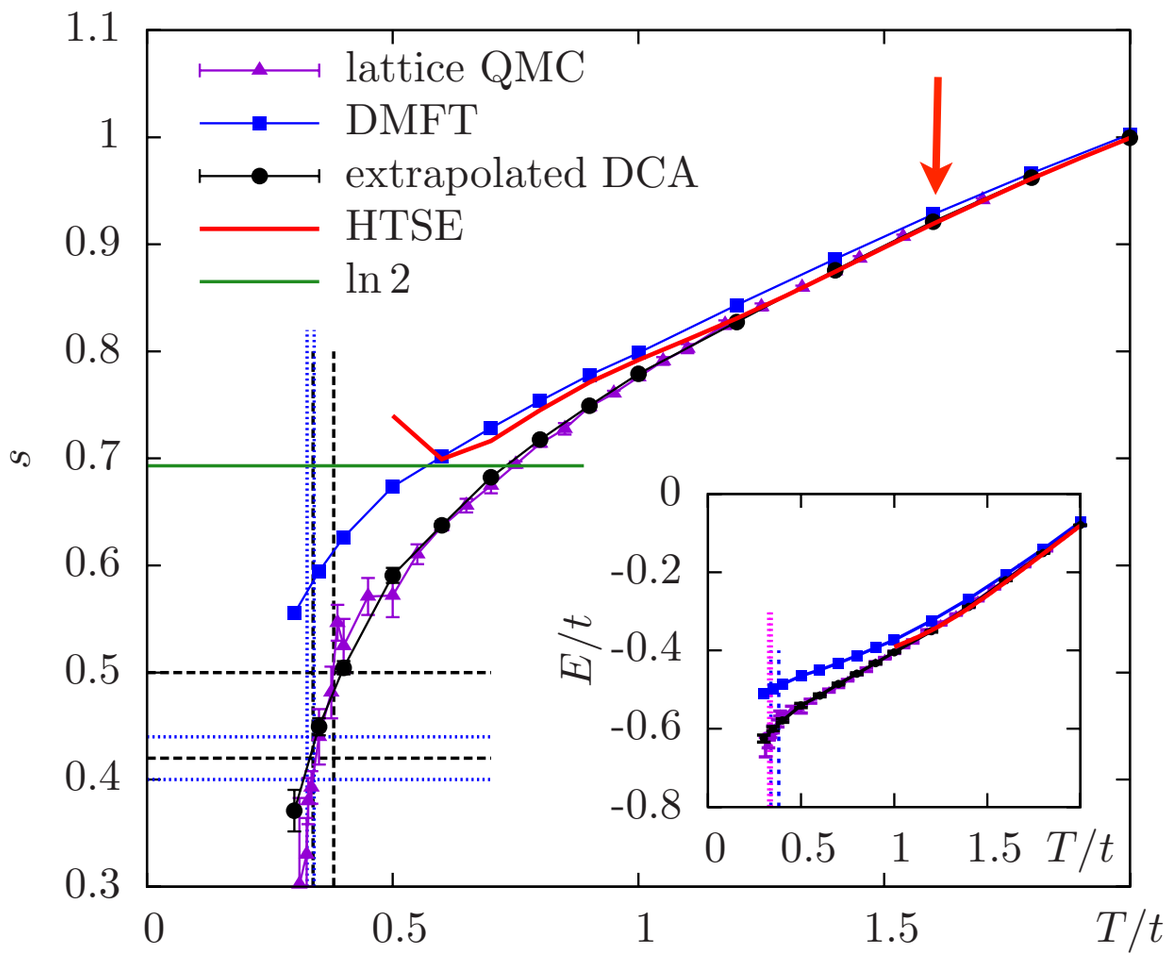

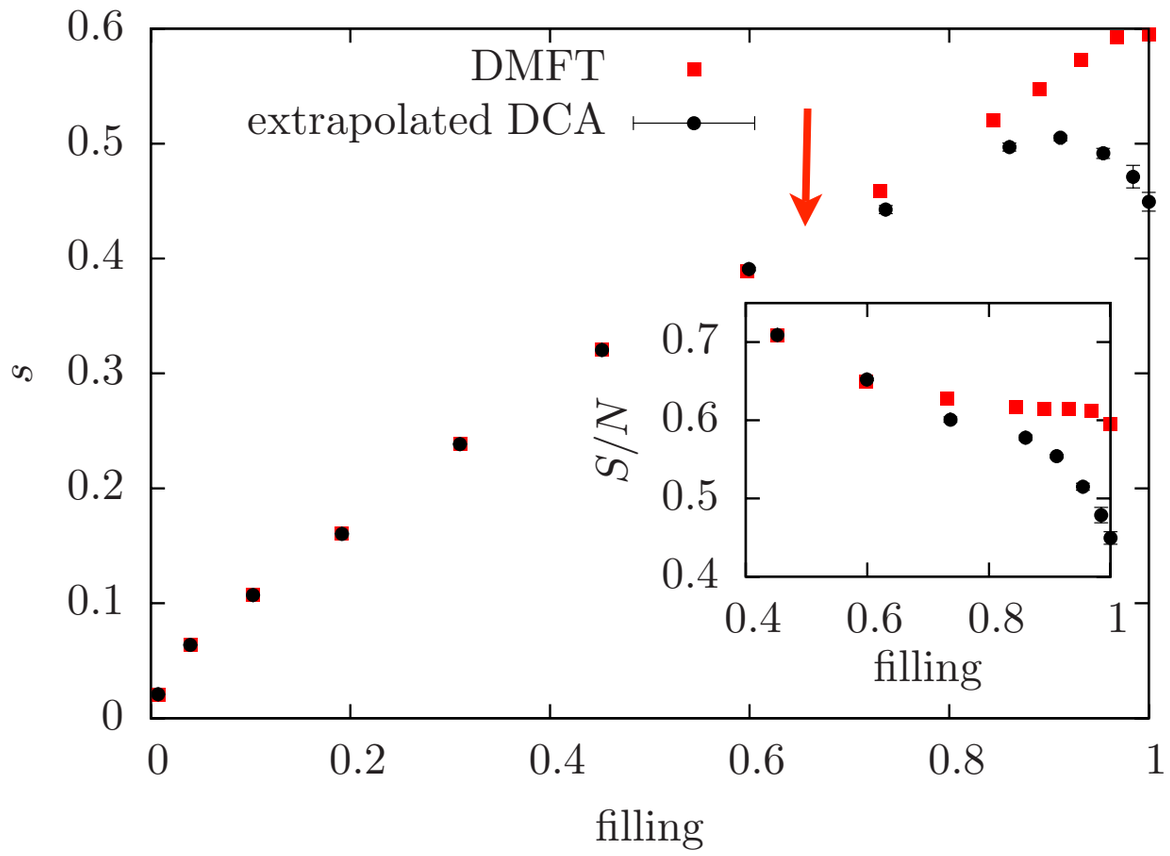

Away from half filling, for n ≤ 0.7: same behavior as in 2D; DMFT is essentially exact, no momentum dependence of the self energy:

$$\Sigma(k,\omega) = \sum_n \Sigma_n(\omega)\phi_n(k) = \Sigma_{\mathrm{DMFT}}(\omega)$$

n < 0.7

Phys. Rev. Lett. 106, 030401 (2011)

Controlling DCA

Solve quantum impurity model self-consistently for a range of cluster sizes:

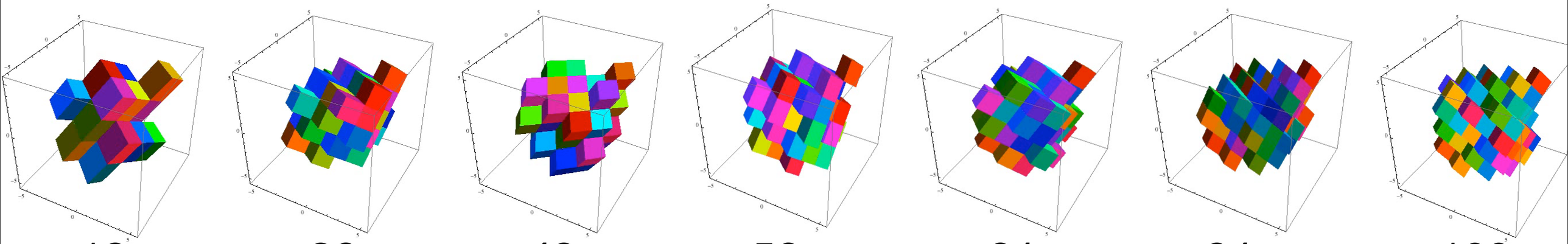

18 36 48 56 64 84 100

Compute thermodynamics: energy, density, entropy, free energy, double occupancy, spin correlation functions, …: Observable estimates and errors for a finite size system.

Extrapolate observable estimate to the infinite system size limit using known finite size scaling

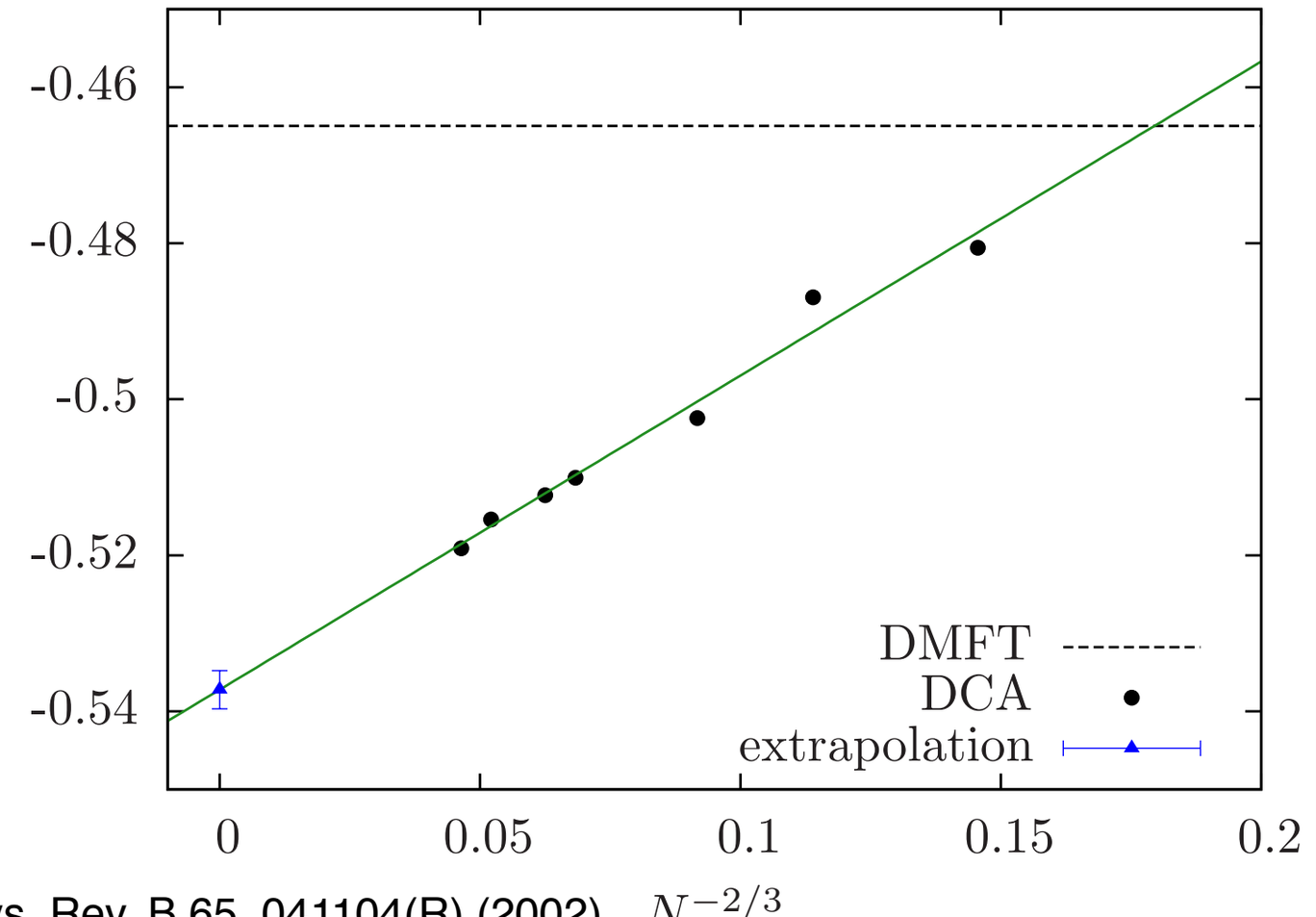

Fine size scaling behavior: Maier, Jarrell, Phys. Rev. B 65, 041104(R) (2002)

Phys. Rev. Lett. 106, 030401 (2011)

Controlling DCA

Solve quantum impurity model self-consistently for a range of cluster sizes:

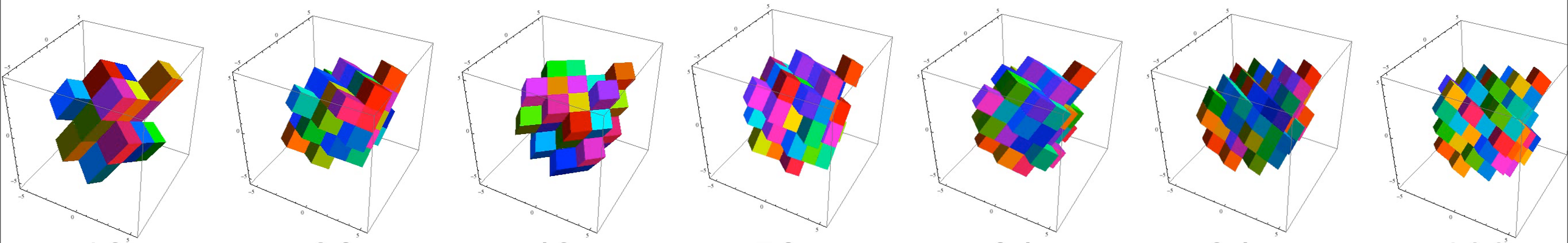

18 36 48 56 64 84 100

Compute thermodynamics: energy, density, entropy, free[illegible], double occupancy, correlation functions, …: Obs[illegible] and errors for a fini[illegible]

Results for finite clusters without extrapolations are not accurate!

Extrapolate observable estimate to the infinite system size limit using known finite size scaling

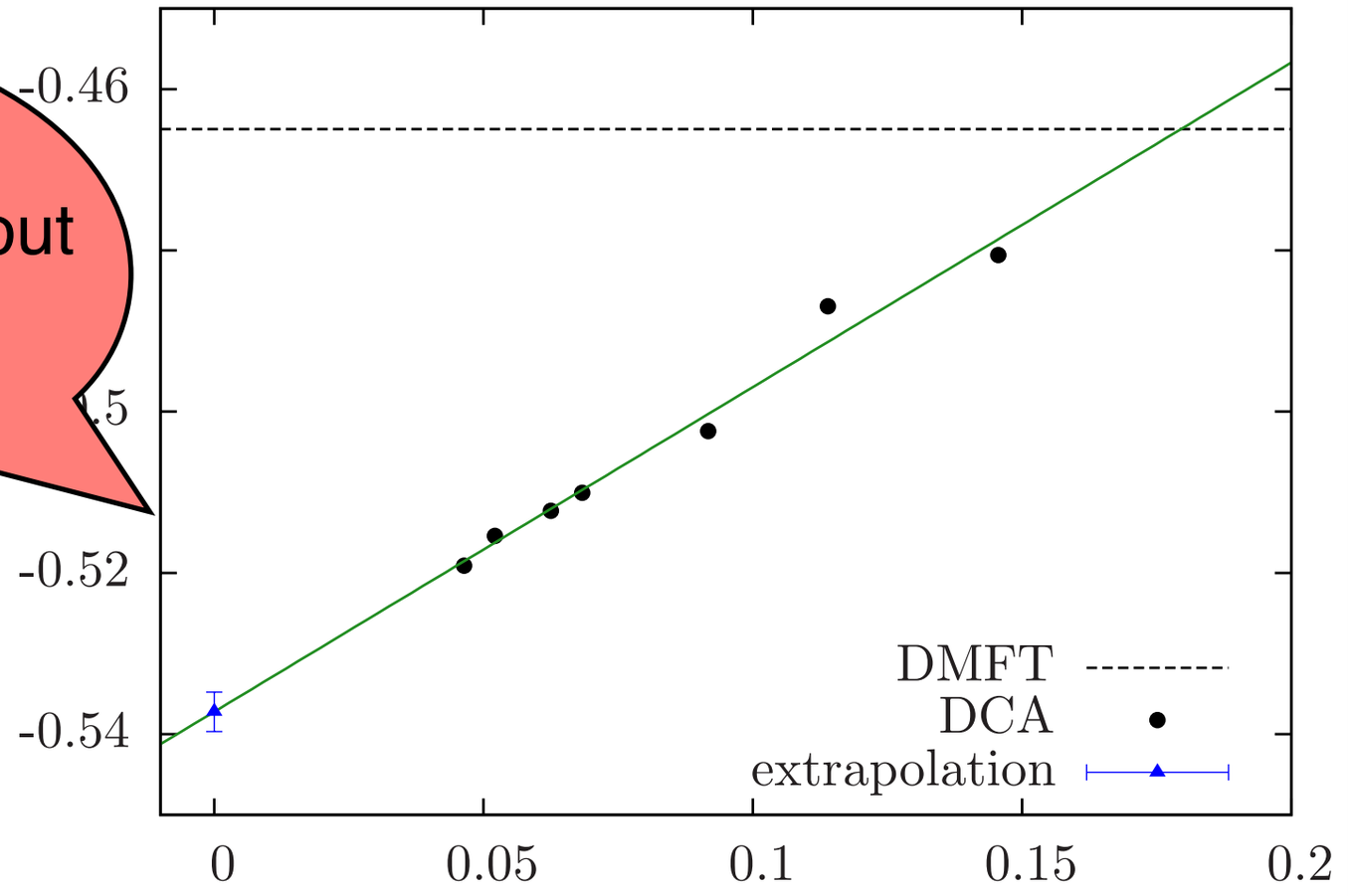

Fine size scaling behavior: Maier, Jarrell, Phys. Rev. B 65, 041104(R) (2002)

Phys. Rev. Lett. 106, 030401 (2011)

Controlling DCA

Solve quantum impurity model self-consistently for a range of cluster sizes:

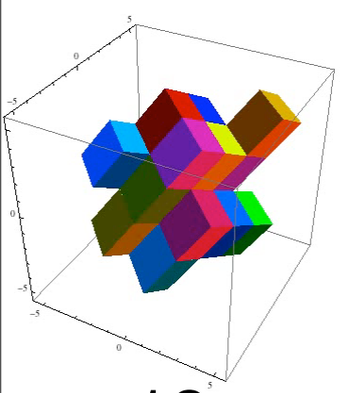
18

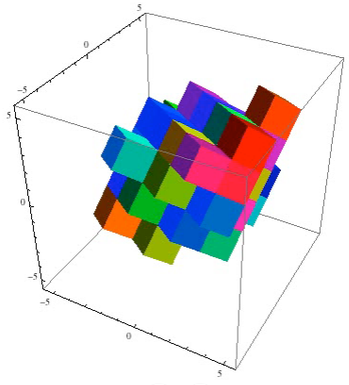
36

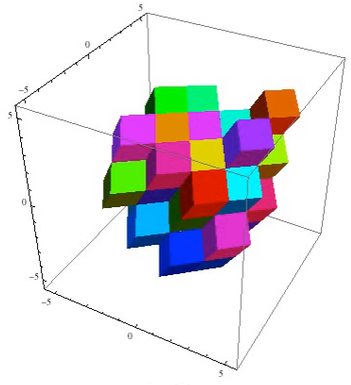
48

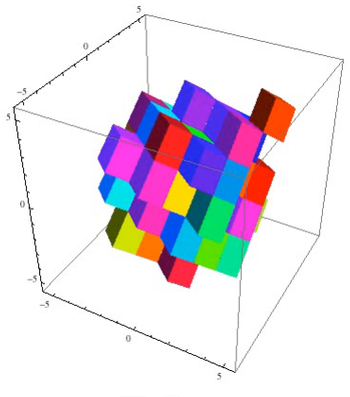
56

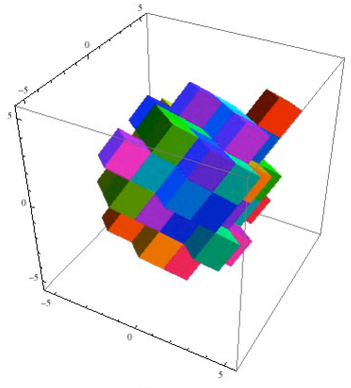
64

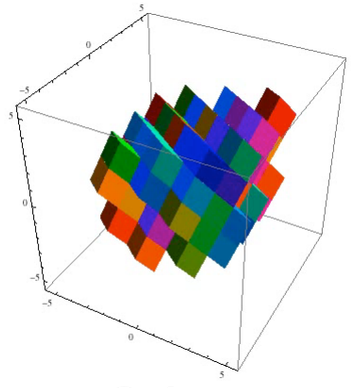
84

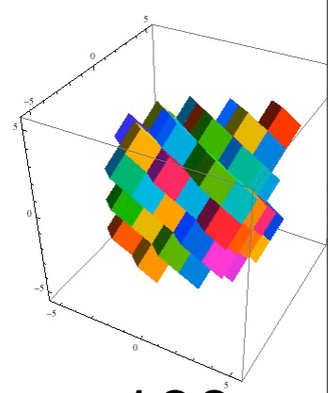
100

Compute thermodynamics: energy density, entropy, free energy, double occupancy, spin correla functions, …: Observable estima and errors for a finite size system.

Finite Size Scaling can be done controlled and with high accuracy

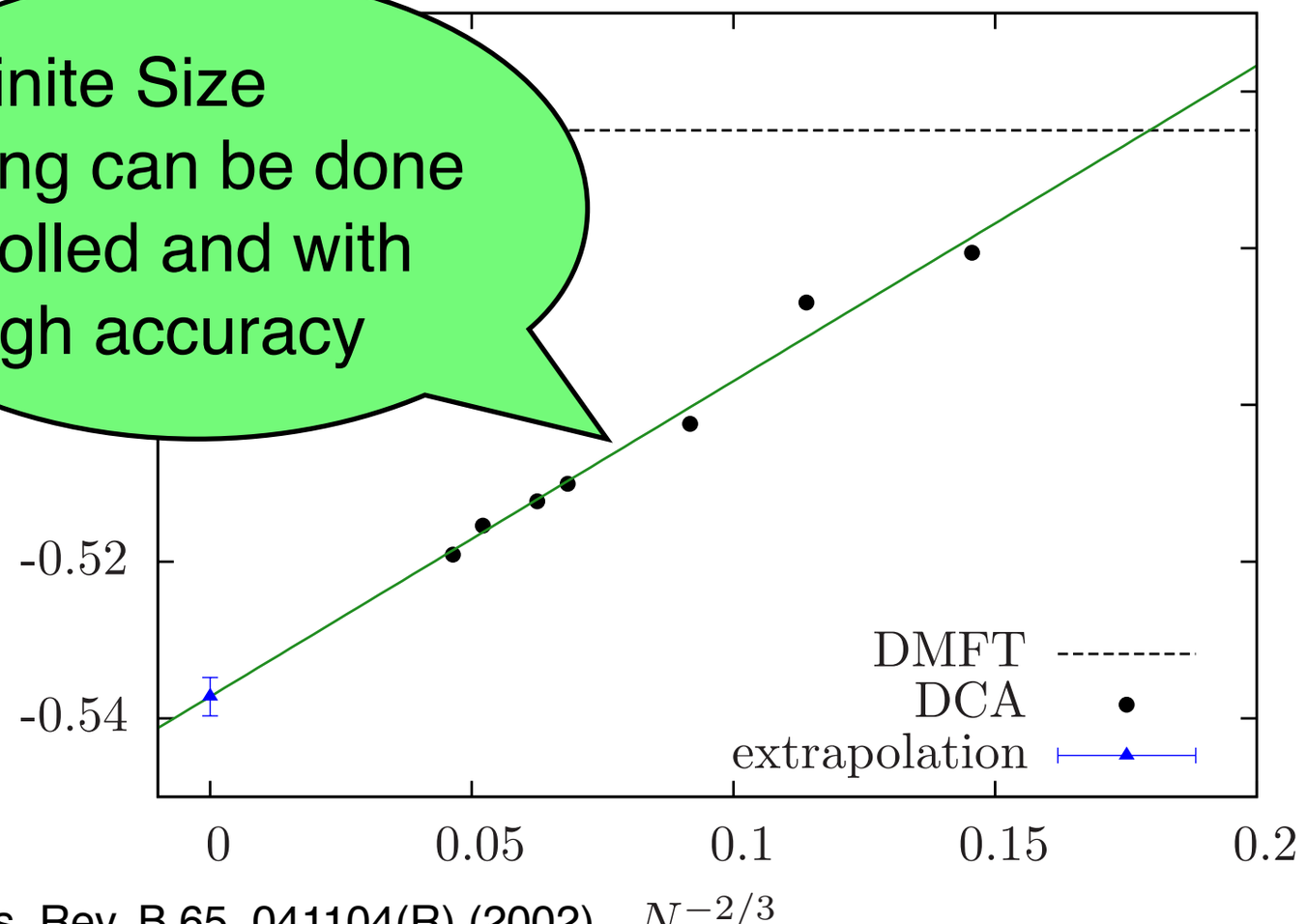

Extrapolate observable estimate to the infinite system size limit using known finite size scaling

Fine size scaling behavior: Maier, Jarrell, Phys. Rev. B 65, 041104(R) (2002)

Phys. Rev. Lett. 106, 030401 (2011)

Controlling DCA

k-dependence of the self energy systematically reintroduced, convergence for self energy observed: Approximation controlled

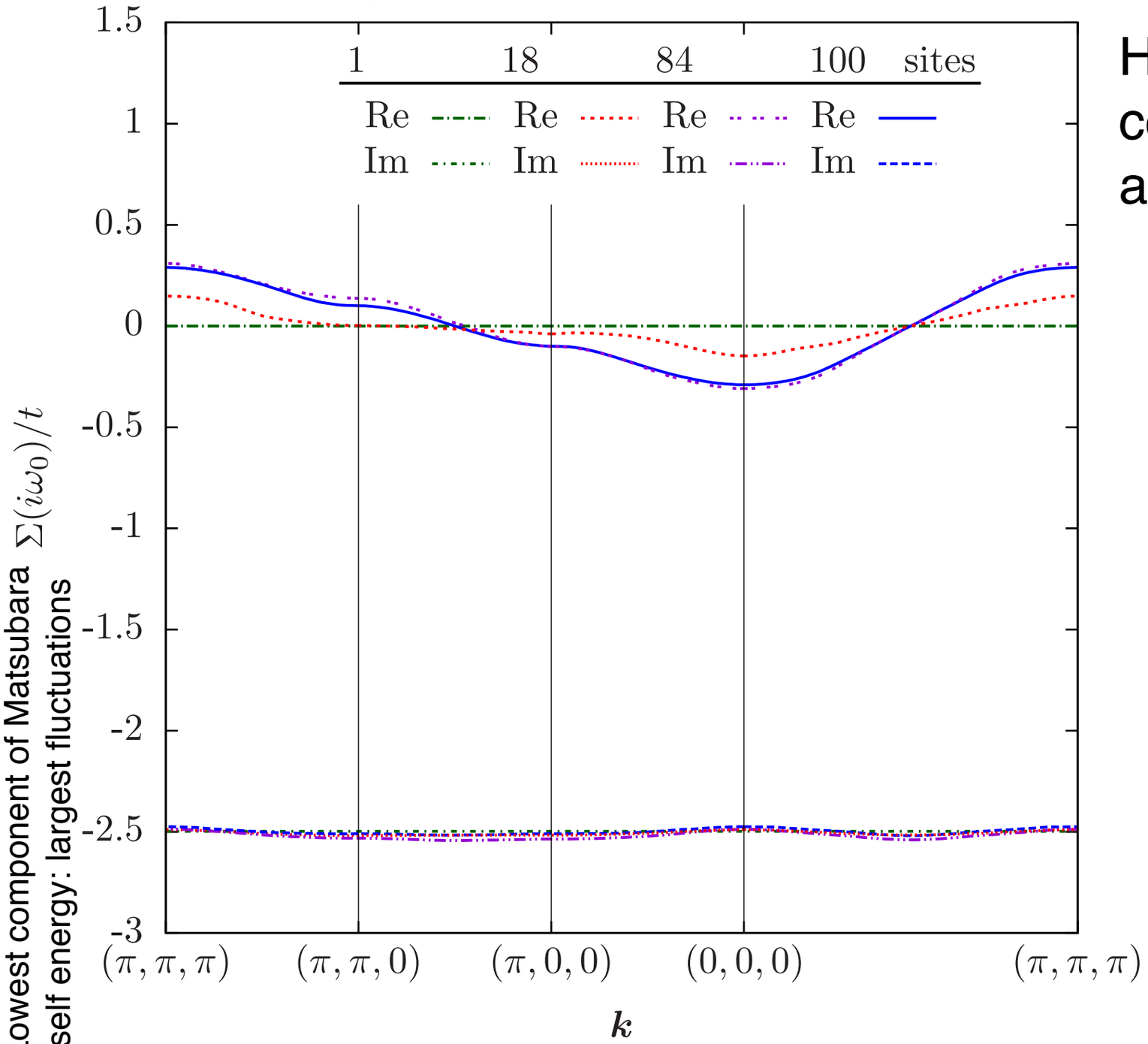

High temperature T/t = 1: Exact convergence of the self energy as a function of cluster size.

Phys. Rev. Lett. 106, 030401 (2011)

Controlling DCA

k-dependence of the self energy systematically reintroduced, convergence for self energy observed: Approximation controlled

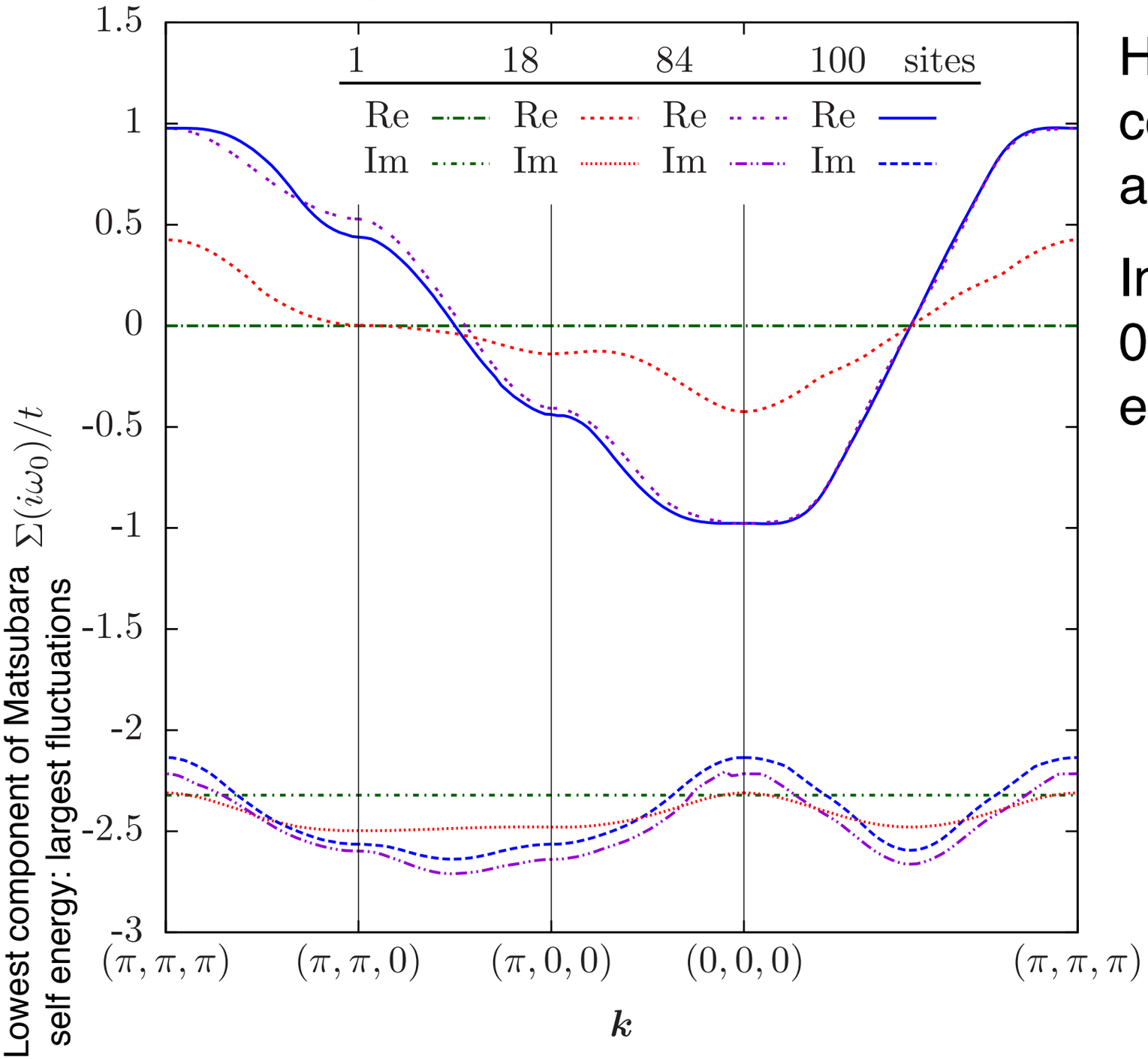

High temperature T/t = 1: Exact convergence of the self energy as a function of cluster size.

Intermediate temperature T/t = 0.5: Convergence visible, extrapolation needed.

Phys. Rev. Lett. 106, 030401 (2011)

Controlling DCA

k-dependence of the self energy systematically reintroduced, convergence for self energy observed: Approximation controlled

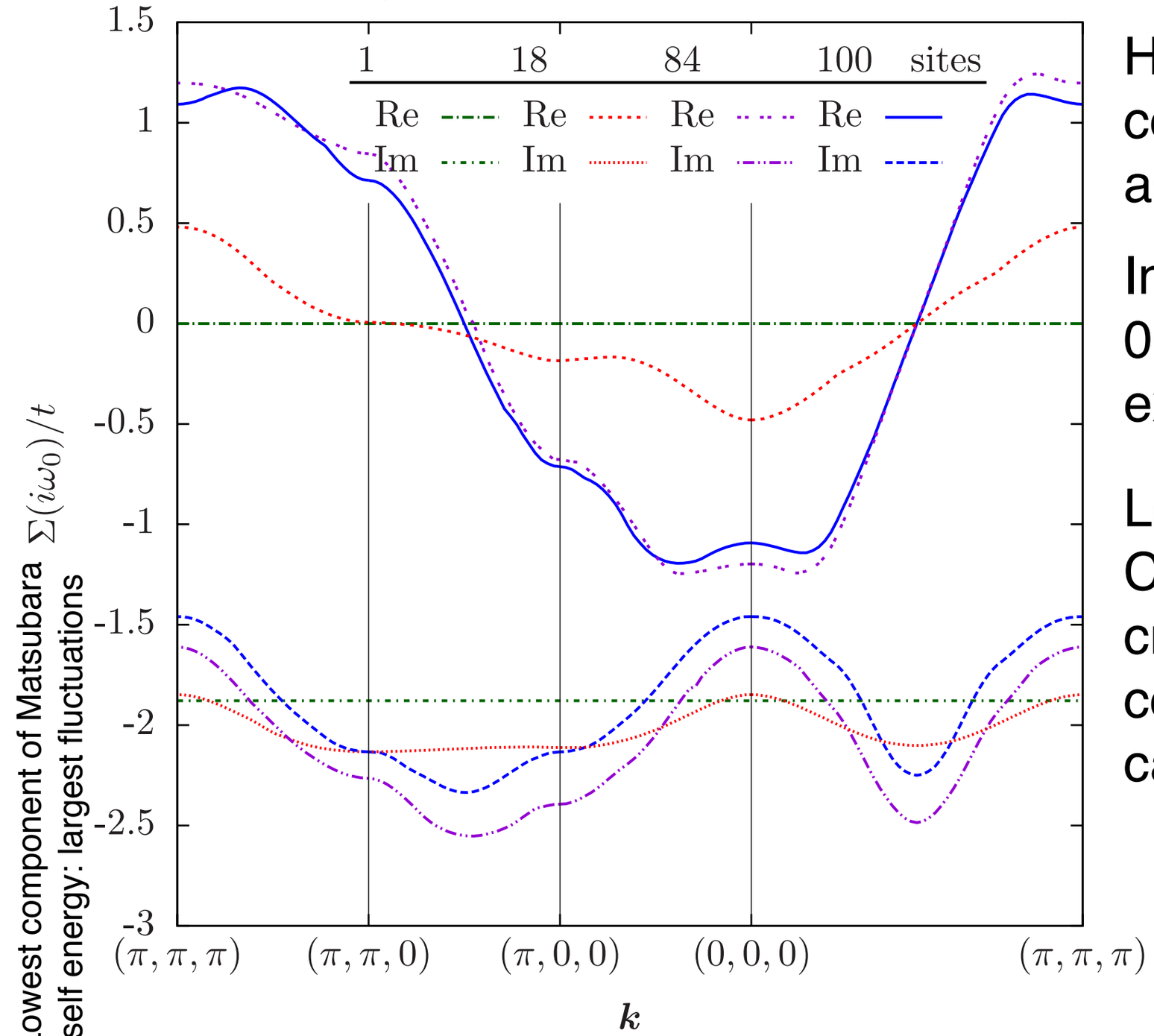

High temperature T/t = 1: Exact convergence of the self energy as a function of cluster size.

Intermediate temperature T/t = 0.5: Convergence visible, extrapolation needed.

Low temperature T/t = 0.35: Convergence not obvious, critical regime with diverging correlation length not well captured. ($\sim T_N$)

Phys. Rev. Lett. 106, 030401 (2011)

Finite Size Simulations vs DCA

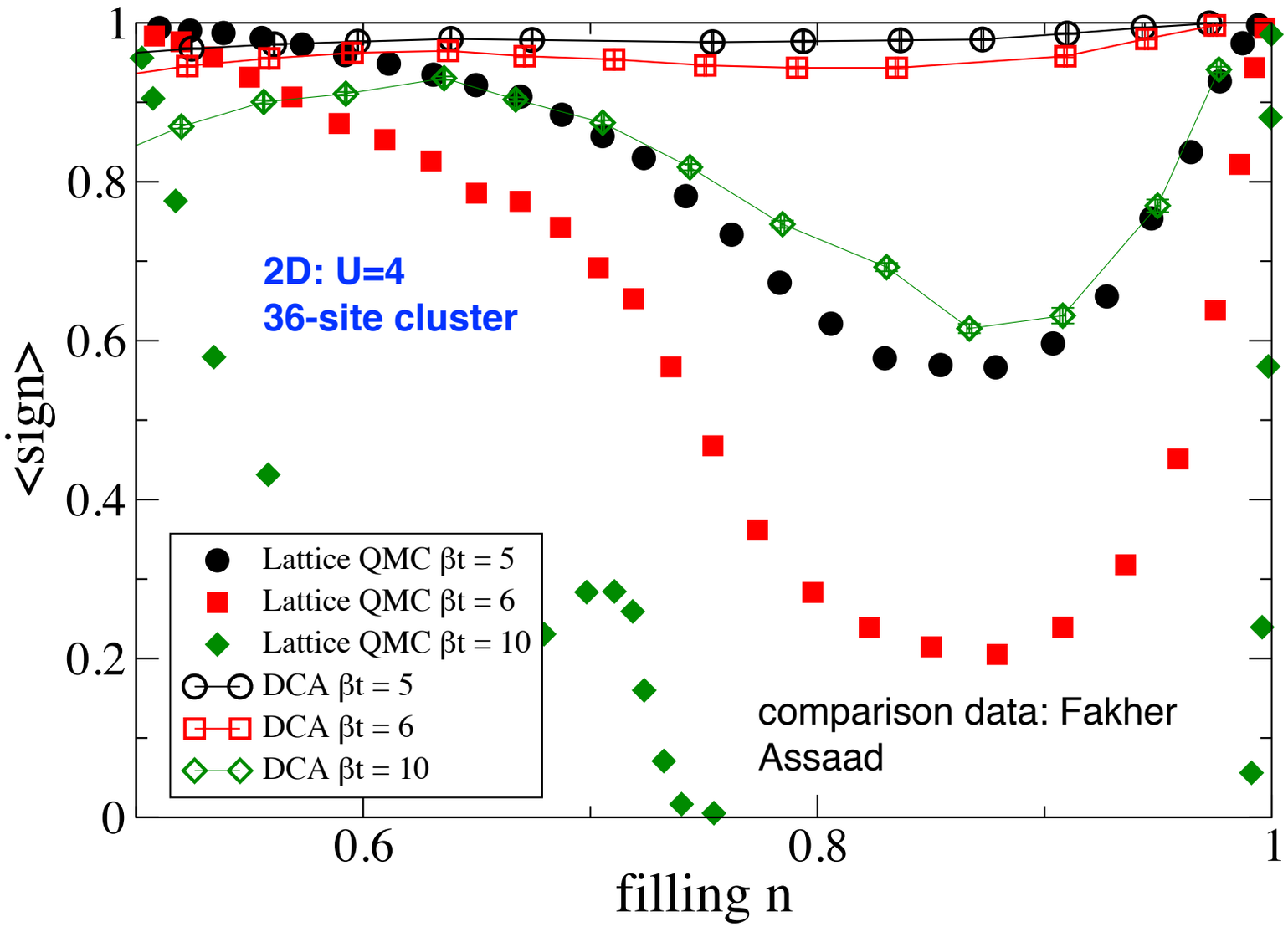

- Convergence in DCA is faster: results from 64-84-100 sites comparable to 6^3, 8^3, 10^3 sites in lattice simulation.

- Sign problem is better ('bath helps with sign problem') near half filling.

Phys. Rev. Lett. 106, 030401 (2011)

3D Hubbard Model (conclusions)

We have solved the 3D Hubbard model (at high temperature)! Full tables, entire phase diagram with energies, densities, entropies, double occupancies, spin correlation functions available online

http://prl.aps.org/supplemental/PRL/v106/i3/e030401

Finite size scaling feasible for non-trivial systems in practice: change the status of cluster DMFT from an uncontrolled approximation to a method for obtaining **controlled results** with **accurate error bars**, similar to BSS / finite Lattice simulations

Nontrivial regime accessible: about 5x lower in temperature than HTSE & DMFT.

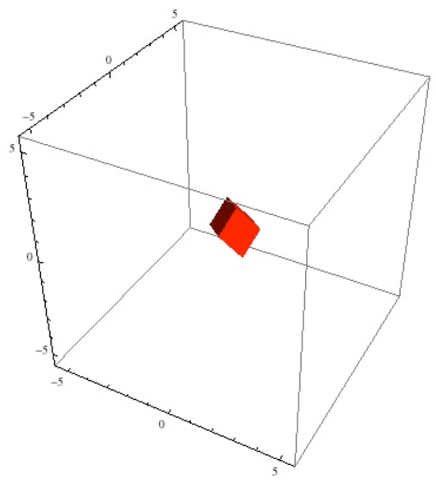

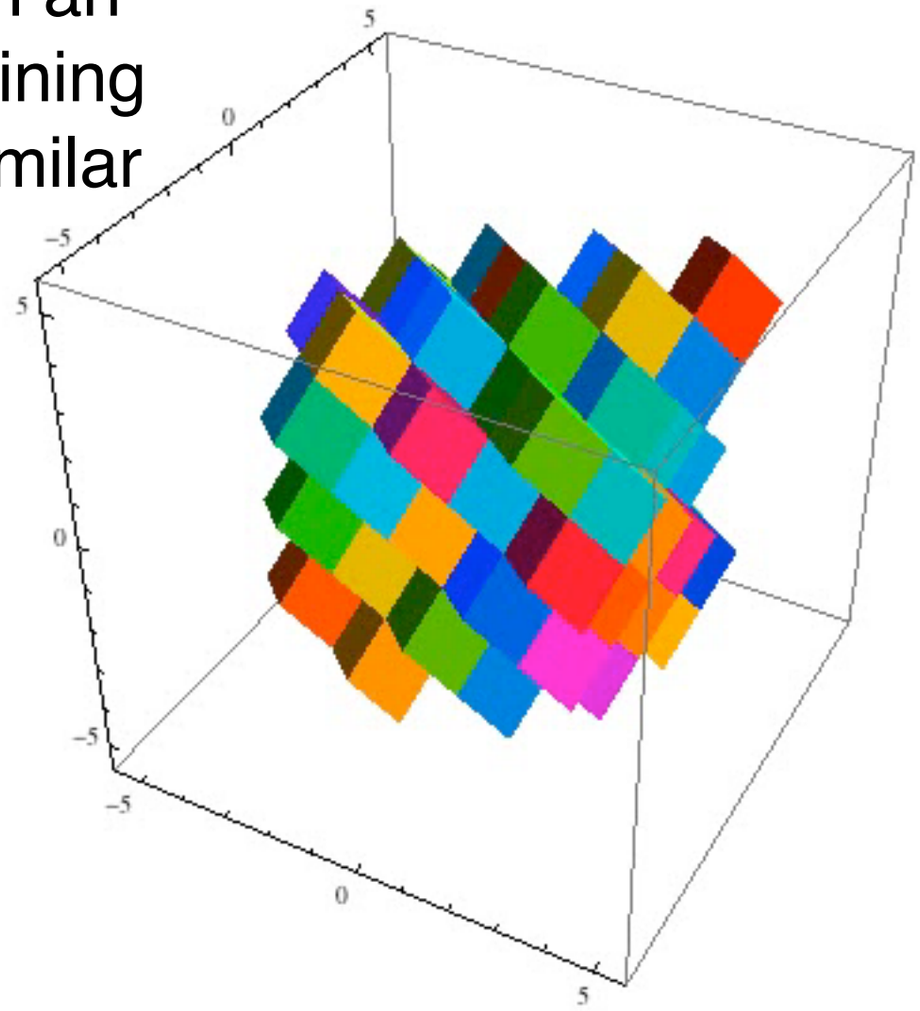

Cluster DMFT

Variation of cluster sizes and geometries, crucial to establish robustness of features!

In DCA: No periodization / interpolation schemes.

In this talk: cluster geometries of size 2–16 (larger: hampered by sign problem)

Clear Nodal / Antinodal separation on clusters large enough.

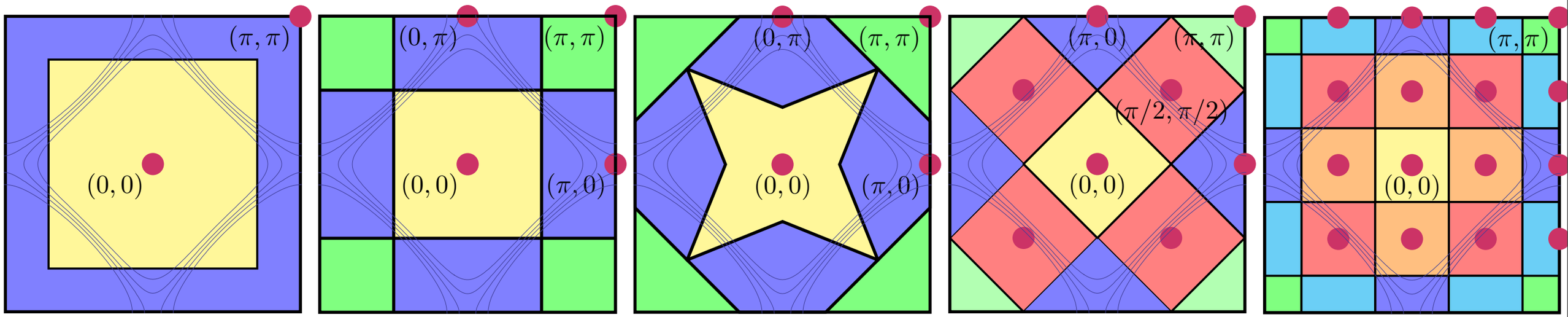

Cluster DMFT

Variation of cluster sizes and geometries, crucial to establish robustness of features!

In DCA: No periodization / interpolation schemes.

In this talk: cluster geometries of size 2–16 (larger: hampered by sign problem)

Clear Nodal / Antinodal separation on clusters large enough.

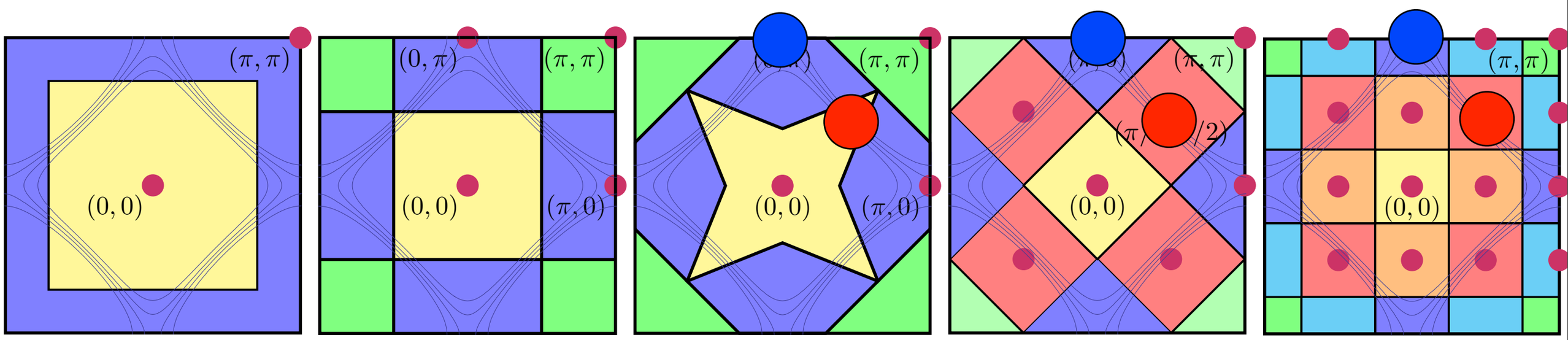

2D Hubbard with t': Generic Phase Diagram

See also:
C. Huscroft et al., Phys. Rev. Lett. 86, 139 (2001),
A. Macridin, et al., Phys. Rev. Lett. 97, 036401 (2006),
O. Parcollet, G. Biroli, and G. Kotliar, Phys. Rev. Lett. 92, 226402 (2004),
Park et al., Phys. Rev. Lett. 101, 186403 (2008)
E. Gull, P. Werner, X. Wang, M. Troyer, and A. J. Millis, EPL 84, 37009 (2008),
Y. Z. Zhang and M. Imada, Phys. Rev. B 76, 045108 (2007),
M. Ferrero, P. S. Cornaglia, L. De Leo, O. Parcollet, G. Kotliar, and A. Georges, EPL 85, 57009 (2009)
…and several other studies…

New aspects:
Larger clusters, lower temperatures, scans of entire phase diagrams:
enabled by new computational methods.

P. Werner, E. Gull, O. Parcollet, A. J. Millis, Phys. Rev. B 80, 045120 (2009) (**short version, 8-site**)
E. Gull, O. Parcollet, P. Werner, A. J. Millis, Phys. Rev. B 80, 245102 (2009) (**long version, t', 8-site**)
E. Gull, M. Ferrero, O. Parcollet,A. Georges, A.J. Millis, Phys. Rev. B 82, 155101 (2010) (**cluster size dependence**)
N. Lin, E. Gull, and A.J. Millis, Phys. Rev. B 82, 045104 (2010) (**analytic continuations, Raman, c-axis**)

Generic Phase Diagram

2D Hubbard: Phase diagram as a function of interaction and doping, on large clusters

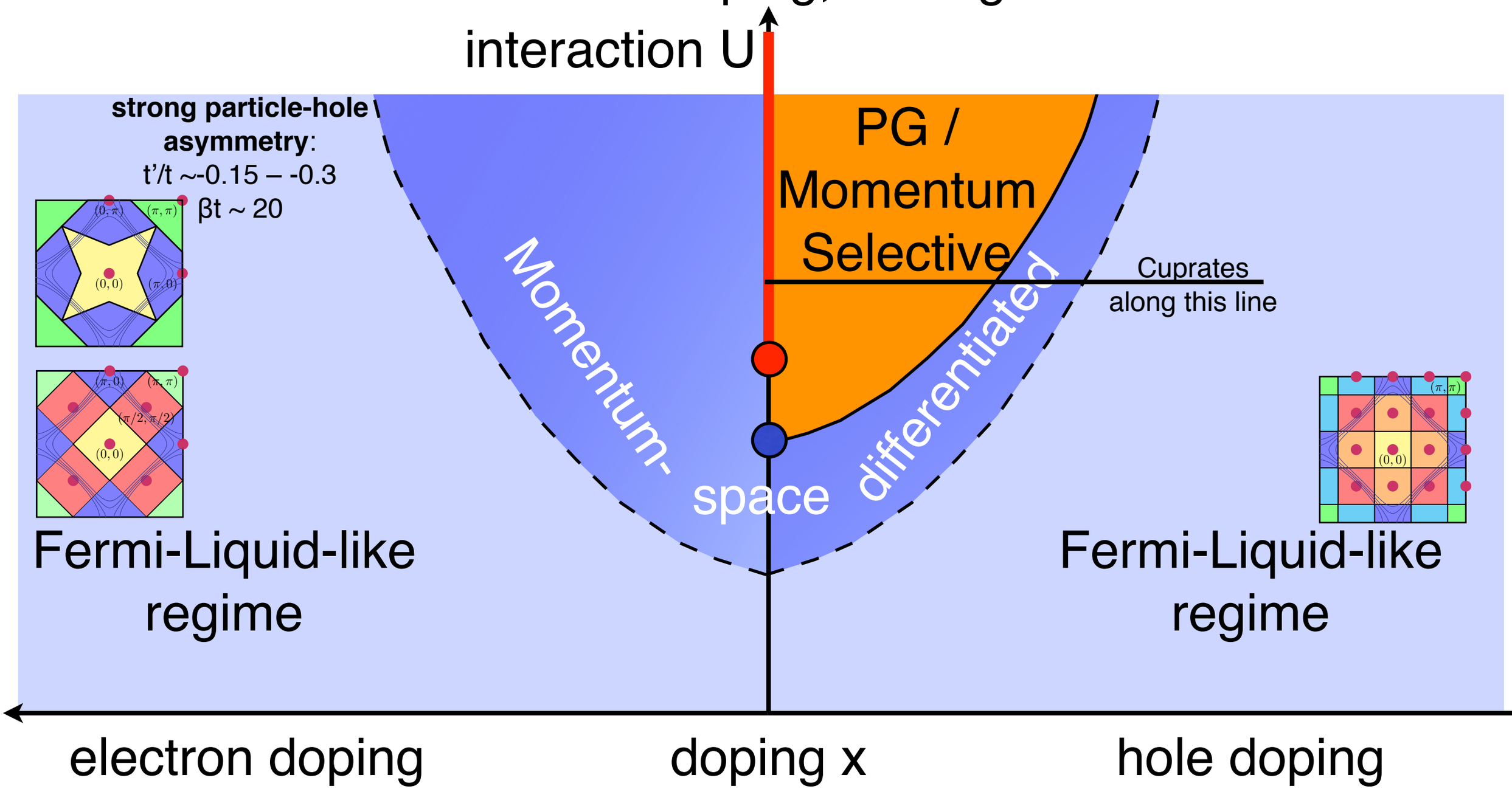

P. Werner, E. Gull, O. Parcollet, A. J. Millis, Phys. Rev. B 80, 045120 (2009) (interaction)
E. Gull, O. Parcollet, P. Werner, A. J. Millis, Phys. Rev. B 80, 245102 (2009) (doping, t')
E. Gull, M. Ferrero, O. Parcollet,A. Georges, A.J. Millis, Phys. Rev. B 82, 155101 (2010) (cluster size)

Generic Phase Diagram

2D Hubbard: Phase diagram as a function of interaction and doping, on large clusters

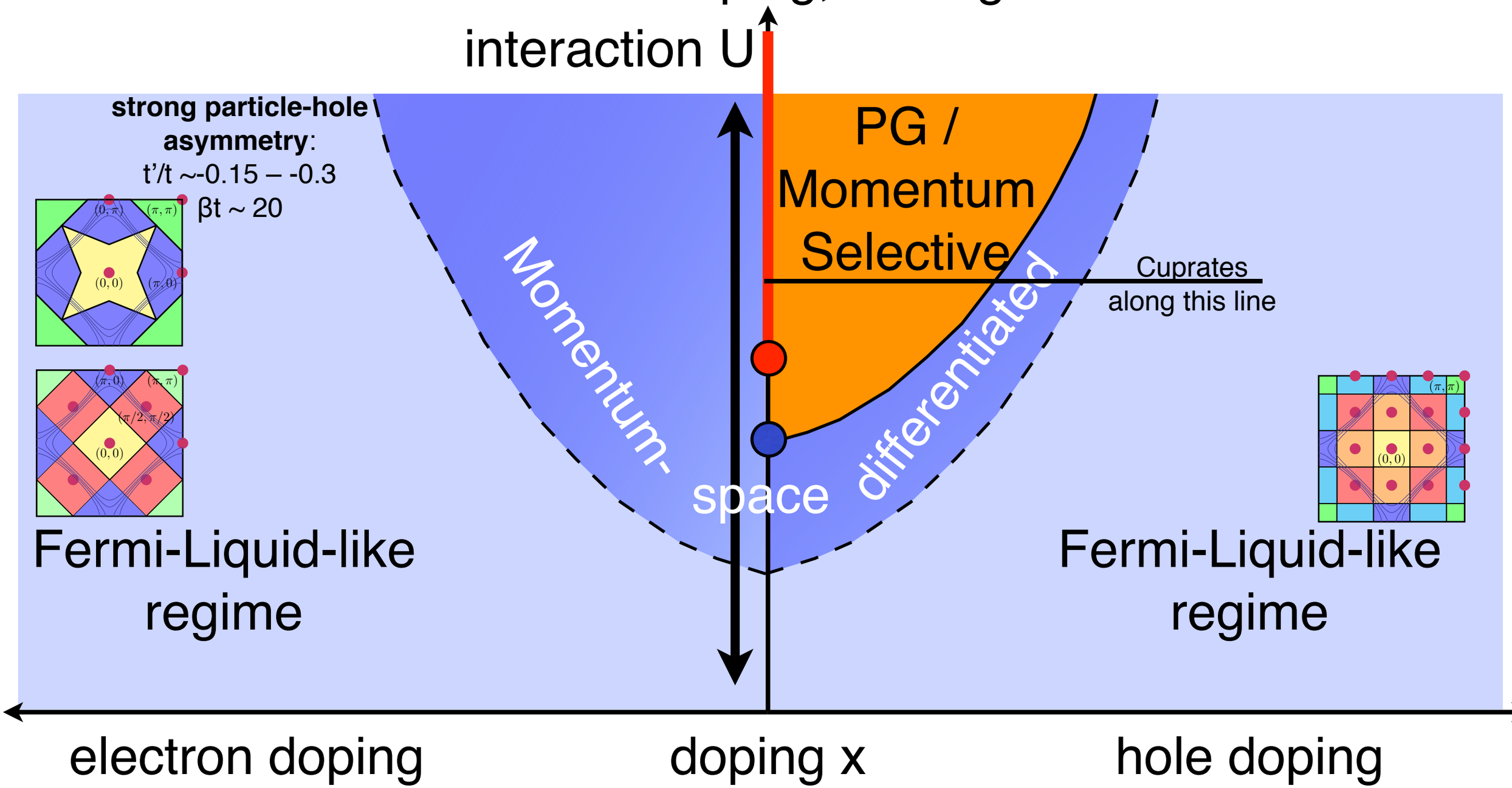

P. Werner, E. Gull, O. Parcollet, A. J. Millis, Phys. Rev. B 80, 045120 (2009) (interaction)
E. Gull, O. Parcollet, P. Werner, A. J. Millis, Phys. Rev. B 80, 245102 (2009) (doping, t')
E. Gull, M. Ferrero, O. Parcollet,A. Georges, A.J. Millis, Phys. Rev. B 82, 155101 (2010) (cluster size)

Generic Phase Diagram

2D Hubbard: Phase diagram as a function of interaction and doping, on large clusters

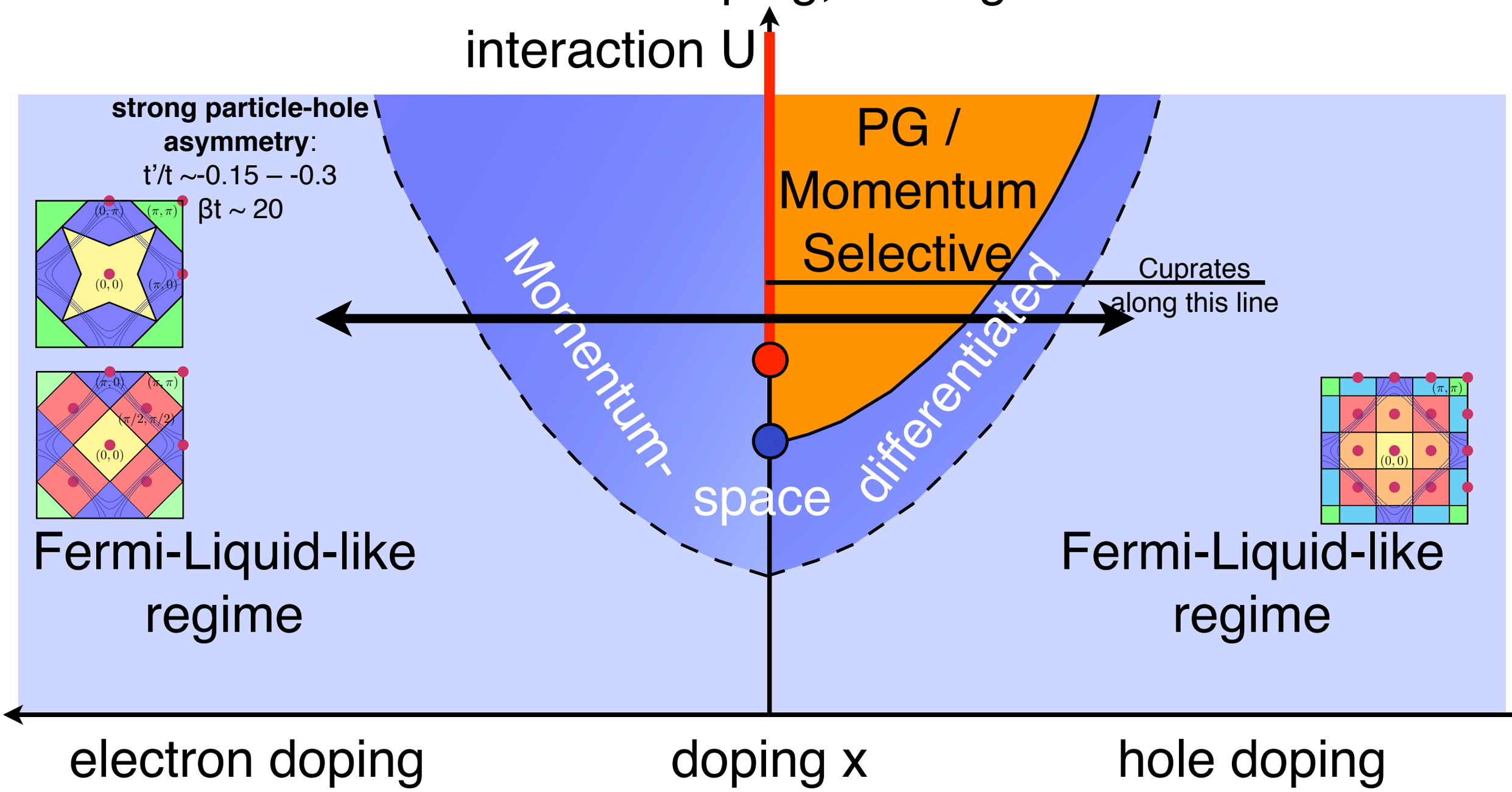

P. Werner, E. Gull, O. Parcollet, A. J. Millis, Phys. Rev. B 80, 045120 (2009) (interaction)
E. Gull, O. Parcollet, P. Werner, A. J. Millis, Phys. Rev. B 80, 245102 (2009) (doping, t')
E. Gull, M. Ferrero, O. Parcollet,A. Georges, A.J. Millis, Phys. Rev. B 82, 155101 (2010) (cluster size)

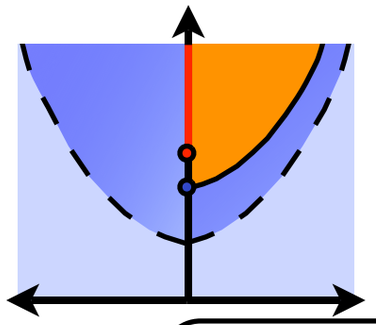

Phase Diagram

8-site Matsubara self-energy: blue: antinode. red: node

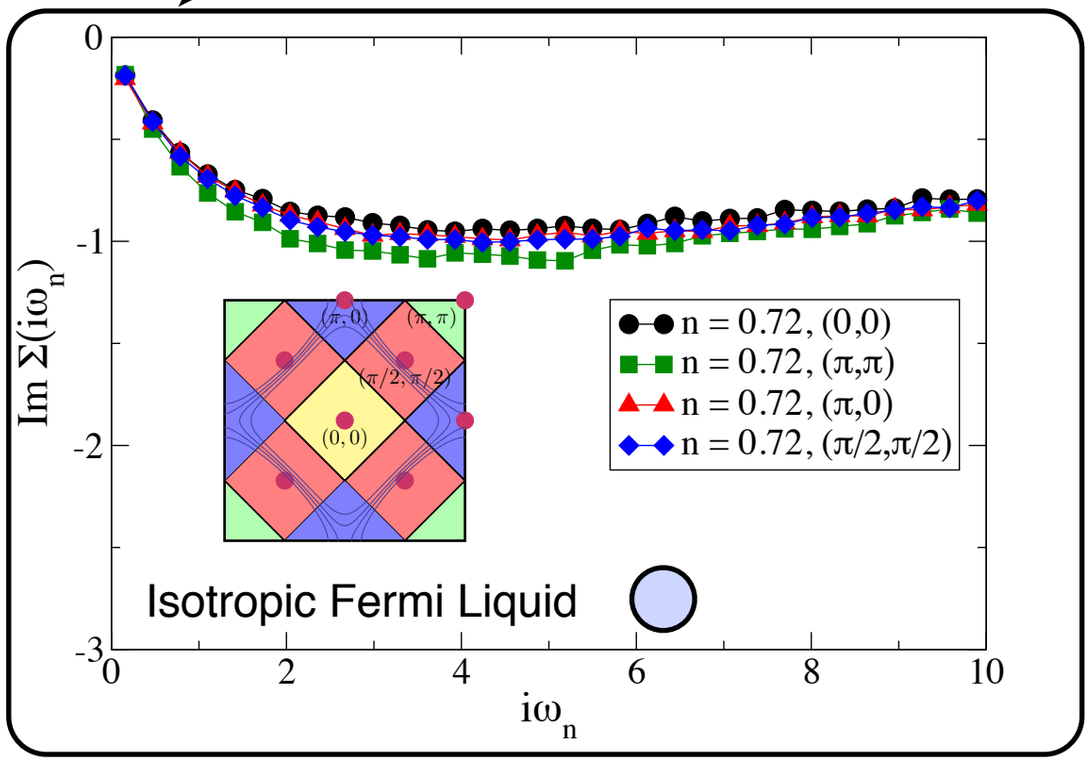

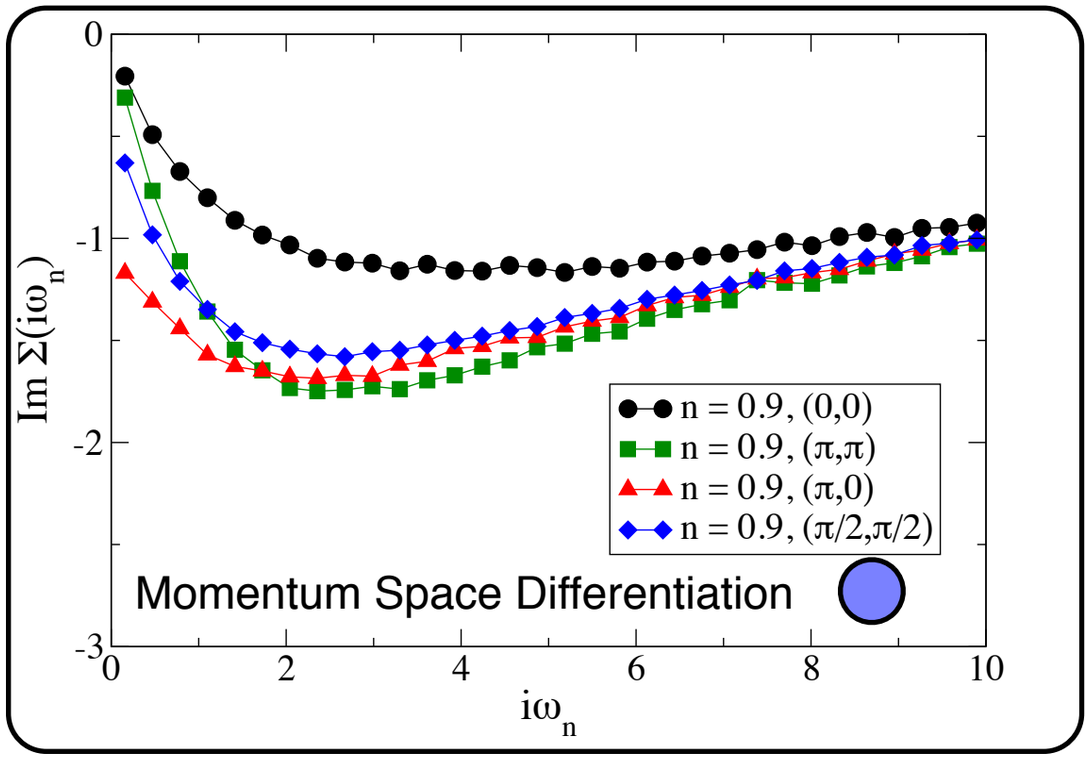

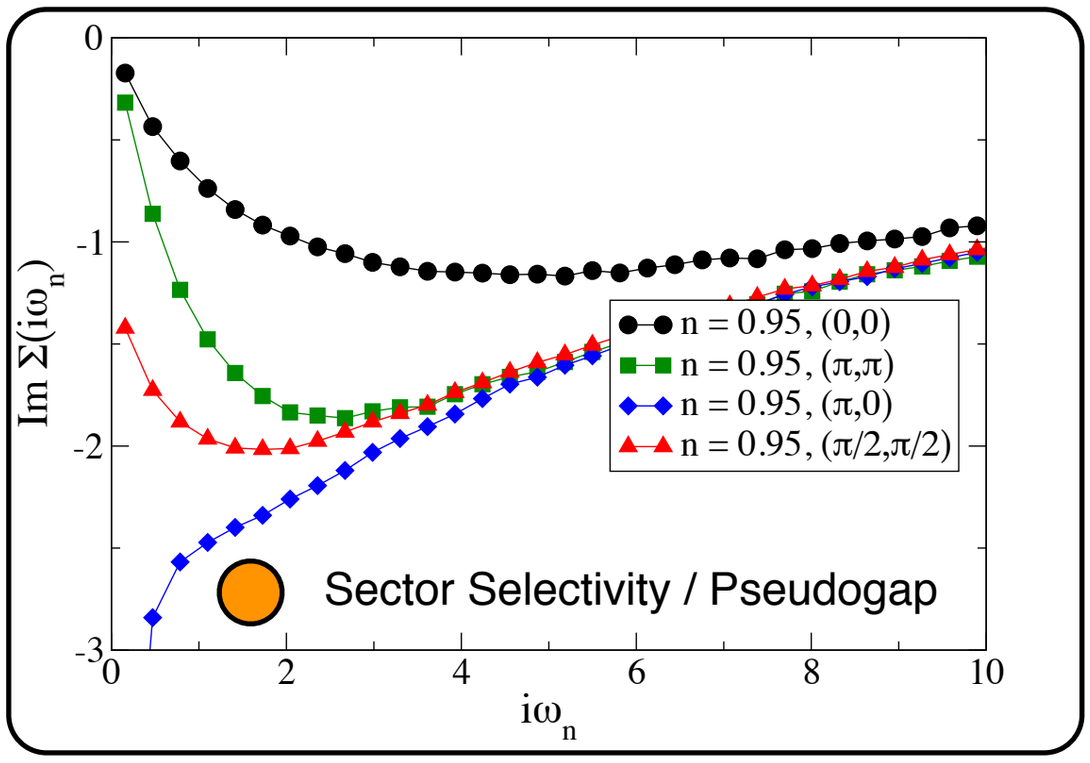

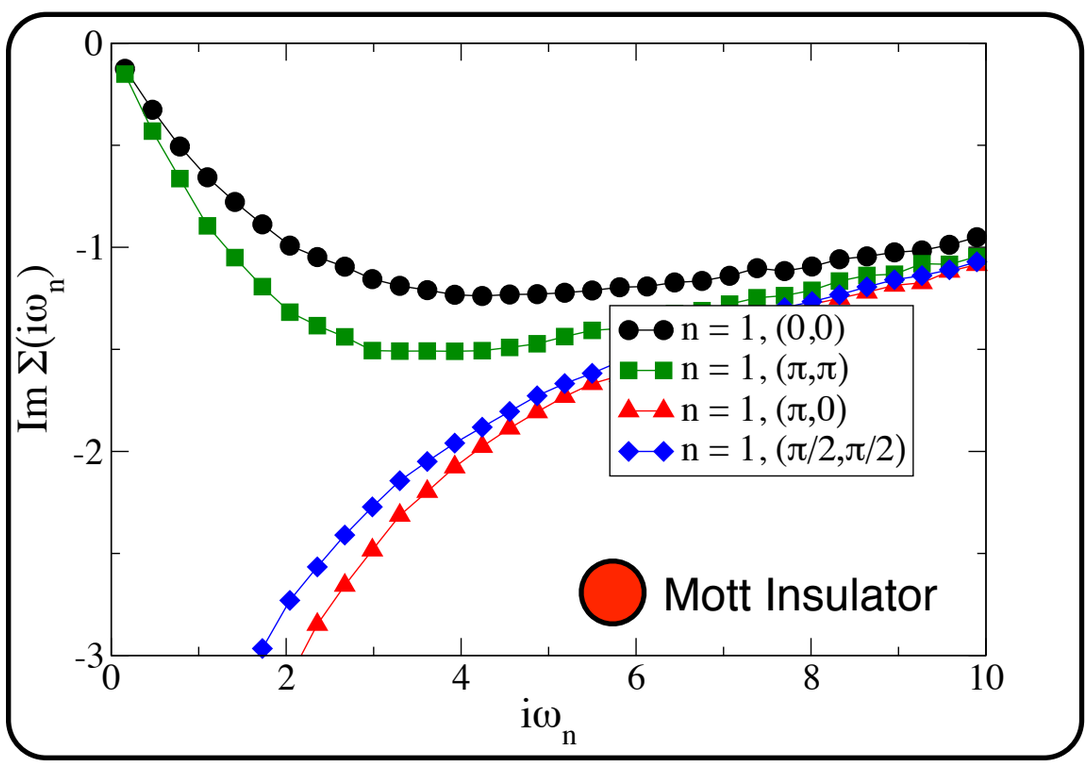

Interaction transitions at half filling

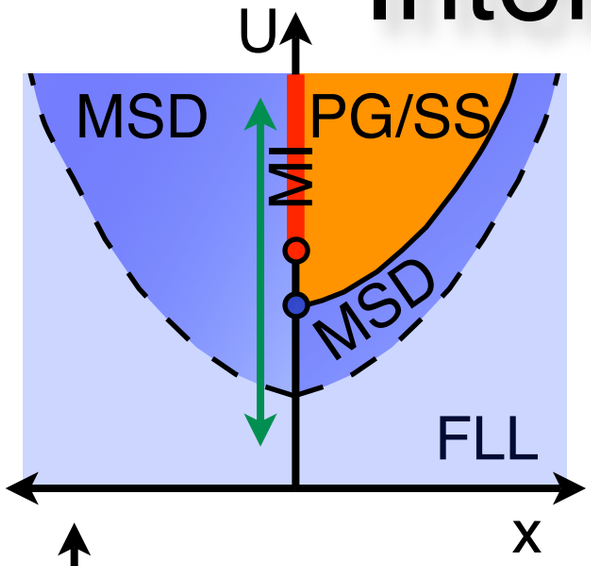

For weak interaction: **Fermi-Liquid** (-like) phase (FLL)

Crossover: At slightly larger interaction **Momentum-Space Differentiation** (MSD), Each momentum sector consistent with Fermi Liquid, but variations between momentum sectors

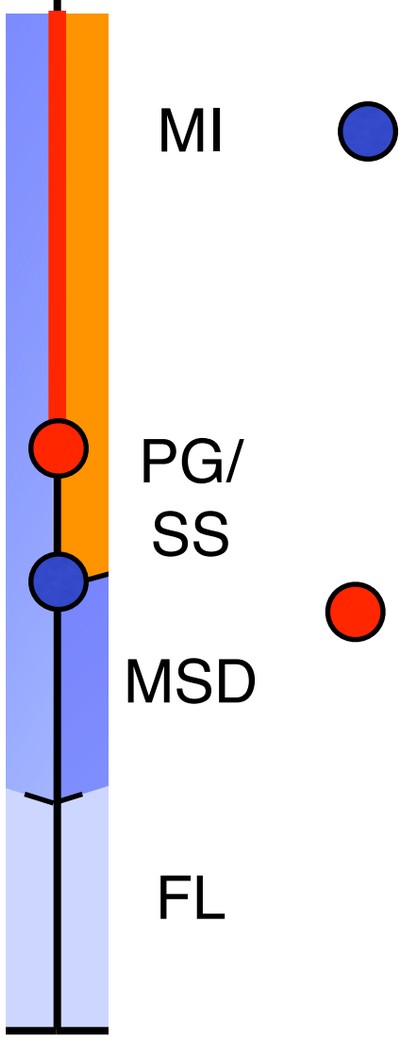

Transition 1: (Continuous, at the T accessible) to a **Sector Selective Phase**: Anti-nodal part of the Fermi surface gapped), nodal part metallic. Analogous to orbitally selective Mott transition

Momentum selectivity proposed in minimal 2-site model: M. Ferrero, P. S. Cornaglia, L. De Leo, O. Parcollet, G. Kotliar, and A. Georges, EPL 85, 57009

Transition 2: (First Order) to a **Mott insulating** Phase. All parts of the noninteracting Fermi surface gapped

P. Werner, E. Gull, O. Parcollet, A. J. Millis, Phys. Rev. B 80, 045120 (2009)
E. Gull, O. Parcollet, P. Werner, A. J. Millis, Phys. Rev. B 80, 245102 (2009)
E. Gull, M. Ferrero, O. Parcollet,A. Georges, A.J. Millis, Phys. Rev. B 82, 155101 (2010)

see also: Liebsch, Tong, Phys. Rev. B 80, 165126 (2009) for CDMFT

Doping transition at intermediate U

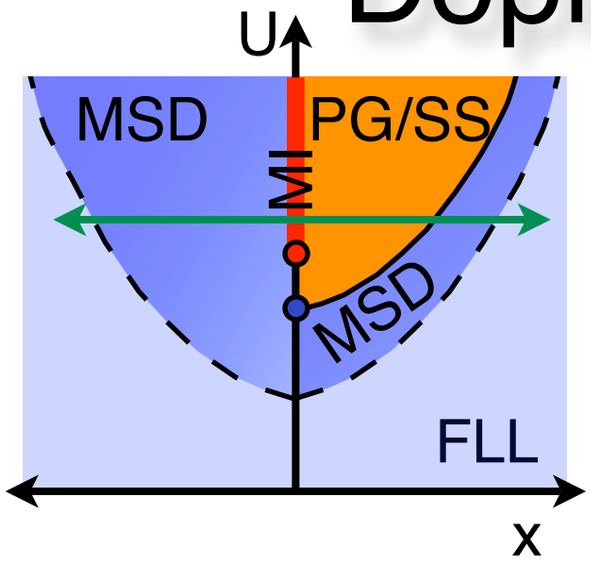

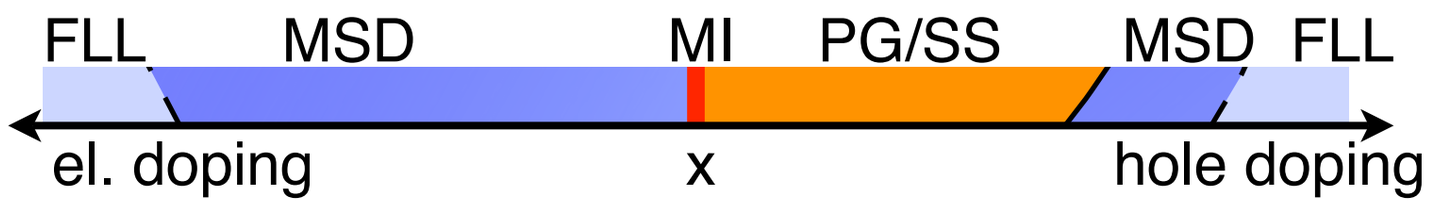

On the hole doped side: same story as in interaction transition.

On the electron-doped side: direct transition to the **Mott Insulator**. Large t': first order. Small t': intermittent sector selective phase, continuous.

[1st order: see also Macridin et al., Phys. Rev. B 74, 085104 (2006)]

E. Gull, O. Parcollet, P. Werner, A. J. Millis, Phys. Rev. B 80, 245102 (2009)
E. Gull, M. Ferrero, O. Parcollet,A. Georges, A.J. Millis, Phys. Rev. B 82, 155101 (2010)

see also: M. Ferrero, P. S. Cornaglia, L. De Leo, O. Parcollet, G. Kotliar, and A. Georges, EPL 85, 57009
Liebsch, Tong, Phys. Rev. B 80, 165126 (2009) and Sordi, Haule, Tremblay, Phys. Rev. Lett. 104, 226402 (2010)

Doping transition at intermediate U

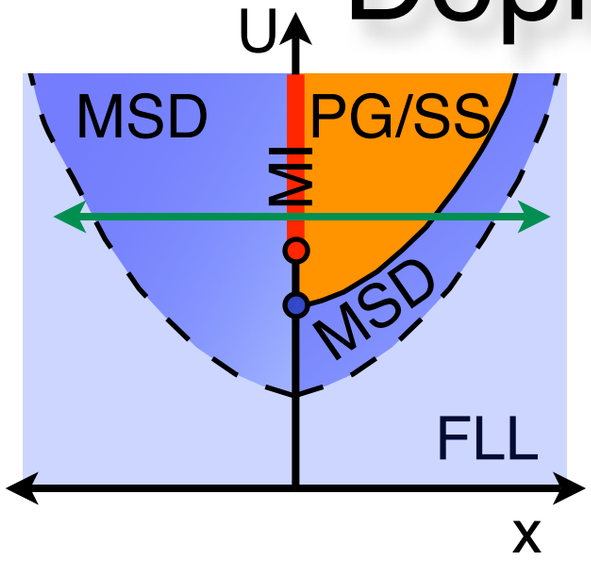

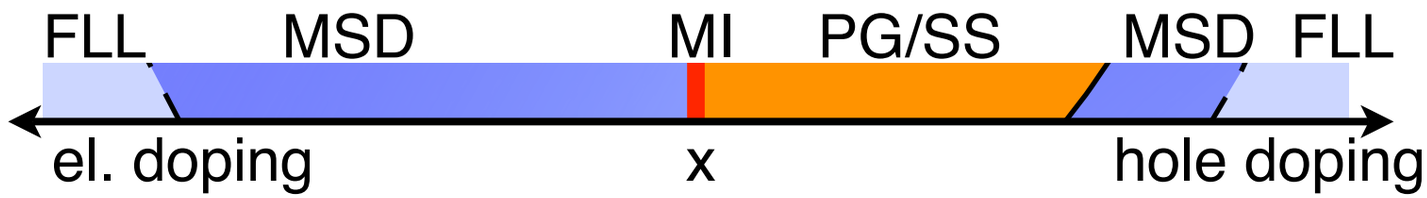

Direct Fermi level DOS estimator:

$$\beta G\left(\frac{\beta}{2}\right) = \int \frac{d\omega}{2\pi T} \frac{A_K(\omega)}{\cosh \frac{\omega}{2t}} \xrightarrow{T\to 0} A_K(0)$$

Antinodal Fermi level DOS

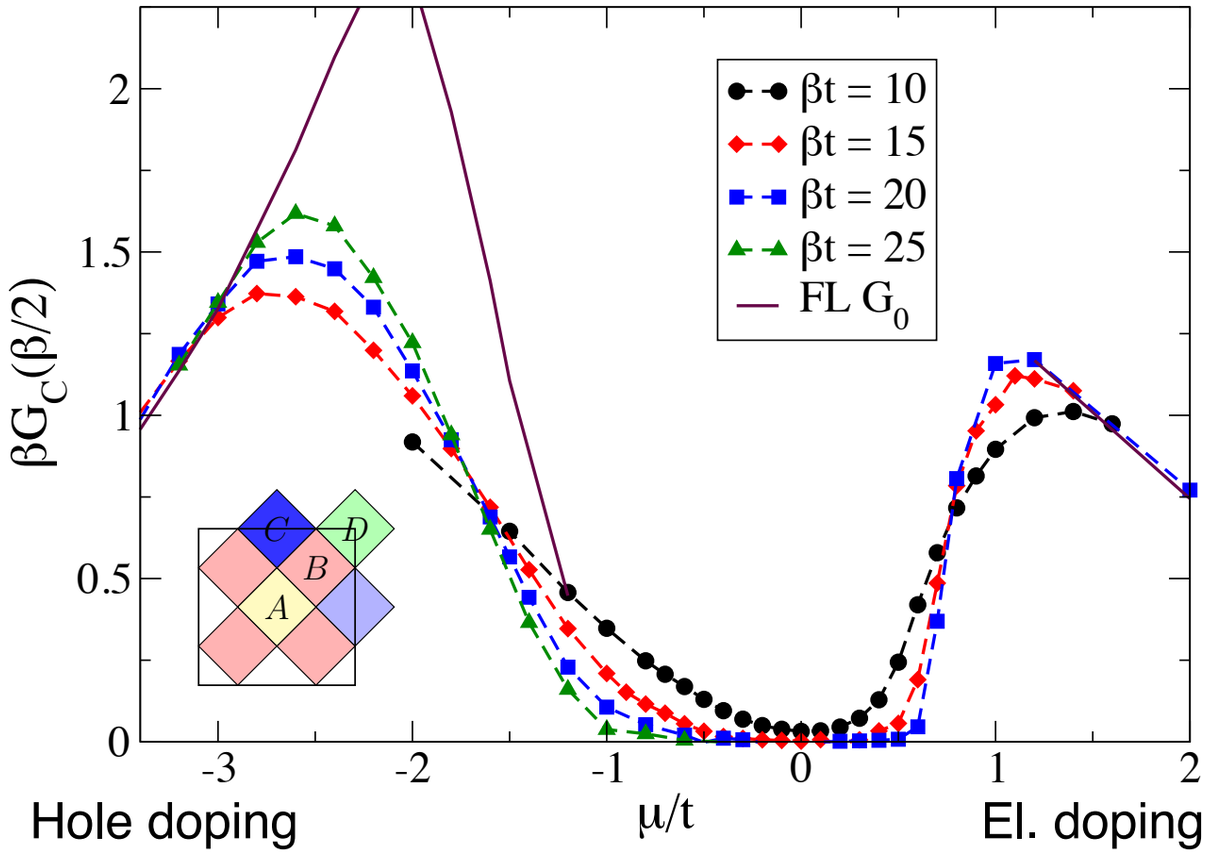

Nodal Fermi level DOS

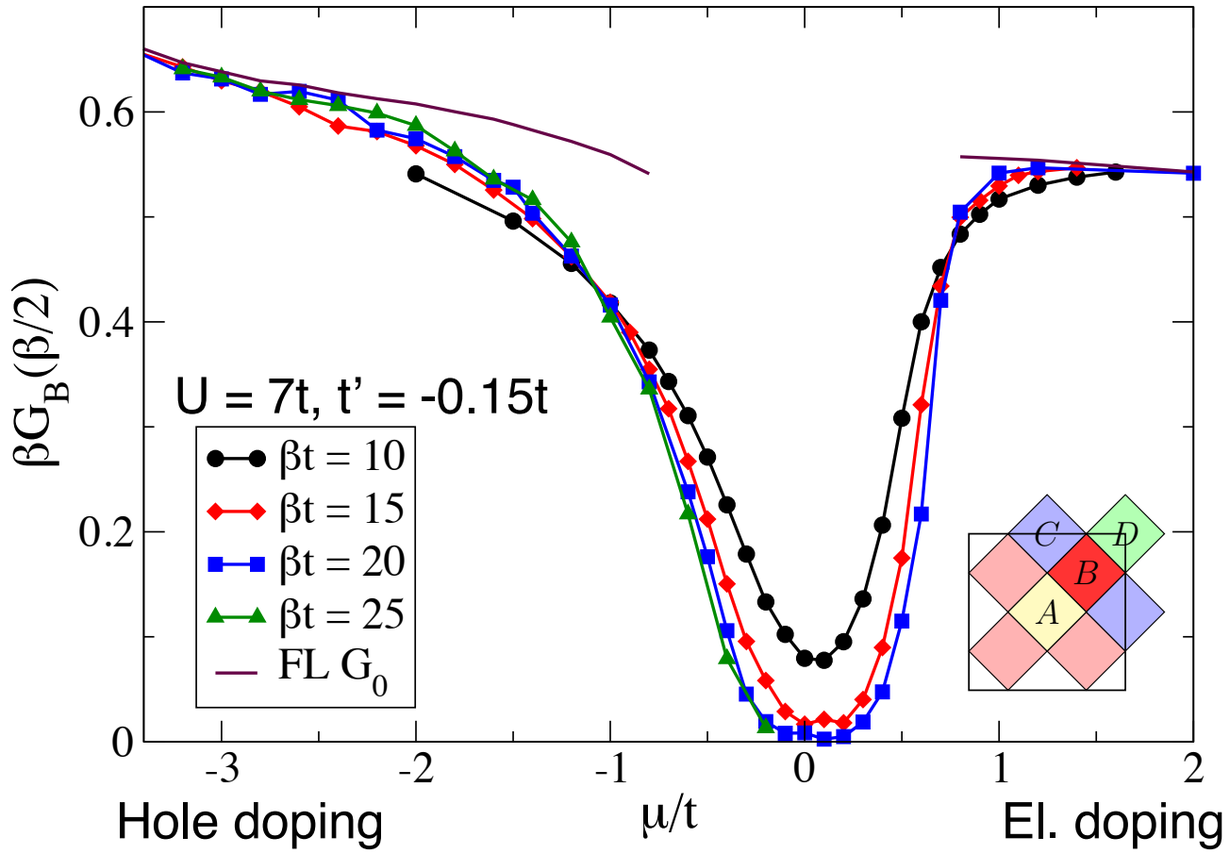

U = 7t, t' = -0.15t

E. Gull, O. Parcollet, P. Werner, A. J. Millis, Phys. Rev. B 80, 245102 (2009)

E. Gull, M. Ferrero, O. Parcollet,A. Georges, A.J. Millis, Phys. Rev. B 82, 155101 (2010)

Doping transition at intermediate U

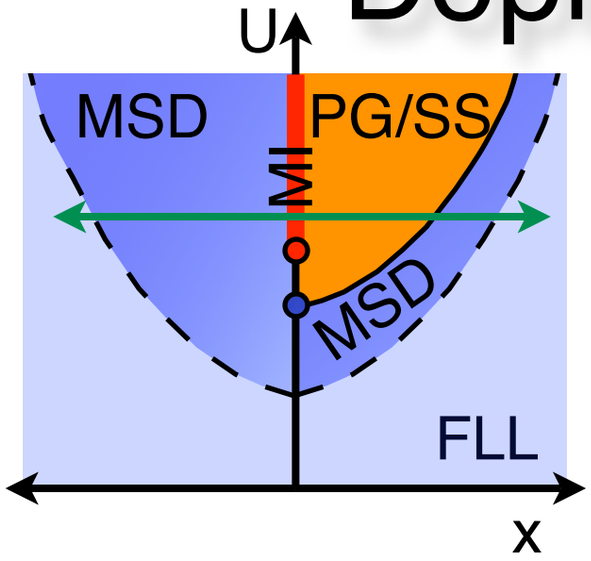

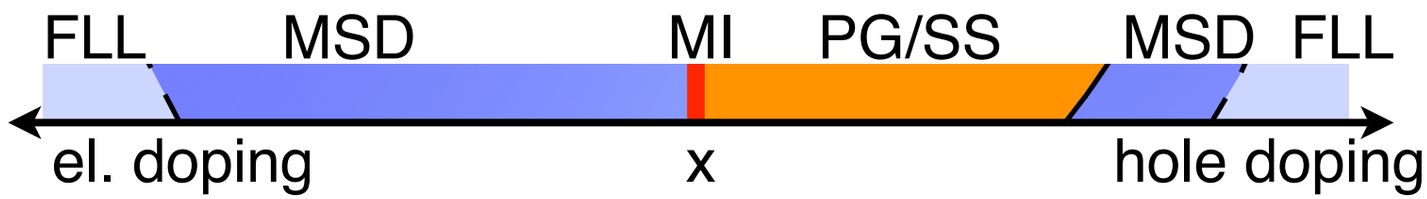

Direct Fermi level DOS estimator:

$$\beta G\left(\frac{\beta}{2}\right) = \int \frac{d\omega}{2\pi T} \frac{A_K(\omega)}{\cosh \frac{\omega}{2t}} \xrightarrow{T\to 0} A_K(0)$$

Antinodal Fermi level DOS

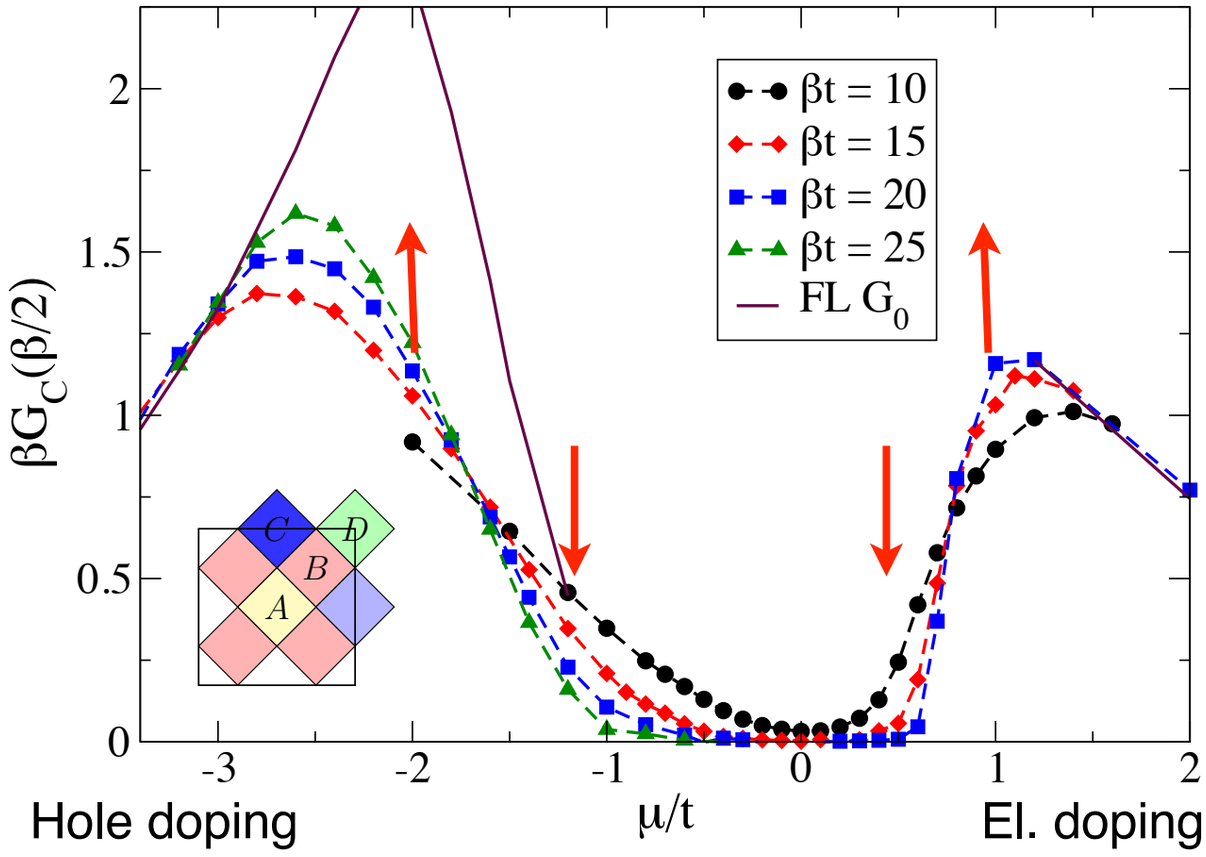

Nodal Fermi level DOS

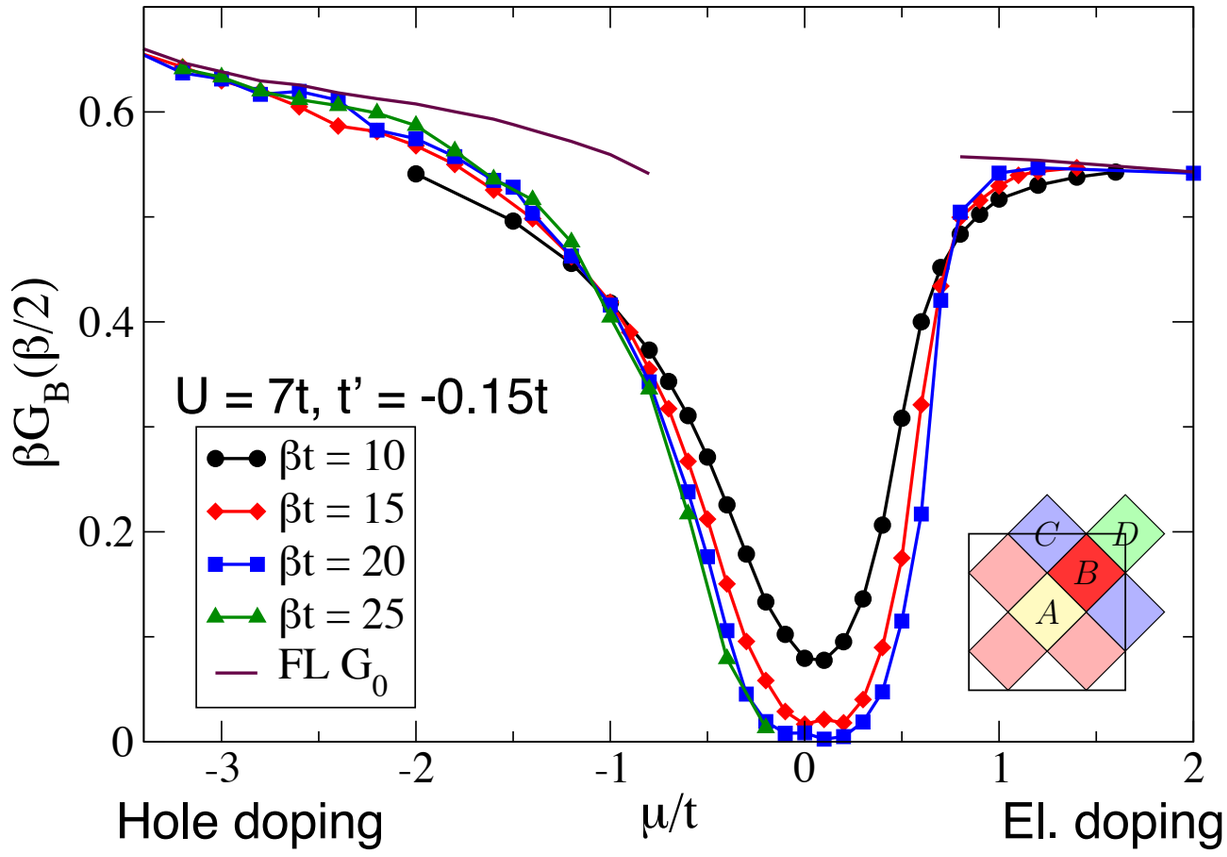

U = 7t, t' = -0.15t

E. Gull, O. Parcollet, P. Werner, A. J. Millis, Phys. Rev. B 80, 245102 (2009)

E. Gull, M. Ferrero, O. Parcollet,A. Georges, A.J. Millis, Phys. Rev. B 82, 155101 (2010)

Doping transition at intermediate U

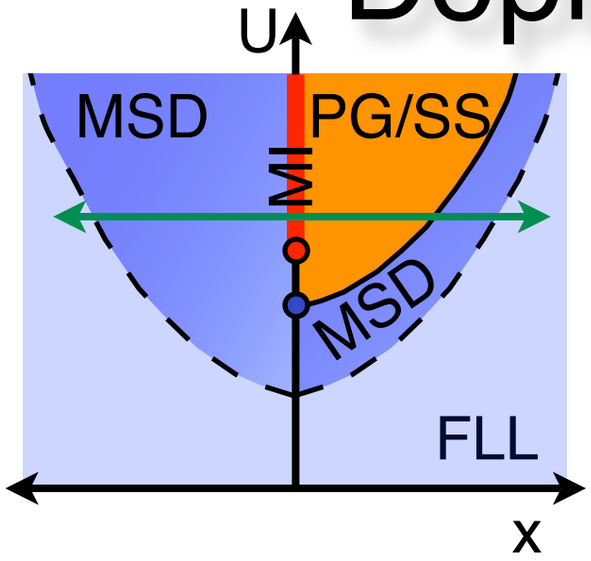

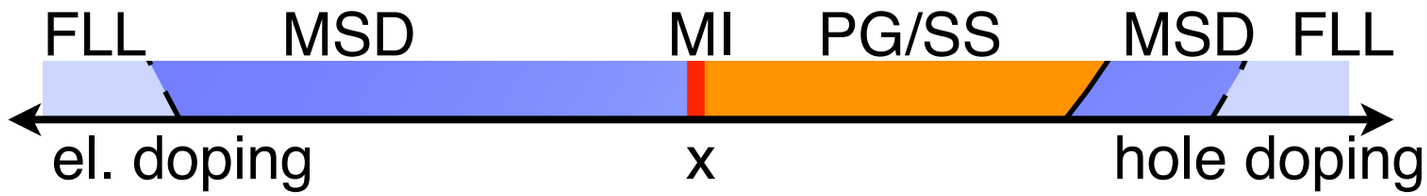

Direct Fermi level DOS estimator:

$$\beta G\left(\frac{\beta}{2}\right) = \int \frac{d\omega}{2\pi T} \frac{A_K(\omega)}{\cosh \frac{\omega}{2t}} \xrightarrow{T\to 0} A_K(0)$$

Antinodal Fermi level DOS

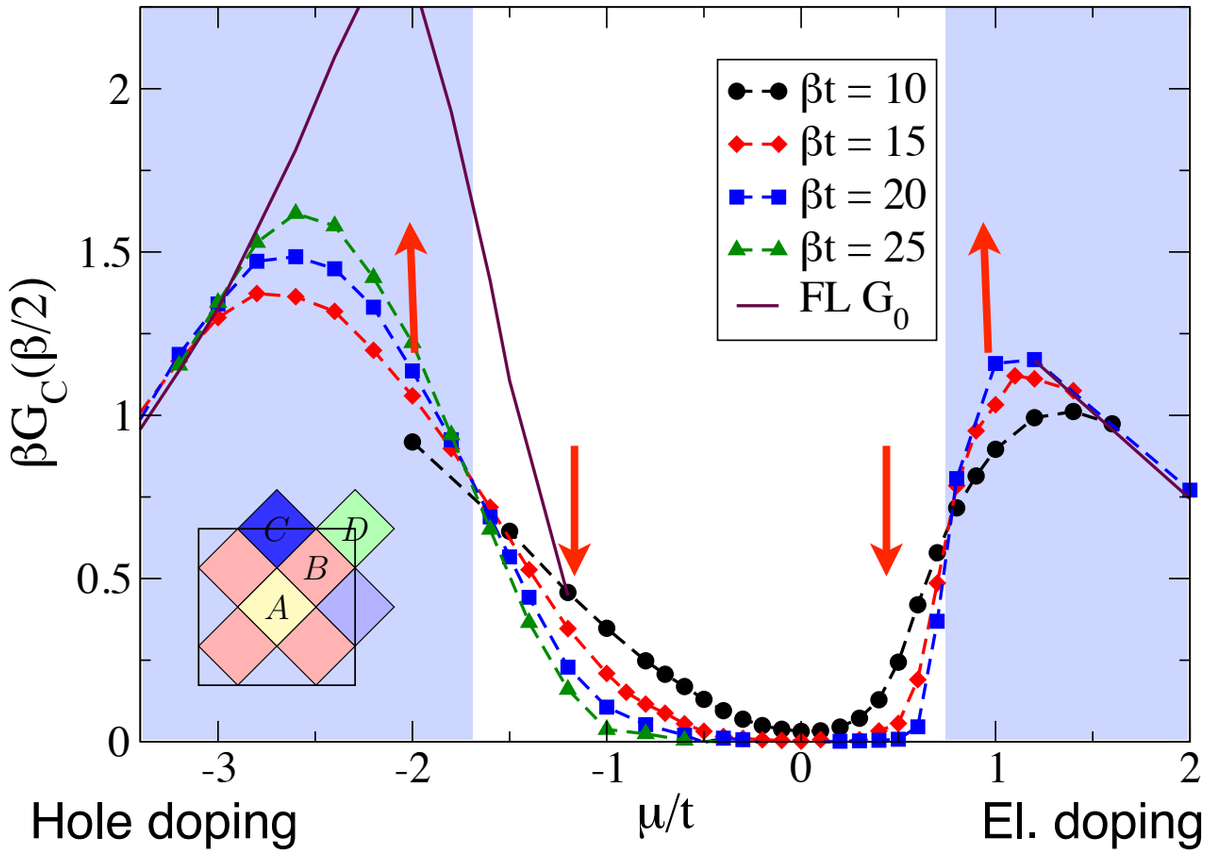

Nodal Fermi level DOS

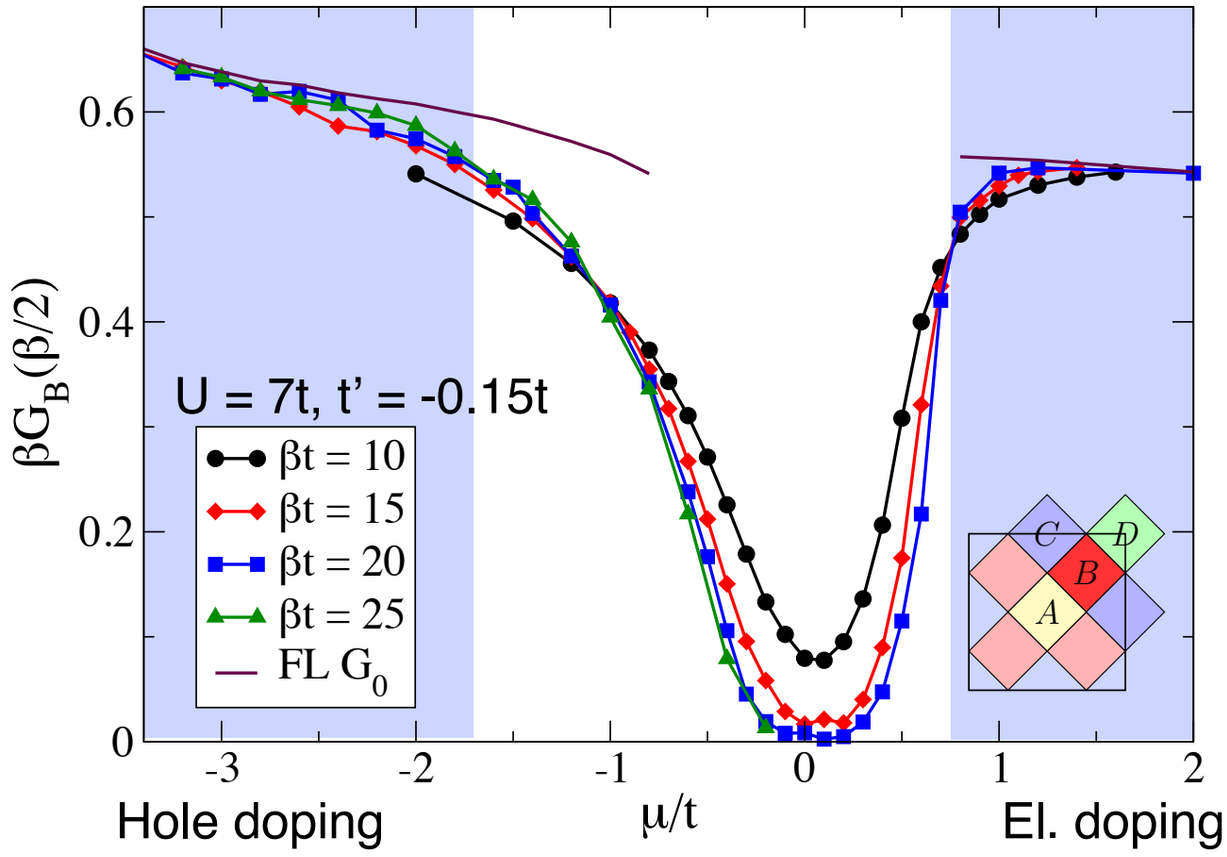

U = 7t, t' = -0.15t

E. Gull, O. Parcollet, P. Werner, A. J. Millis, Phys. Rev. B 80, 245102 (2009)

E. Gull, M. Ferrero, O. Parcollet,A. Georges, A.J. Millis, Phys. Rev. B 82, 155101 (2010)

Doping transition at intermediate U

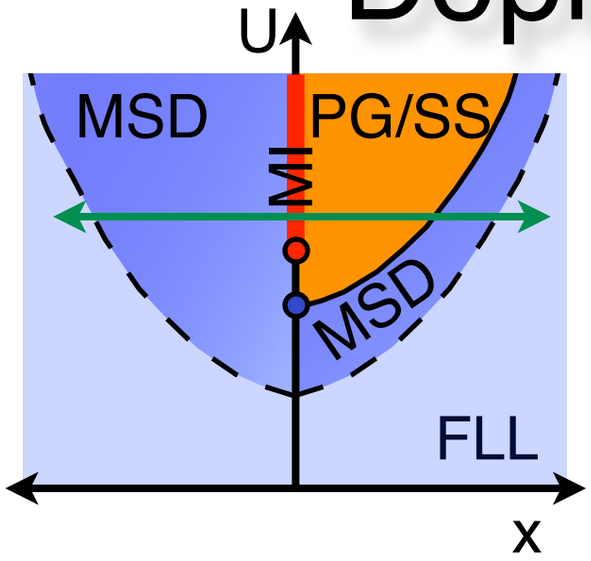

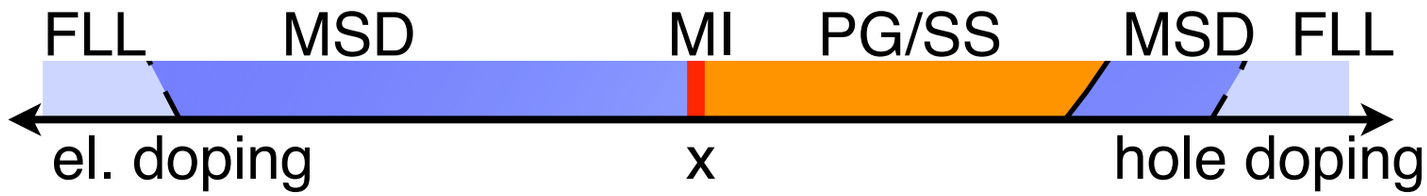

Direct Fermi level DOS estimator:

$$\beta G\left(\frac{\beta}{2}\right) = \int \frac{d\omega}{2\pi T} \frac{A_K(\omega)}{\cosh \frac{\omega}{2t}} \xrightarrow{T\to 0} A_K(0)$$

Antinodal Fermi level DOS

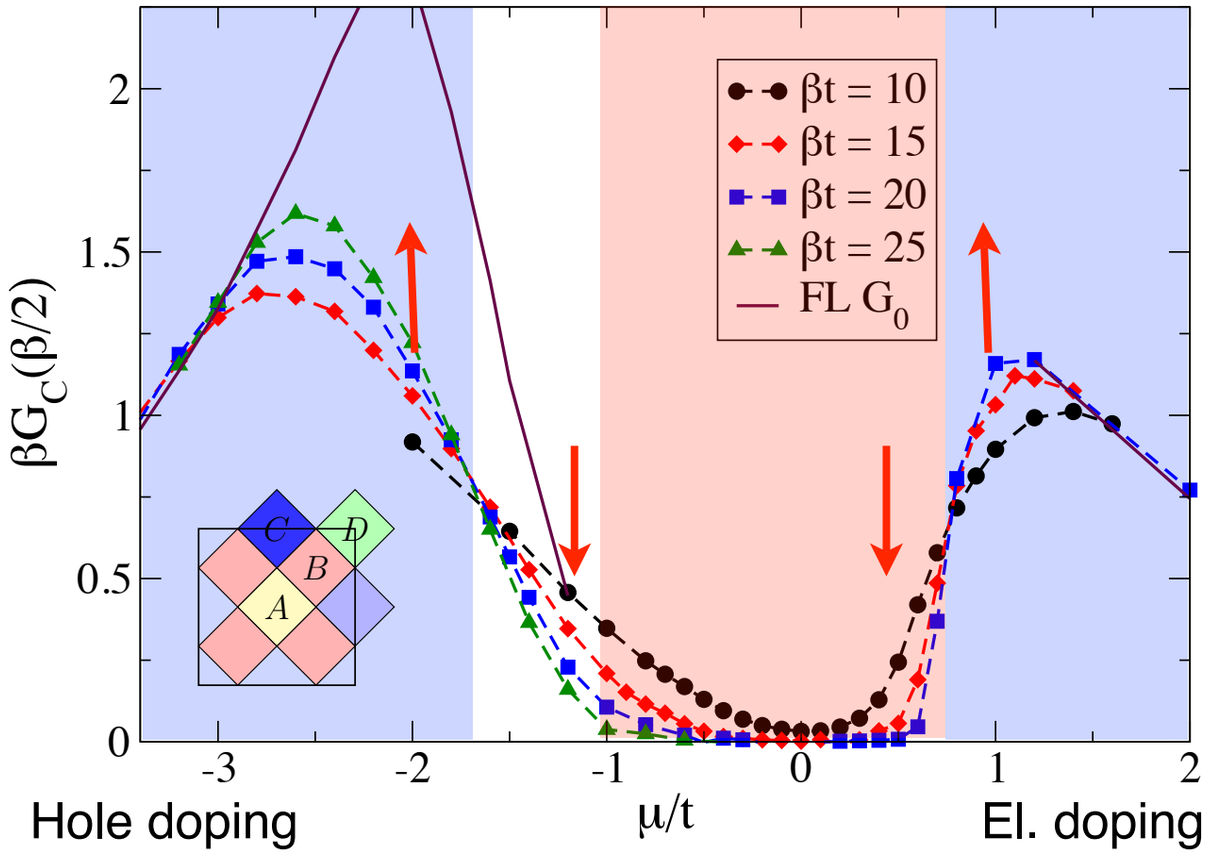

Nodal Fermi level DOS

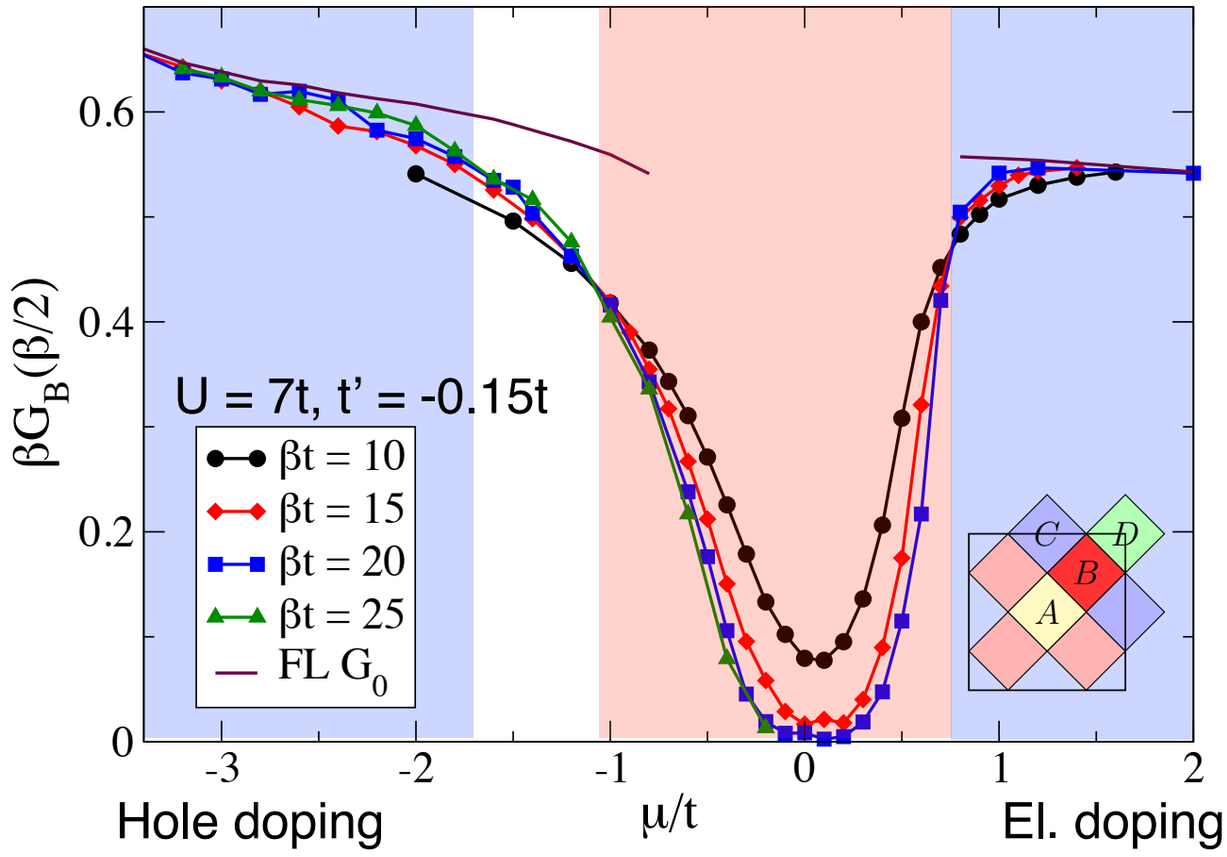

U = 7t, t' = -0.15t

E. Gull, O. Parcollet, P. Werner, A. J. Millis, Phys. Rev. B 80, 245102 (2009)

E. Gull, M. Ferrero, O. Parcollet,A. Georges, A.J. Millis, Phys. Rev. B 82, 155101 (2010)

Doping transition at intermediate U

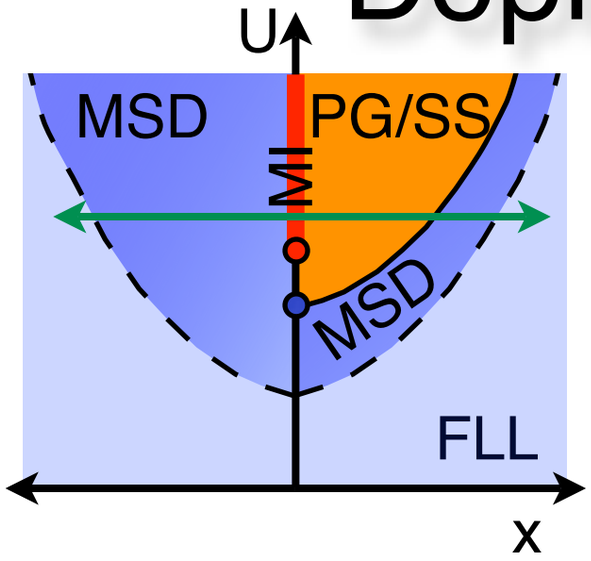

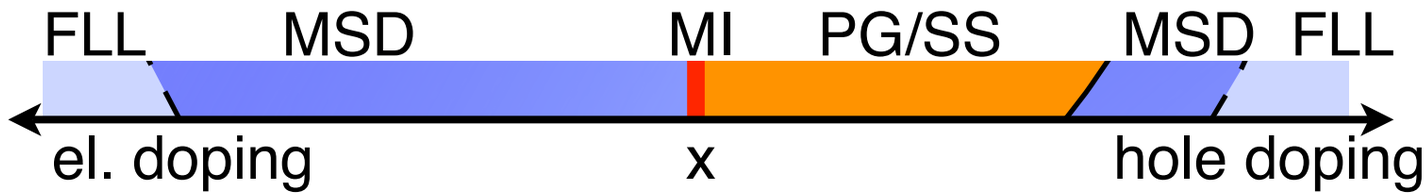

Direct Fermi level DOS estimator:

$$\beta G\left(\frac{\beta}{2}\right) = \int \frac{d\omega}{2\pi T} \frac{A_K(\omega)}{\cosh \frac{\omega}{2t}} \xrightarrow{T\to 0} A_K(0)$$

Antinodal Fermi level DOS

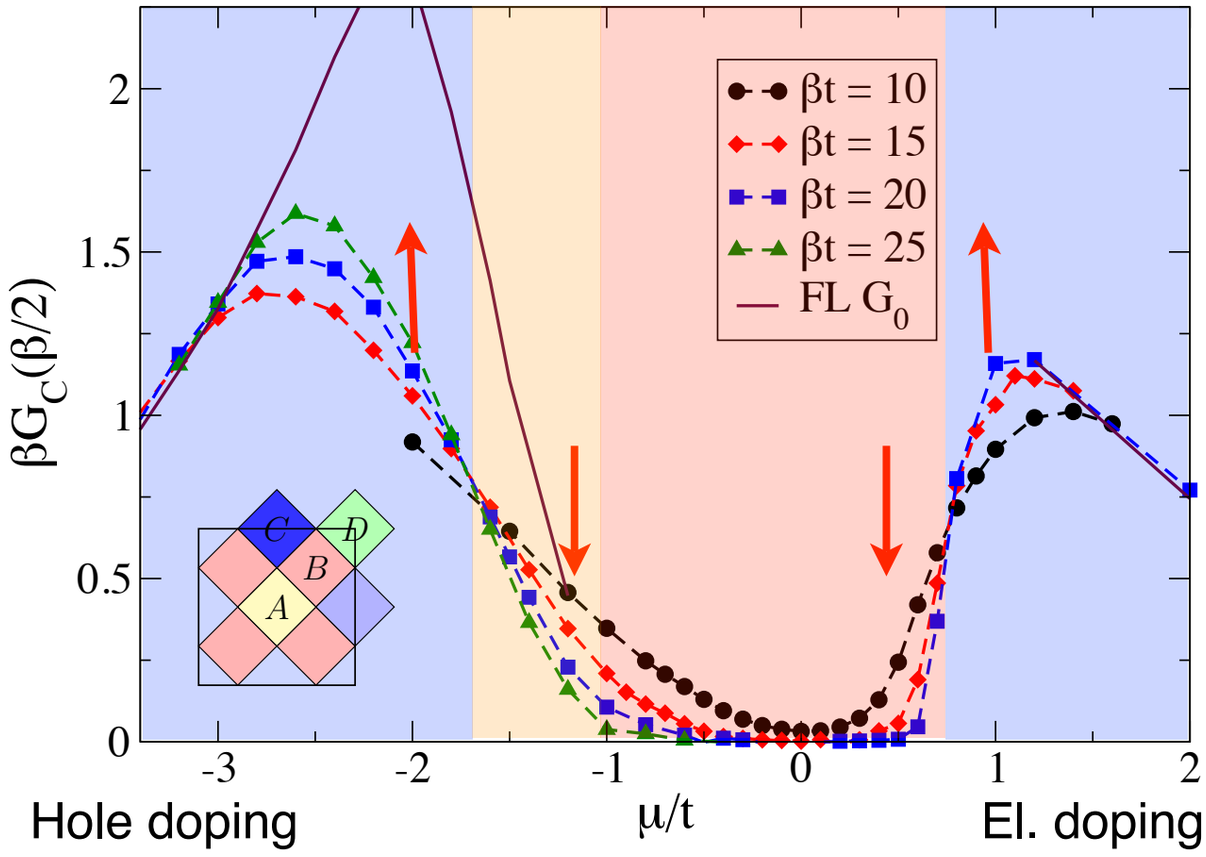

Nodal Fermi level DOS

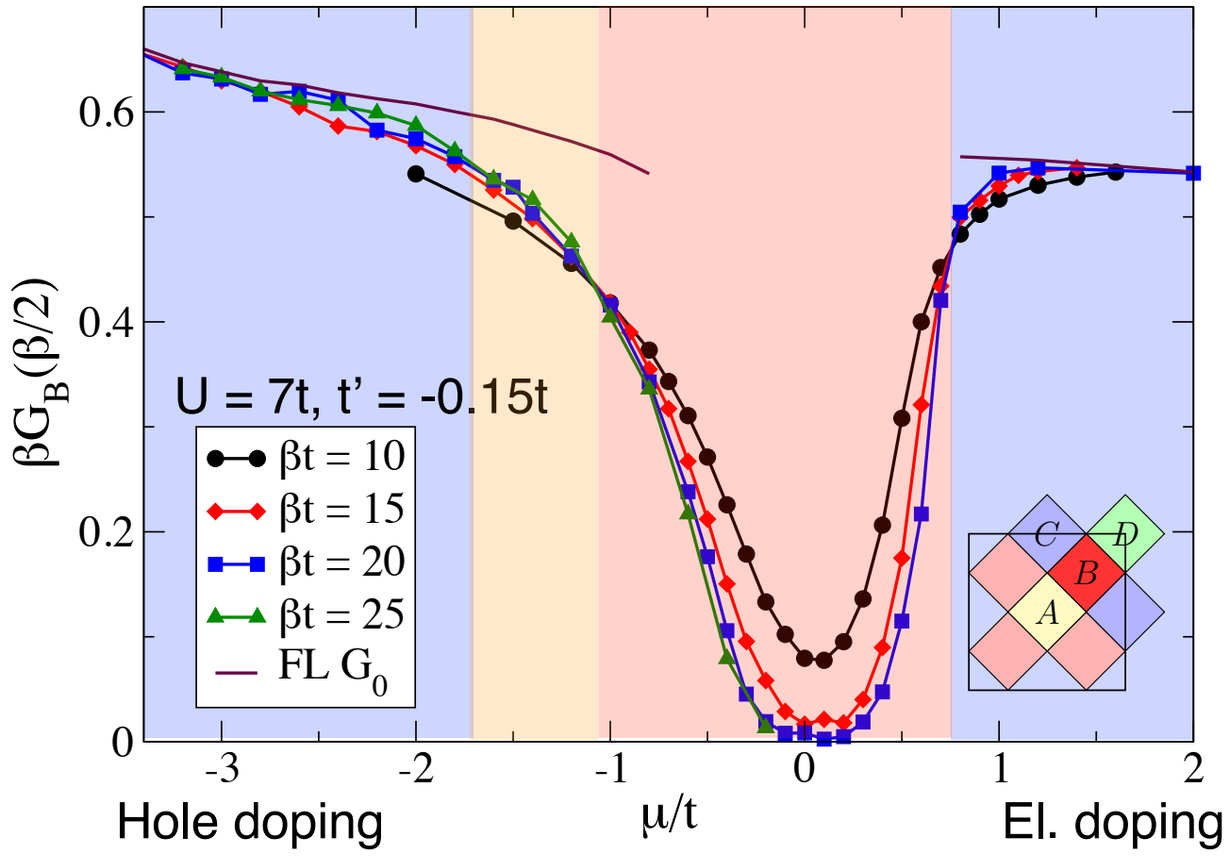

U = 7t, t' = -0.15t

E. Gull, O. Parcollet, P. Werner, A. J. Millis, Phys. Rev. B 80, 245102 (2009)

E. Gull, M. Ferrero, O. Parcollet,A. Georges, A.J. Millis, Phys. Rev. B 82, 155101 (2010)

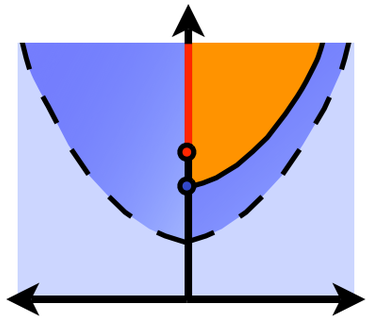

Phase Diagram

Partial occupancy in each momentum sector:

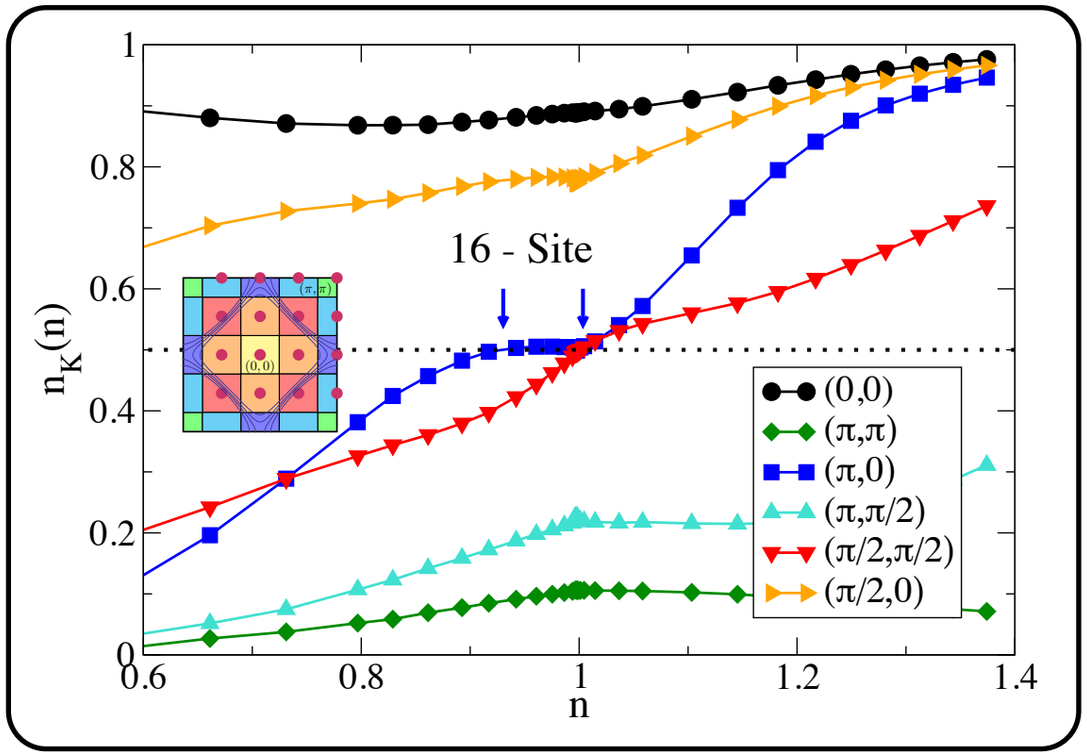

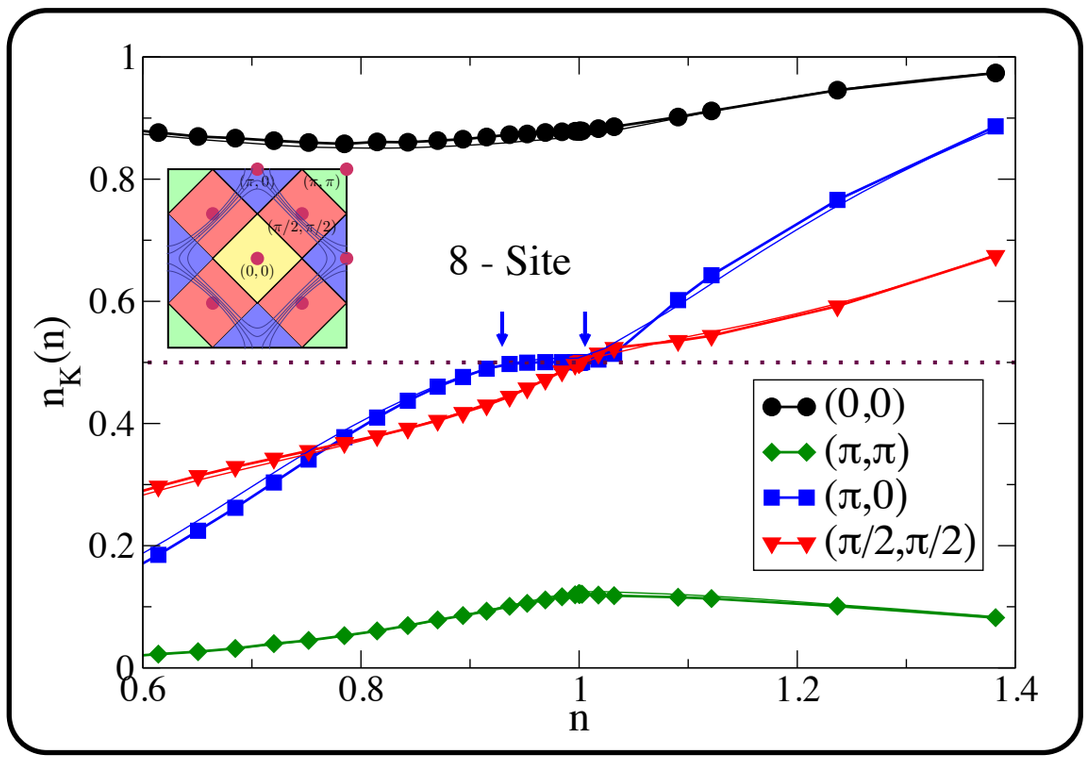

In momentum-selective phase pinned to Mott insulating value: antinode is incompressible, node is metallic.

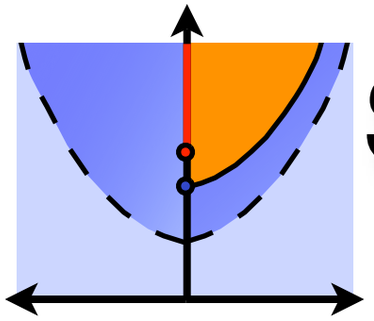

N. Lin, E. Gull, and A.J. Millis, Phys. Rev. B 82, 045104 (2010)

Sector Selective Regime: Spectra

Analytically continued spectral function A(ω): U = 7t, t'/t=0.15, βt=20

for the antinodal sector.

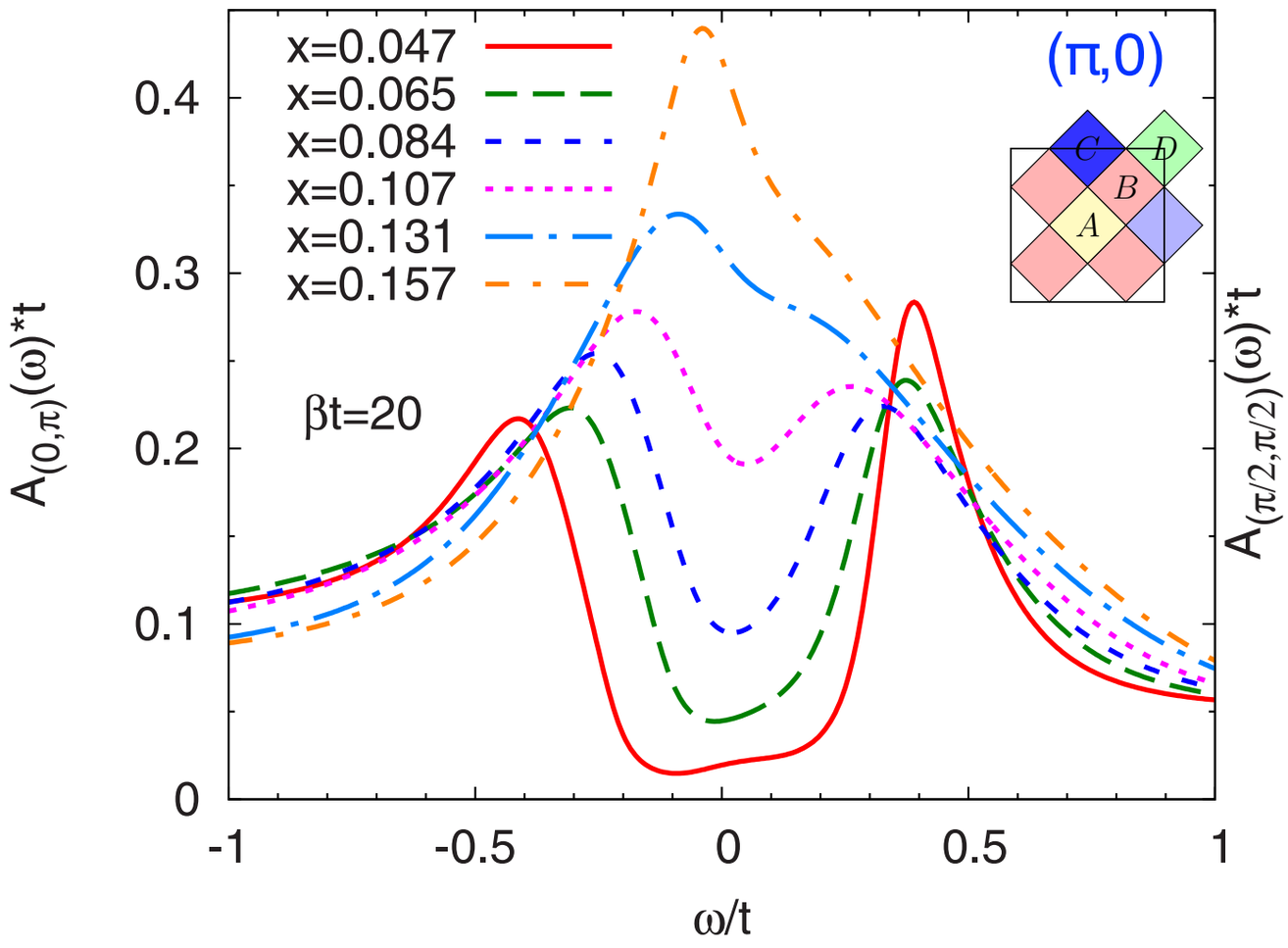

for the nodal sector.

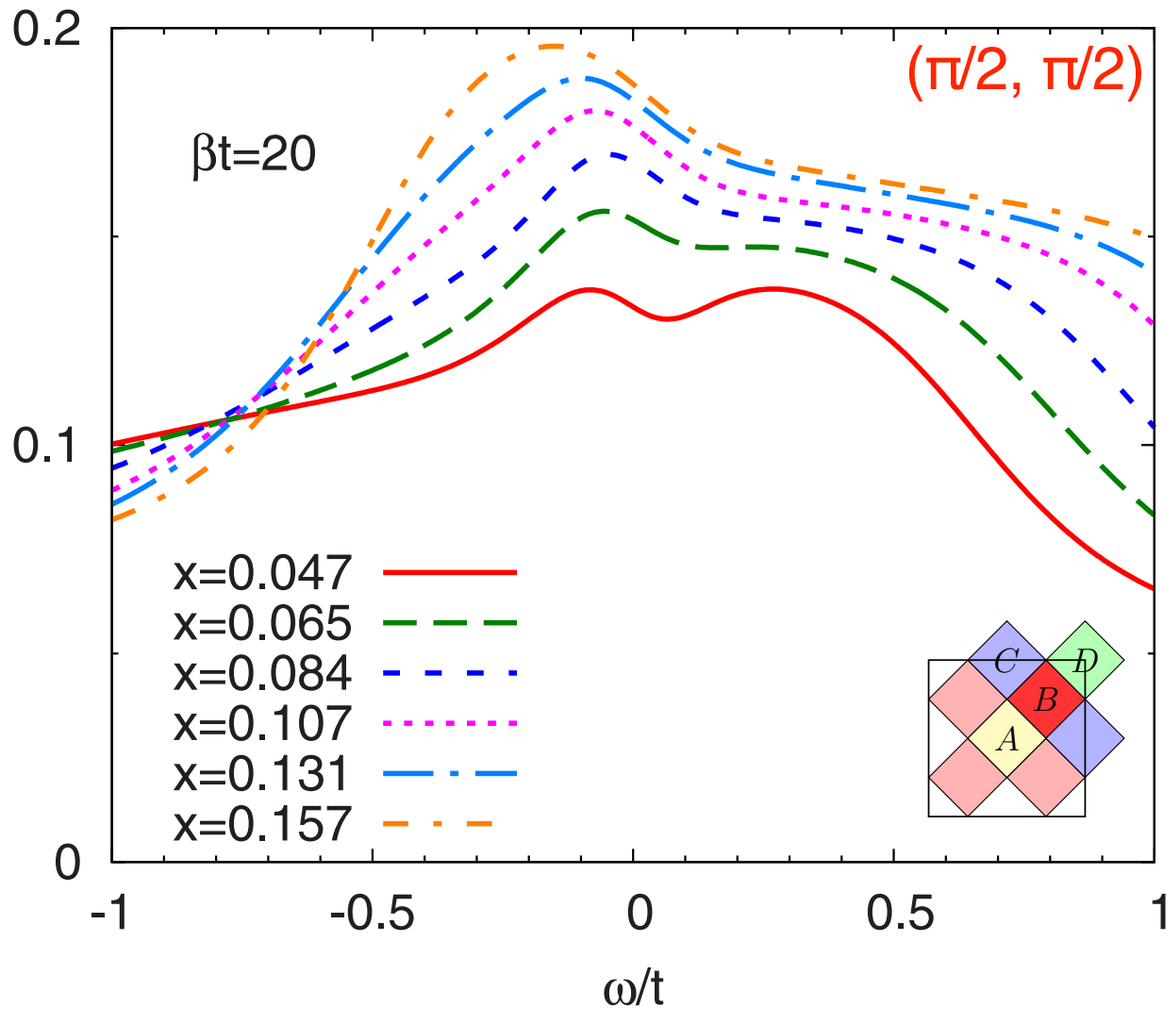

when reducing doping from x=0.157 to x=0.047: gap develops in the antinodal part of BZ, nodal part stays metallic.

Generic Phase Diagram

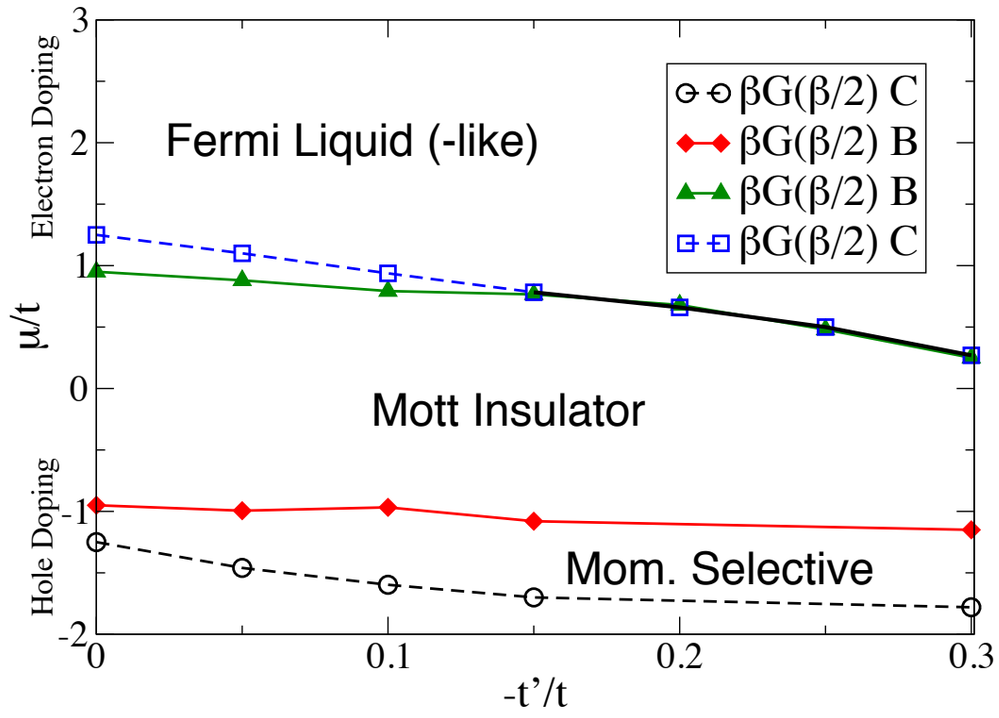

As a function of t'/t: Two transitions merging into one first order transition on the electron doped side

E. Gull, O. Parcollet, P. Werner, A. J. Millis, Phys. Rev. B 80, 245102 (2009)

First order transition: see also A. Macridin et al., Phys. Rev. B 74, 085104 (2006).

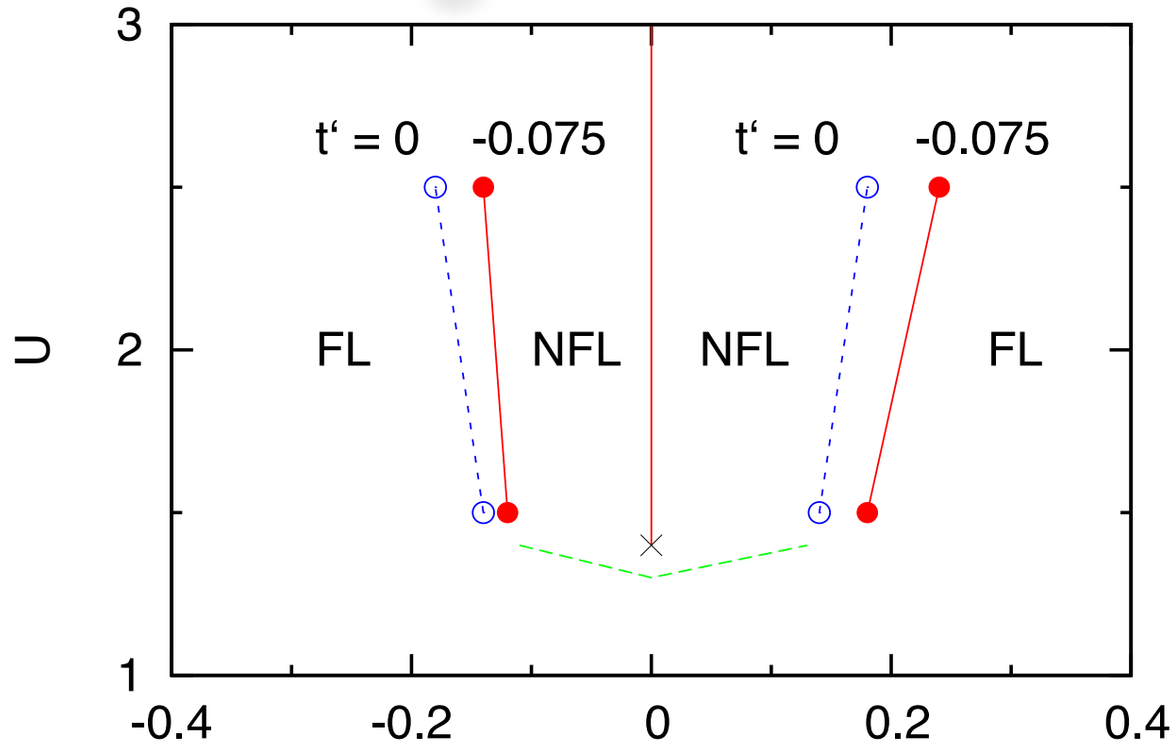

In 2x2 CDMFT (&ED)

A. Liebsch, N.-H. Tong, Phys. Rev. B 80, 165126 (2009)

CDMFT/ED

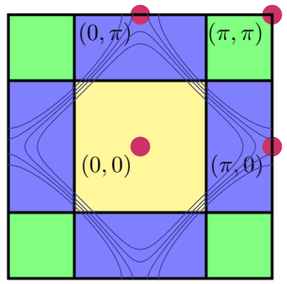

P. Werner, E. Gull, O. Parcollet, A.J. Millis, Phys. Rev. B 80, 045120 (2009),
E. Gull, P. Werner, O. Parcollet, A.J. Millis, Phys. Rev. B 80, 245102 (2009)

Cluster Size Dependence

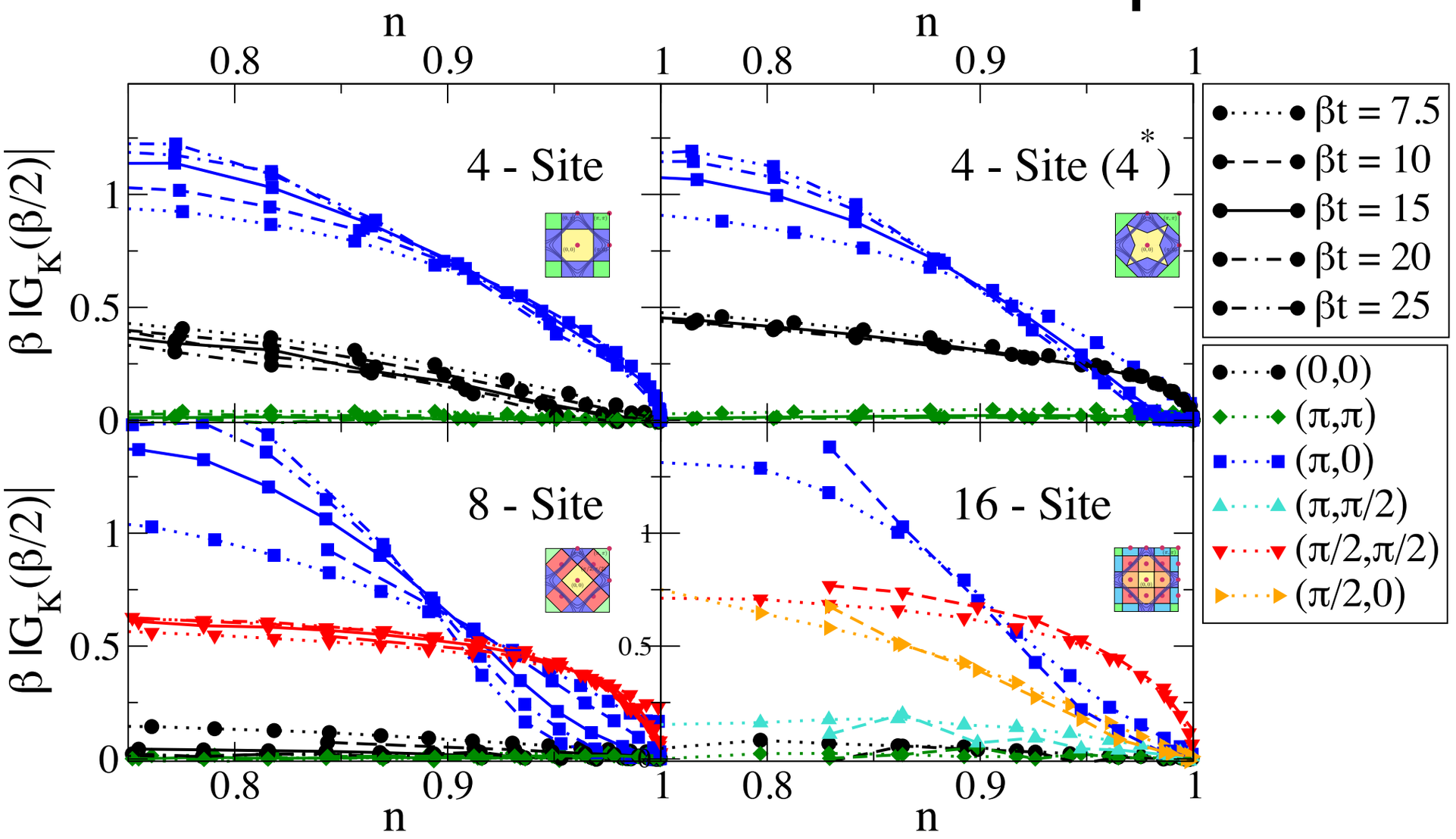

Sector selective transition is robust in DCA (for all clusters large enough to have nodal antinodal differentiation), is the DCA representation of pseudogap physics.

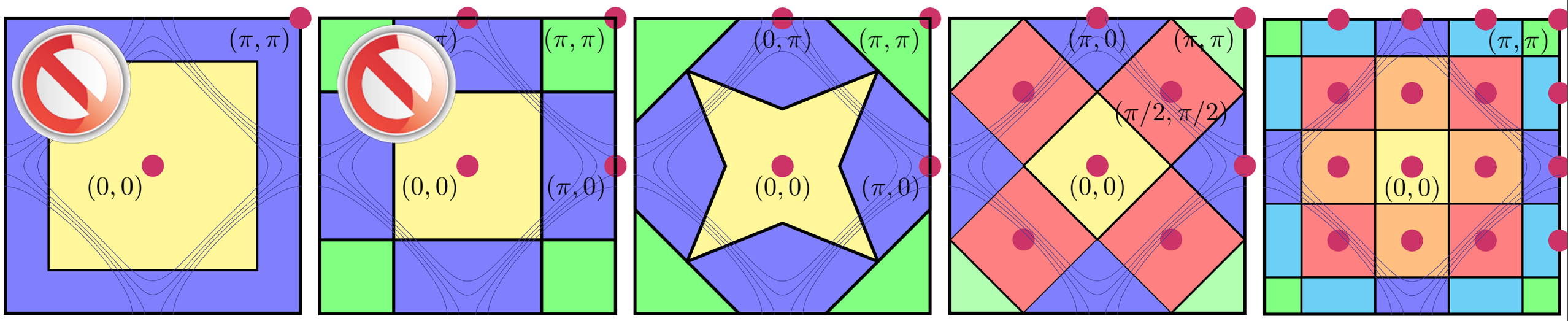

P. Werner, E. Gull, O. Parcollet, A.J. Millis, Phys. Rev. B 80, 045120 (2009),
E. Gull, P. Werner, O. Parcollet, A.J. Millis, Phys. Rev. B 80, 245102 (2009)

Cluster Size Dependence

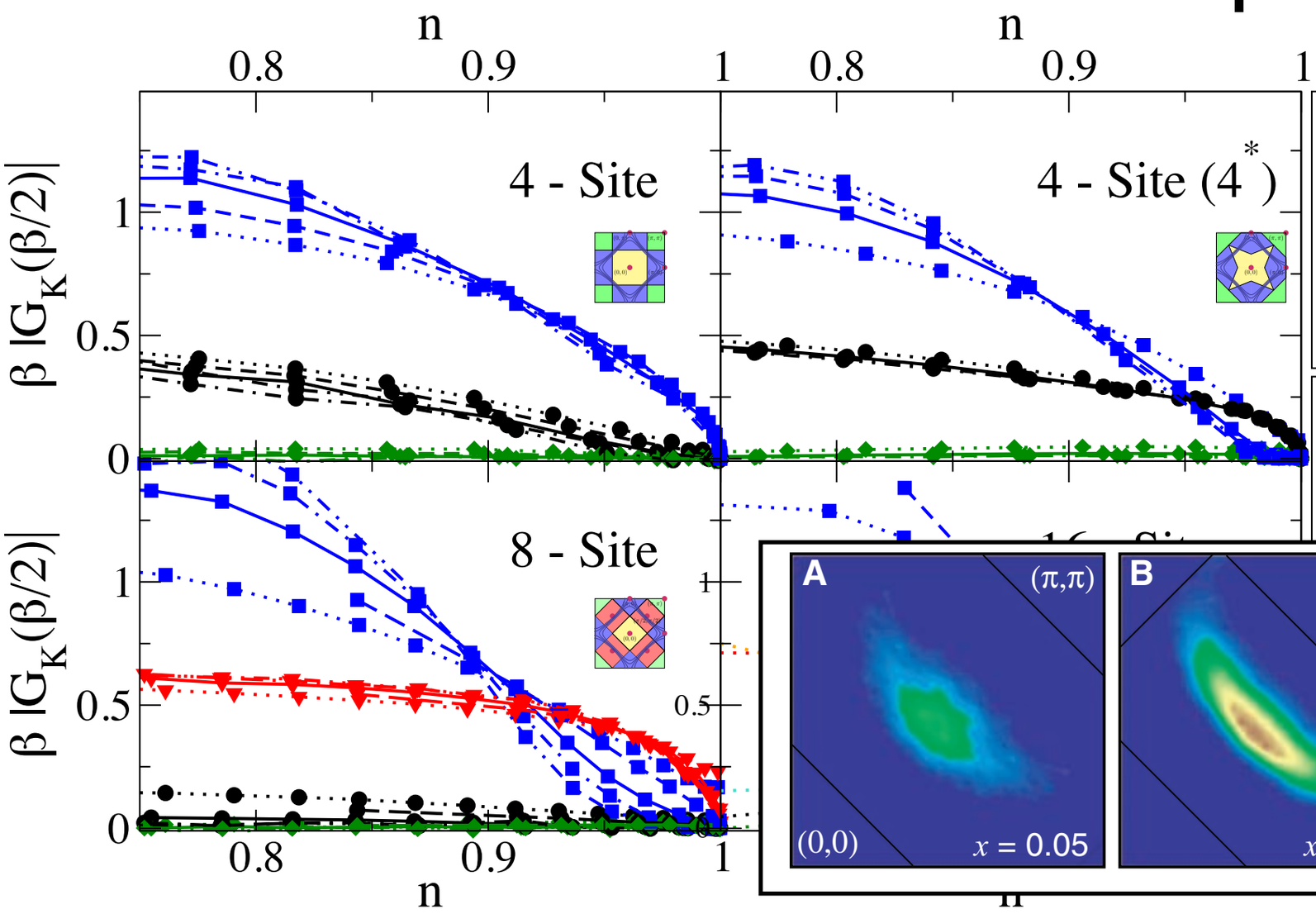

Sector selective transition is robust in DCA (for all clusters large enough to have nodal antinodal
tiation), is
A
entation of
gap
s.

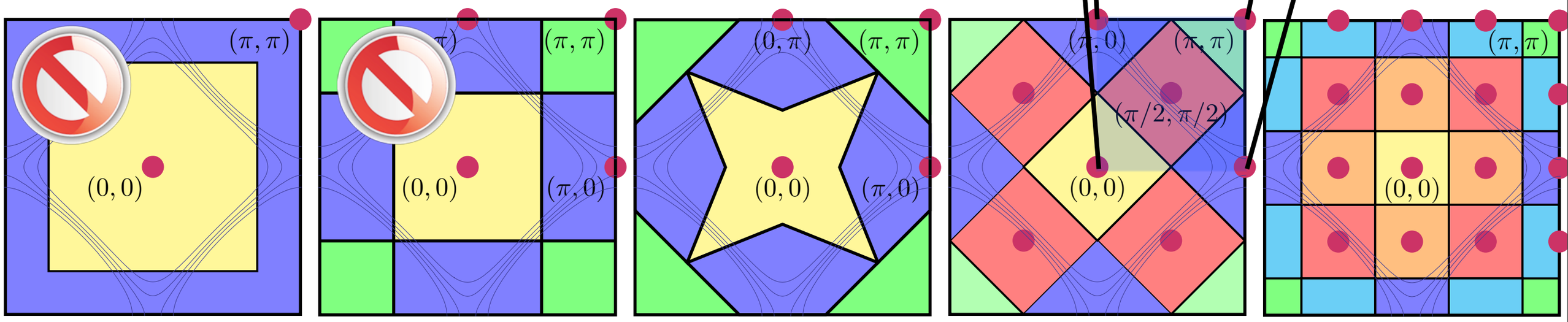

N. Lin, E. Gull, and A.J. Millis, Phys. Rev. B 82, 045104 (2010)

Sector Selective Regime: ARPES & Pseudogap

Sector selective transition is the cluster DMFT representation of pseudogap physics.

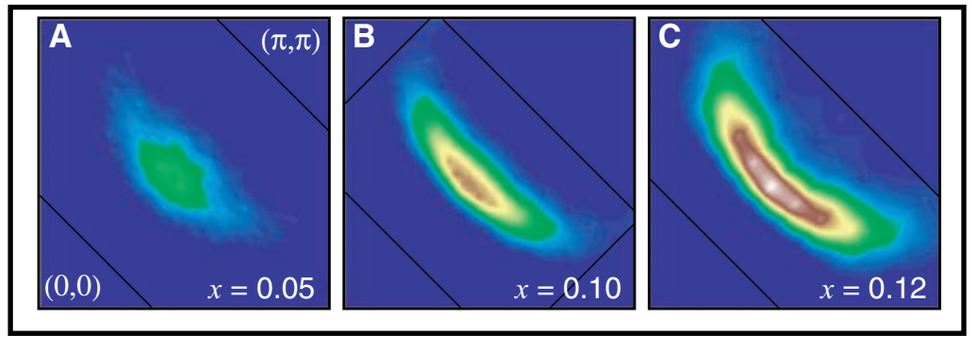

ARPES: Shen *et al.*, Science 307, 901 (2005)

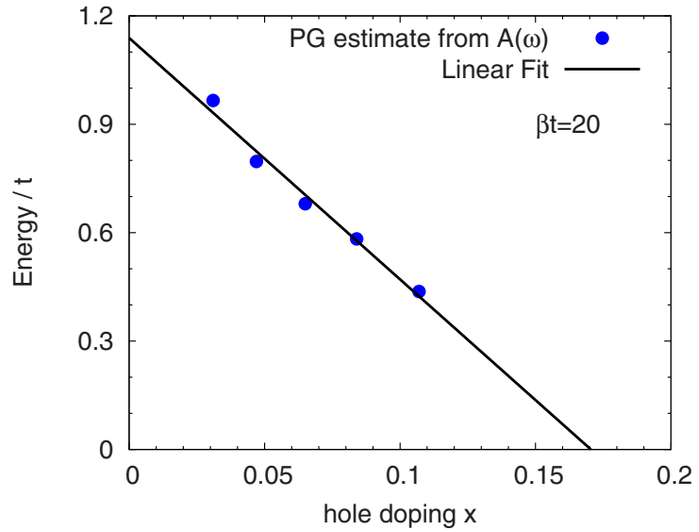

FIG. 15. (Color online) Points: pseudogap size determined from electron spectral function as a function of hole doping x for $U=7t$ and inverse temperature $\beta=20/t\approx 200$ K. Line: linear fit to results.

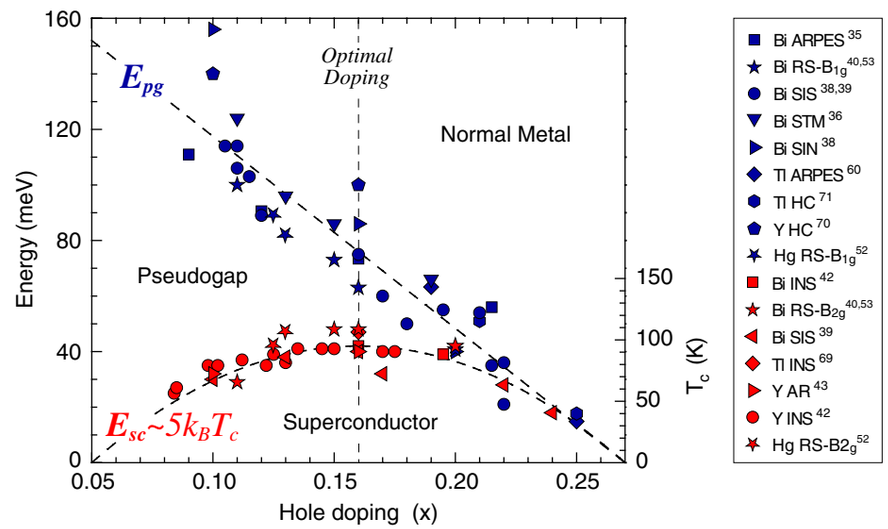

Hüfner *et al.*, Rep. Prog. Phys. 71, 062501(2008)

The pseudogap is a feature of the Hubbard model at intermediate correlation strength.

No long range order is required.

Remarkable agreement with other experimental probes: c-axis, in-plane optical conductivity, Raman.

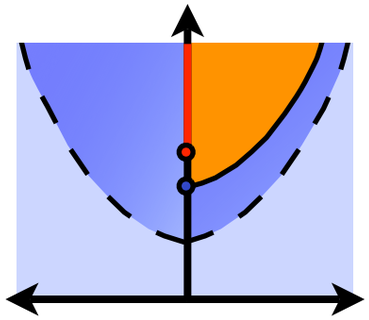

Momentum Space Differentiation

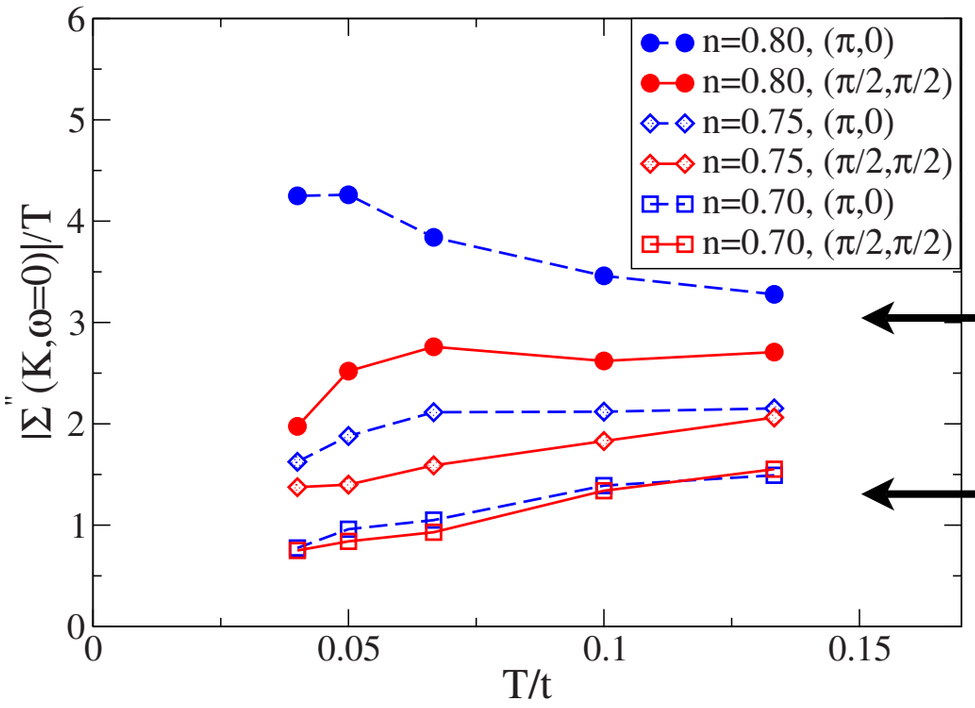

Red: Nodal scattering rates
Blue: Antinodal scattering rates

Momentum Space Differentiation

Isotropic Fermi Liquid regime

Momentum space differentiation (n ~ 0.8): Nodal scattering rate vanishing more rapidly than antinodal scattering rate.
Isotropic Fermi Liquid regime (n ~ 0.7): Nodal and Antinodal scattering rate identical.

Similar to anisotropic component observed in Angle-Dependent Magneto-Resistance

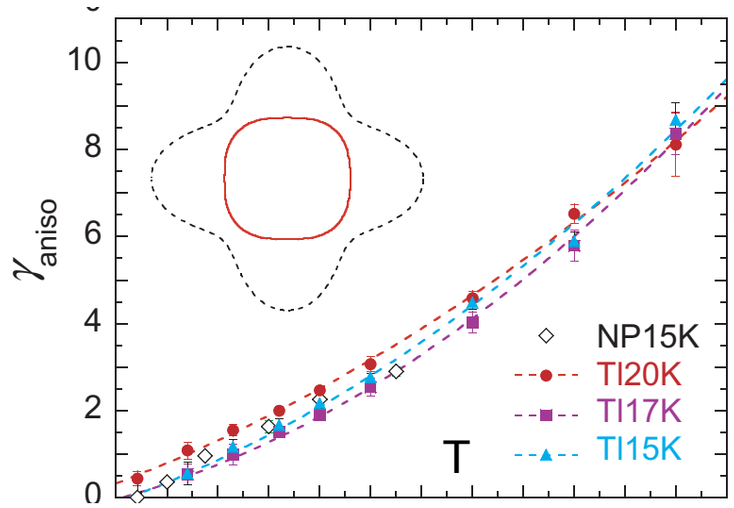

French, Analytis, Carrington, Balicas, Hussey: NJP 11, 05595 (2009)

Conclusions

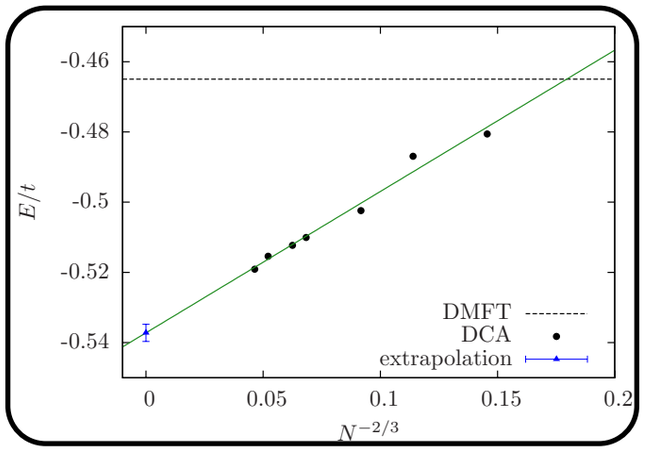

We have established DCA as a reliable tool to obtain results for the thermodynamic limit (for the infinite (lattice) system).

Algorithmic and **numerical** improvements: much larger systems accessible, scans of phase space possible.

Fermi Liquid | Momentum-Space Diff. | Sector Selective | Mott

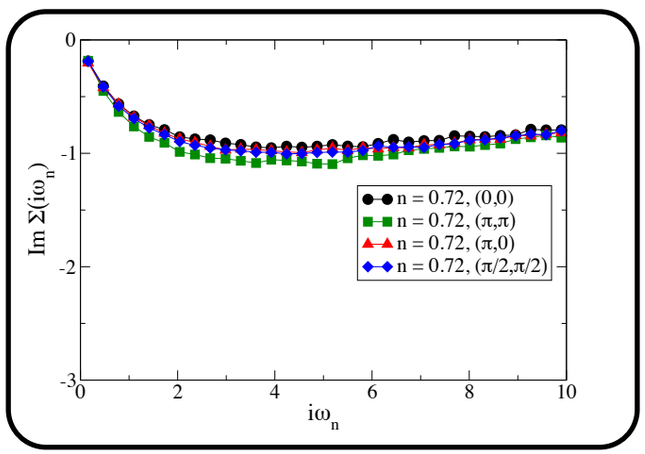

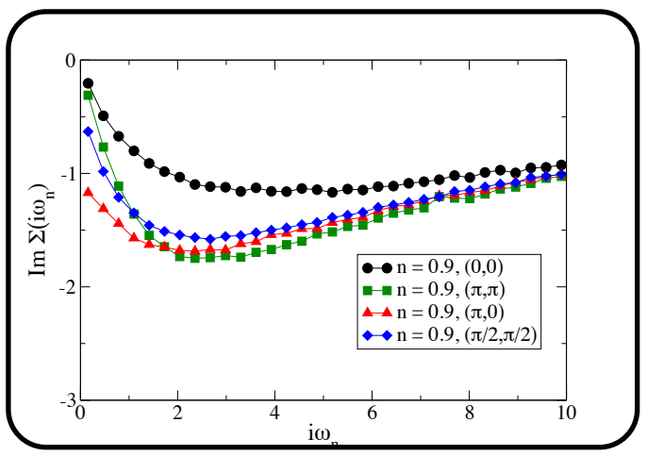

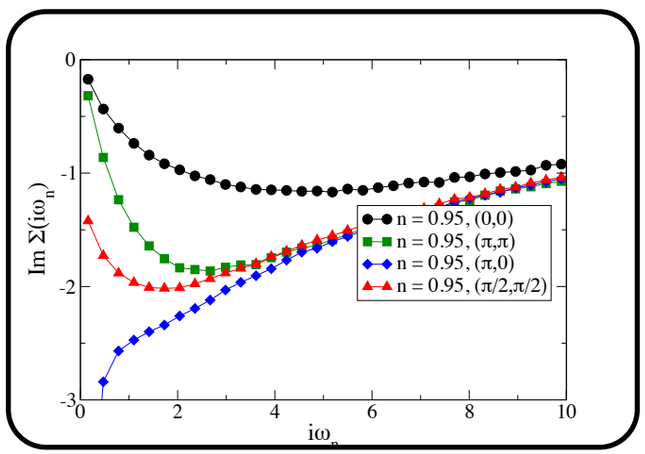

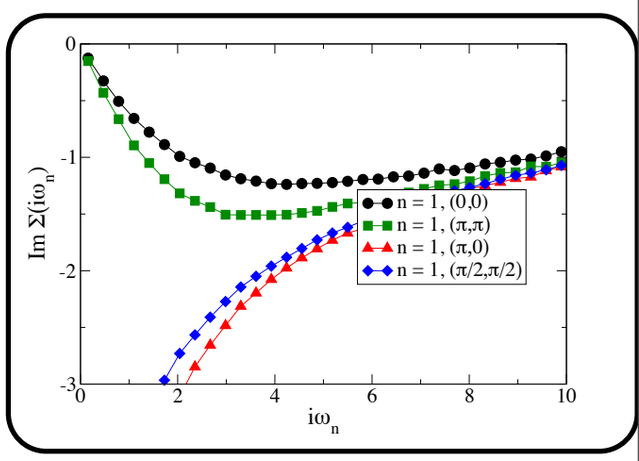

2D Hubbard model, phase diagram: contains many features observed in High-Tc experiments: Momentum space differentiation, pseudogap: Node metallic, antinode insulating. No long-ranged order required.

Sector selectivity is the Cluster DMFT signature of the pseudogap, Features are robust: observed for all clusters large enough, also in CDMFT, no interpolation / analytical continuation

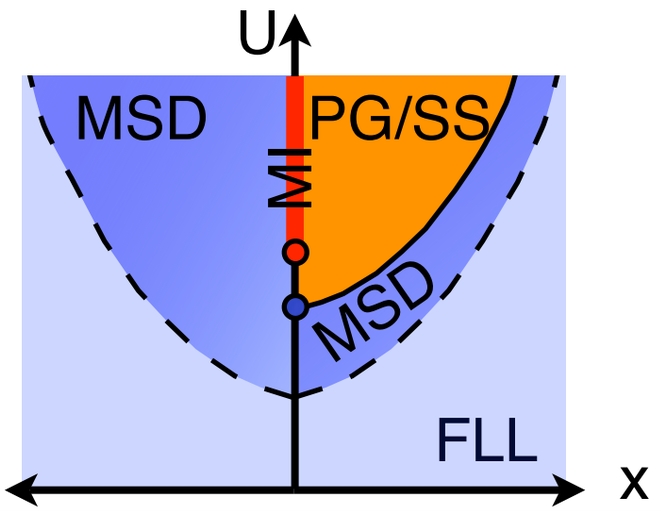

Acknowledgments

Many thanks to my collaborators:

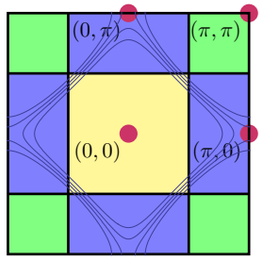

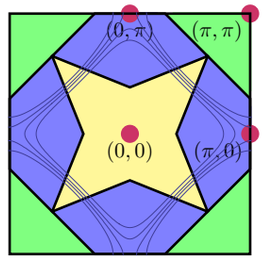

A. J. Millis

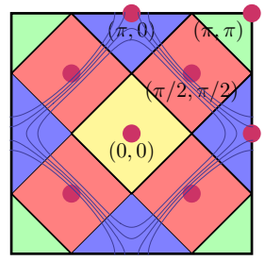

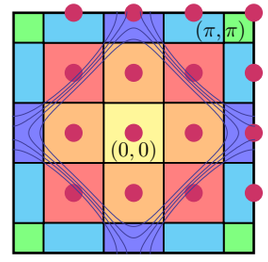

2d Hubbard:

M. Ferrero, A. Georges, N. Lin, O. Parcollet, P. Werner

3d Hubbard, algorithmics:

S. Fuchs, T. Maier, P. Nukala, L. Pollet, T. Pruschke, P. Staar, T. Schulthess, M. Summers, M. Troyer

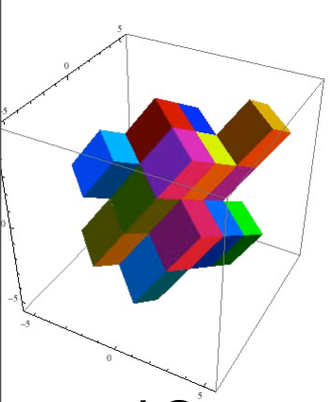

18

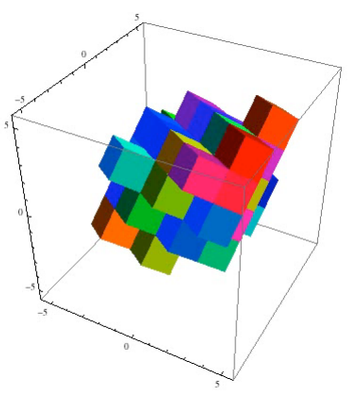

36

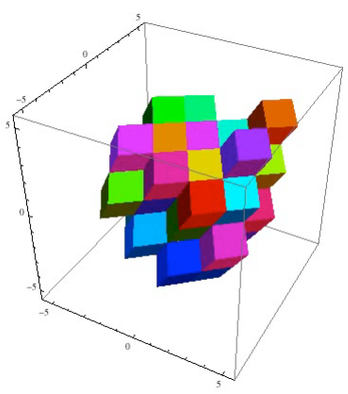

48

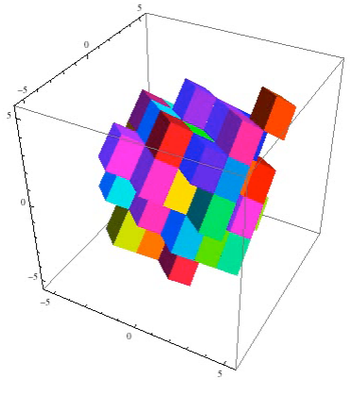

56

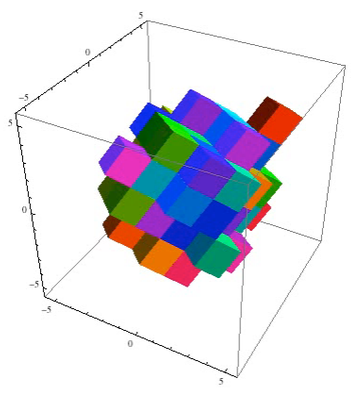

64

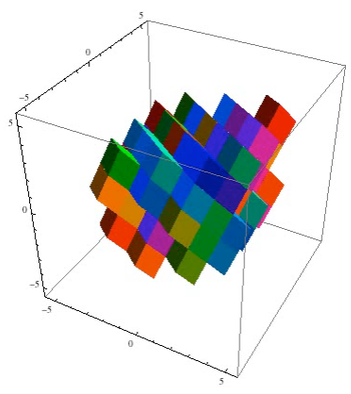

84

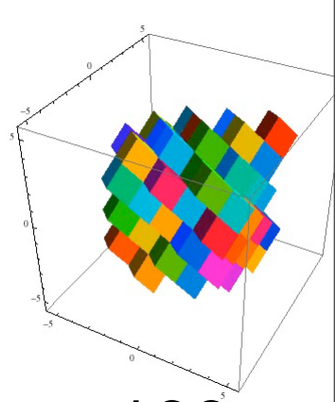

100

COLUMBIA UNIVERSITY
IN THE CITY OF NEW YORK

Funding: NSF-DMR-1006282

Computer time: Brutus cluster, ETH Zurich and the Center for Nanophase Materials Sciences at ORNL